Russian Original Vol. 35, No. 4, October, 1973

April, 1974

SATEAZ 35(4) 883-976 (1973)

SOVIET ATOMIC ENERGY

АТОМНАЯ ЭНЕРГИЯ
(ATOMNAYA ÉNERGIYA)

TRANSLATED FROM RUSSIAN

CONSULTANTS BUREAU, NEW YORK

SOVIET ATOMIC ENERGY

Soviet Atomic Energy is a cover-to-cover translation of *Atomnaya Énergiya*, a publication of the Academy of Sciences of the USSR.

An arrangement with Mezhdunarodnaya Kniga, the Soviet book export agency, makes available both advance copies of the Russian journal and original glossy photographs and artwork. This serves to decrease the necessary time lag between publication of the original and publication of the translation and helps to improve the quality of the latter. The translation began with the first issue of the Russian journal.

Consultants Bureau journals appear about six months after the publication of the original Russian issue. For bibliographic accuracy, the English issue published by Consultants Bureau carries the same number and date as the original Russian from which it was translated. For example, a Russian issue published in December will appear in a Consultants Bureau English translation about the following June, but the translation issue will carry the December date. When ordering any volume or particular issue of a Consultants Bureau journal, please specify the date and, where applicable, the volume and issue numbers of the original Russian. The material you will receive will be a translation of that Russian volume or issue.

Subscription
$80 per volume (6 issues)
2 volumes per year
(Add $5 for orders outside the United States and Canada.)

Single Issue: $30
Single Article: $15

CONSULTANTS BUREAU, NEW YORK AND LONDON

227 West 17th Street
New York, New York 10011

Davis House
8 Scrubs Lane
Harlesden, NW10 6SE
England

Published monthly. Second-class postage paid at Jamaica, New York 11431.

Soviet Atomic Energy, is abstracted or indexed in *Applied Mechanics Reviews, Chemical Abstracts, Engineering Index, INSPEC—Physics Abstracts and Electrical and Electronics Abstracts, Current Contents,* and *Nuclear Science Abstracts.*

SOVIET ATOMIC ENERGY

A translation of *Atomnaya Énergiya*

April, 1974

Volume 35, Number 4 October, 1973

CONTENTS

CONTENTS

(continued)

The Russian press date (podpisano k pechati) of this issue was 9/20/1973. Publication therefore did not occur prior to this date, but must be assumed to have taken place reasonably soon thereafter.

DANILA LUKICH SIMONENKO

The editorial staff of the periodical Atomnaya Énergiya expresses its profound grief on the occasion of the untimely demise of Professor Danila Lukich Simonenko, member of the editorial panel of the periodical, head of the I.V. Kurchatov Institute of Atomic Energy sector, winner of the Lenin Prize, and Doctor of Physical and Mathematical Sciences, on August 21, 1973 in the 63rd year of his life, and shares the deep sorrow of that loss with the relatives and close acquaintances of the deceased.

Translated from Atomnaya Énergiya, Vol. 35, No. 4, p. 225, October, 1973.

IN MEMORIAM

ALEKSANDR IL'ICH LEIPUNSKII

A.P. Aleksandrov, I.K. Kikoin,
Yu.B. Khariton, V.V. Orlov,
B.V. Gromov, O.D. Kazachkovskii,
and V.I. Subbotin

The power startup of the BN-350 full-scale industrial fast reactor took place on July 16, 1973, in the town of Shevchenko on the shores of the Caspian Sea.

The founder and scientific pacesetter of developmental work on fast breeder reactors in our country was Academician Aleksandr Il'ich Leipunskii of the Academy of Sciences of the Ukrainian SSR, the anniversary of whose death is marked by August 14. Thanks to the work which he initiated in good time, our country has taken the leading position in the development of several of the principal aspects of fast power reactors, and in building fast power reactors. Fast reactors are instrumental in the thorough solution of the problem of fuel reserves for the nuclear power industry, and are presently acknowledged the world over as one of the principal areas of promise in the overall power picture.

A.I. Leipunskii was an outstanding Soviet physicist, one of the founders of Soviet nuclear physics and nuclear power.

The scientific activities of A.I. Leipunskii began in 1926 at the Leningrad Physics and Engineering Institute [LFTI] with his research into elementary atomic processes. Among the most significant research achievements of that period was the detection and study of energy transfer from excited atoms and molecules to free electrons (impacts of the second kind). An extensive research program was devised for studying molecular dissociation and recombination phenomena, and the formation of negative ions.

Translated from Atomnaya Énergiya, Vol.35, No.4, p.226, October, 1973.

Starting with 1930, the basic interests entertained by A.I. Leipunskii shifted to problems in the physics of the nucleus. As one of the organizers of the Ukrainian Physics and Engineering Institute [UFTI], A.I. Leipunskii developed an extensive research program at Khar'kov geared to investigations of nuclear reactions, and one of its first projects dealt with neutron physics research. He studied processes involving interactions between thermal neutrons and matter, and photoneutron production and scattering processes. Specifically, A.I. Leipunskii was the first to detect resonance effects in scattering of neutrons on light nuclei. His neutrino detection experiment (1936) was one of A.I. Leipunskii's significant contributions to nuclear physics.

A.I. Leipunskii devoted his last twenty-five years, with all his energies, to the development of Soviet nuclear power. He was in fact the first in the world to point out how fast reactors can provide the most effective solution to the problem of reproduction of nuclear fuel. While arriving at this concept in the 1948-1949 period, A.I. Leipunskii headed up the work on fast-neutron breeder reactors in the country.

At the Power Physics Institute [FEI] in Obninsk, A.I. Leipunskii devoted a broad program of research on nuclear physics, reactor physics, heat transfer and technology of liquid-metal coolants. This research, backed up by operating experience with the BR-2, BR-5, and BOR-60 fast reactors build under his supervision, laid down solid scientific and technical foundations for future full-scale power generating stations using fast reactors.

A.I. Leipunskii died only one year before the startup of the first full-scale nuclear power station based on a BN-350 fast reactor, and built under his scientific supervision. An even more productive power station using a BN-600 fast reactor is now under construction in the Urals, and large power generating stations are being developed to bring fast reactors definitely into the nuclear power picture in the country.

In addition to his many-sided scientific research activities and activities in organizing scientific programs, A.I. Leipunskii has also devoted many of his efforts to the training and education of scientific cadres. As one of the founders of MIFI [Moscow Engineering and Physical Institute], he continued in his capacity as head of a department of that institute up until his very last days. Many of his pupils developed into major scientists at the head of leading scientific teams.

A.I. Leipunskii's contribution to the cause of developing Soviet nuclear physics and the Soviet nuclear power industry has received a high estimate from the Soviet government. He was awarded three Orders of Lenin, the Order of the October Revolution, the Badge of Honor order, and various medals. For his work on fast reactors, A.I. Leipunskii, together with some of his colleagues, was awarded the Lenin Prize. In 1963, A.I. Leipunskii was awarded the title of Hero of Socialist Labor.

As a scientists and as a person, Aleksandr Il'ich Leipunskii won the most profound respect of all those who worked with him, and of all those fortunate enough to know him. His bright memory will always be cherished in our hearts.

ARTICLES

FIRST RESULTS OF WORKING WITH BEAMS OF SEPARATED PARTICLES IN THE INSTITUTE OF HIGH-ENERGY PHYSICS ACCELERATOR

F. Bernard,* N.A. Galyaev,
A. Grand,* V.E. Zelenin,
V.I. Kotov, R. Lazerus,*
G. Lengeler,* B. Marechal,*
J. Prela,* A.A. Prilepin,
B.V. Prosin, and Yu. S. Khodyrev

UDC 621.3.038.617:621.384.8

In accordance with the arrangements which have been made for cooperation between the Institute of High-Energy Physics and CERN, a magnetooptical channel forming a beam of separated particles and a high-frequency separator have been developed and constructed for the French liquid-hydrogen chamber "Mirabelle." This channel provides the bubble chamber with kaons and antiprotons over range of momentum 17-40 GeV/c, and pions with momenta up to 50 GeV/c. The high-frequency separator developed and constructed in CERN over the period 1967-1971 was set up and tested in the Institute of High-Energy Physics in August 1971. Over the same period a magnetooptical channel was designed and set up in the Institute of High-Energy Physics. Testing of the whole complex was completed in 1972, and the first photographs in a beam of K^- mesons were obtained in the Mirabelle chamber in May-June, 1972.

*CERN colleagues.

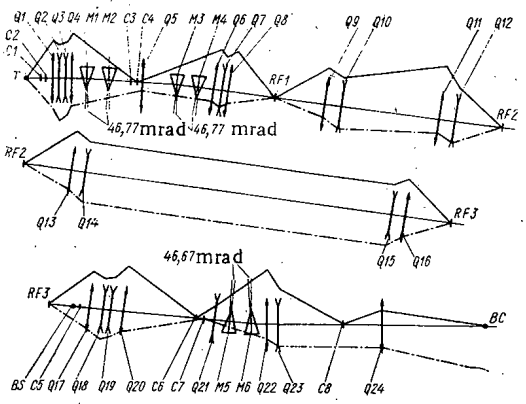

Fig. 1

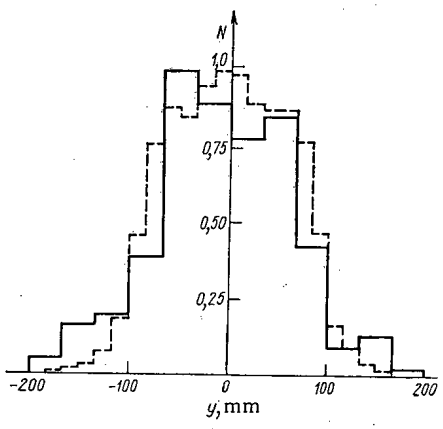

Fig. 2

Fig. 1. Optical system of the channel and course of the rays in the horizontal (———) and vertical (- - - -) planes: T) outer target; C) collimators; Q) quadrupole lenses; M) deflecting magnets; RF) deflectors of the separator; BS) absorber; BC) Mirabelle bubble chamber.

Fig. 2. Vertical profile of the beam in the Mirabelle bubble chamber: ———) experimental distribution of the particles; - - - -) calculated distribution.

Translated from Atomnaya Énergiya, Vol. 35, No. 4, pp. 227-230, October, 1973. Original article submitted February 1, 1973.

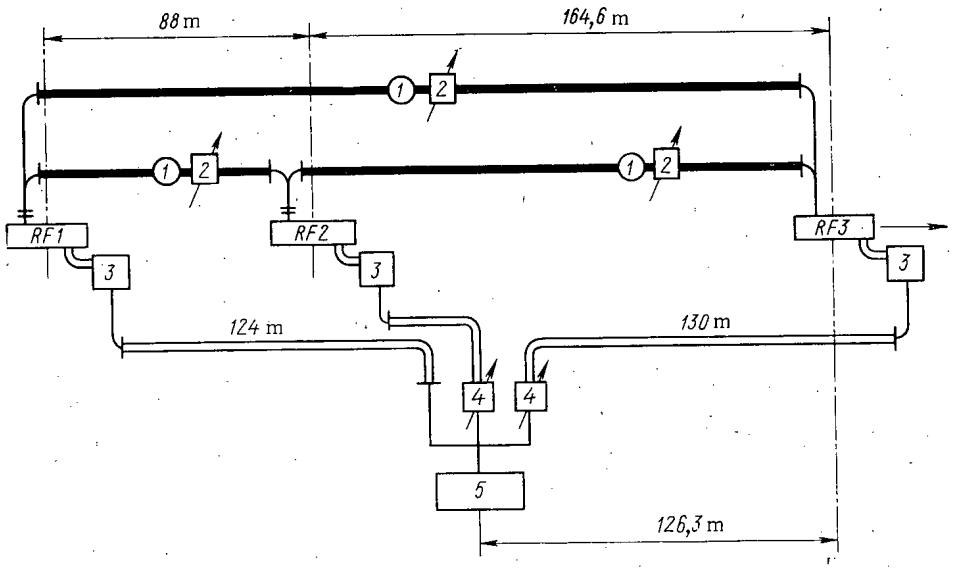

Fig. 3. Block diagram of the separator: 1) phase bridge; 2) reference phase shifter; 3) klystron power amplifier; 4) finishing phase shifter; 5) high-stability master generator.

The main design characteristics of the channel and the high-frequency separator were presented earlier [1]. Figure 1 shows the final version of the optical system of the channel, which differs from that given in [1] mainly in relation to the final section, the latter providing a repeated momentum analysis of the particles and shaping the particle beam passing into the bubble chamber. The new version of the optical system gives a uniform particle distribution in the working space of the bubble chamber (Fig. 2). The main parameters of the optical system of the channel are as follows:

Dimensions of the copper target (horizontal—vertical—length)	$2 \times 1.5 \times 150$ mm^3
Angle of formation of the particles	0°
Angles of capture of the particles into the channel:	
horizontal	±5 mrad
vertical	±3.8 mrad
Maximum solid angle of capture	76 μsr
Momentum resolution	±0.25%
Number of quadrupole lenses (length 2 m)	23
Number of rotating magnets (length 6 m)	6
Number of collimators	8
Interdeflector distances:	
L_{12}	88 m
L_{23}	164.6 m
L_{13}	252.6 m
Total length of the channel	511.5 m

Magnifications	Horizontal	Vertical
First momentum collimator C4	−1.68	-
Center of deflectors	2.31	5.69
Redetermination of target, collimators C6, C7	−3.06	9.83
Second momentum collimator C8	3.33	-

The high-frequency separator was constructed with due allowance for the conditions of optimum acceptance of the particle beam in the momentum range 30 GeV/c, with the maximum possible value of the high-frequency deflecting field. A block diagram of the separator is shown in Fig. 3, and its main characteristics are presented below:

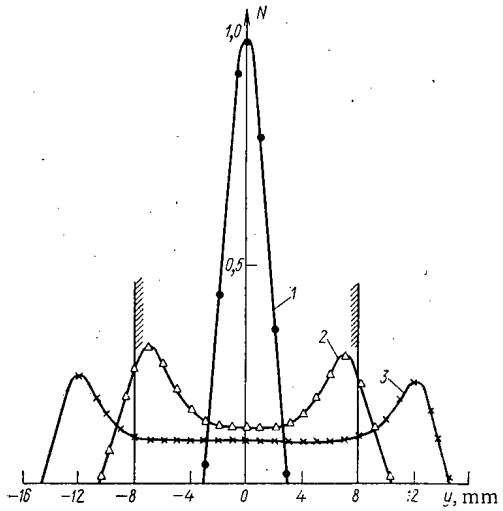

Fig. 4. Profile of the undeflected beam in the absorber in the vertical plane (1), and profiles of the deflected beam when working with one (2), and simultaneously with two deflectors of the separator (3). The vertical straight lines indicate the boundaries of the absorber.

Design frequency (at 25°C, in vacuum, and for $V_{ph} = c$) f_0	2855.167 MHz
Phase shift per cell	$2\pi/3$
Deflector aperture $2a$	45.0 mm
Effective deflector length l	5.845 m
Total deflector length	6.025 m
Group velocity (normalized) $\beta_g = v_g/c$	−0.0248
Amplitude damping factor α	0.102 Np/m
Shunt impedance R	16.3 MΩ/m
Quality factor Q	1180
Series impedance $\sqrt{Z} = [(R/Q) \cdot (2\pi/\lambda) \cdot (1/\beta_g)]^{1/2}$	$1.82\sqrt{k\Omega}/cm$
Deflector constant $kl = \sqrt{Z}\frac{1-e^{-\alpha l}}{\alpha}$	$8.03\sqrt{k\Omega}$
Transverse momentum (for a power of P_0 = 20 MW) $p_\perp = \sqrt{P_0}kl$	35.9 MeV/c

The first setting of the operating conditions of the channel and high-frequency separator was carried out for a particle beam with a momentum of 32.17 GeV/c. For this momentum the phase shift between the pions and protons (antiprotons) on a base of 252.6 m is equal to 360°. It thus follows that by using the first and third deflectors of the separator we may separate kaons from pions and protons (antiprotons). According to calculations, the kaon flux to the bubble chamber reaches a maximum for this value of the momentum [1].

From the measured difference $\Delta\gamma$ between the phases corresponding to the deflections of the π mesons and protons we may accurately determine the momentum of the particles. For a momentum of p = 32.17 GeV/c this difference is equal to zero (or 360°) and the deviation Δp of the momentum from the specified value will be given by the expression

$$\frac{\Delta p}{p} = \frac{\Delta\gamma}{4\pi}.$$

Thus the actual value of the momentum belonging to the separated particles may be determined to an accuracy of better than 0.5%.

From the image of the particle beam in the absorber in the vertical plane (Fig. 4) we may measure the angle of deviation communicated to the particles in each deflector. This is approximately ±0.9 mrad instead of the theoretically expected ±1.0 mrad. The difference is comparable with experimental error.

The purity of the separated beam of kaons was determined by means of Cerenkov and scintillation counters placed in front of the bubble chamber (Fig. 5). The same figure presents the results of some measurements; these show that the background of pions and protons (antiprotons) is no greater than 2%. However, these measurements cannot provide an accurate estimate of the muon background, since the spatial distribution of the muons is considerably greater than the particle beam itself.

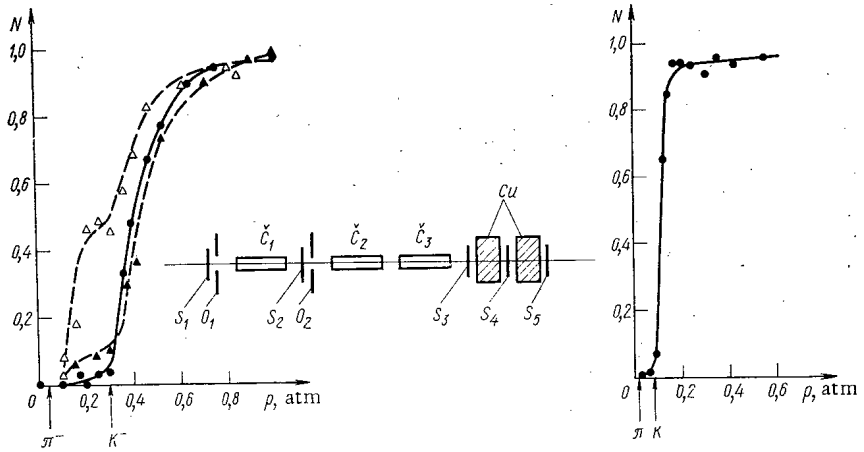

Fig. 5. Arrangement of Cerenkov counters, and threshold curves for $K^{\pm}$ mesons with a momentum of 32.17 GeV/c. The horizontal axis gives the CO_2 (K^-) and freon-12 (K^+) pressure, the vertical axis gives the ratio of the readings in the counters $S_1S_2C_2S_3$ to $S_1S_2S_3$ set for coincidence. The continuous curves correspond to the set phase between the deflectors; the broken curves are obtained on changing this phase by 27 (△) and 32° (△).

In order to carry out these measurements we used a special rapid-extraction operating mode [2, 3]: instead of a single group of accelerated protons (with a duration of about 15 nsec), approximately 1-2% of the protons which were left after the operation of the other experimental installations were extracted from the accelerator at the end of the flat part of the magnetic field. The proton beam was thus conveyed to the external target over a period of some 5 μsec. This enabled us to use standard electronics with coincidences, and also Cerenkov counters.

The first exposure of the Mirabelle bubble chamber was carried out in a beam of K^- mesons with a momentum of 34 GeV/c. In this we used one extracted group of accelerated protons with an intensity of some $3 \cdot 10^{10}$ particles. We obtained about 20,000 photographs with an average number of K^- mesons amounting to 3-4 particles per frame. Preliminary analysis of the photographs gave the following composition of the particle beam: $K^- \approx 80\%$; $\pi^- \approx 2\%$; $\mu^- \approx (18\text{-}20)\%$. In order to reduce the muon background, shielding was installed at several points along the channel, and especially in front of the bubble chamber. In the next irradiation of the Mirabelle chamber in $K^{\pm}$ meson beams the composition of the beam was accordingly much improved: $K^{\pm} \approx 98\%$, traces of other particles $\sim 2\%$.

In conclusion, the authors wish to express their sincere thanks to the Directorates of the Institute of High-Energy Physics and CERN for constant cooperation in the work, and to all colleagues who took part in the present research at various stages of its execution.

LITERATURE CITED

1. N.A. Galyaev et al., Seventh International Conference on High-Energy Charged-Particle Accelerations [in Russian], Vol. 1, Izd. AN ArmSSR, Erevan (1970), p. 531.
2. B. Kuiper et al., ibid., p. 549.
3. A.A. Aseev et al., Preprint of the Institute of High-Energy Physics 72-50 [in Russian], Serpukhov (1972).

CHOICE OF A COOLING MODERATOR IN ORDER TO INCREASE THE INTENSITY OF THE BEAM OF COLD NEUTRONS FROM THE RADIAL CHANNEL OF THE IVV-2 REACTOR

B.N. Goshchitskii, V.V. Gusev,
L.V. Konstantinov, P.M. Korotovskikh,
M.G. Mesropov, S.K. Sidorov,
A.G. Chudin, and V.G. Chudinov

UDC 621.039.556

Cold neutrons ($E_n \leq 0.005$ eV) are widely used for studying the structure and dynamics of matter in the condensed state. However, the number of cold neutrons in ordinary thermal-neutron beams extracted from the channels of a nuclear reactor is very low, and this limits the potentialities of many physical experiments. Special measures are therefore adopted in research reactors in order to increase the intensity of cold-neutron beams, particularly by cooling the volume of the moderator lying close to the reactor channel. As a result of the thermalization of the neutrons, the low-temperature moderator displaces the mean neutron energy into the low-energy region. Devices of this kind have become known as cold-neutron generators. In principle, this method greatly increases the cold-neutron intensity. If we assume that there is a complete thermal equilibrium between the neutron spectrum and the cooled moderator and that no absorption occurs, the transition from an equilibrium neutron distribution at T = 295°K to one at T = 78 and 20°K should increase the intensity of neutrons with an energy of 0.005 eV by 8 and 13 times, respectively [1]. In practical cases this increase is less marked, falling by a factor of 2-4 for a moderator cooled with liquid nitrogen, and by a factor of 5-8 for a moderator cooled with liquid hydrogen [1-7].

Although the use of moderators cooled with liquid hydrogen or deuterium provides far greater cold-neutron intensities, it is in a number of cases preferable (particularly for neutrons with an energy of the order of 0.005 eV) to use cold-neutron generators cooled with liquid nitrogen, bearing in mind their relative operation safety and simplicity of construction. The greatest increase in the intensity of the cold neutrons may be obtained for such weakly-absorbing moderators as graphite, beryllium, and compounds of these [6]. However, owing to the small scattering cross section, the dimensions of the moderators are in this case very considerable, and this leads to an increase in the radiative energy evolution, a greater consumption of the coolant, and so on. On the whole it is therefore better to use hydrogen-containing moderators, which are much less bulky and yield a fairly substantial increase in the cold-neutron intensity.

The efficiency of cold-neutron generators is largely determined by the material, the size, and the shape of the moderator, and also by the position of the latter relative to the active zone of the reactor, the type of reactor employed, and so forth. It is clearly this aspect which explains the contradictions in published experimental and computed data as to the choice of the best moderator dimensions (from 10 to 100 mm [1, 3-5]). Hence in developing a cold-neutron generator for a specific reactor it is essential to determine its optimum physical characteristics experimentally. In the present investigation we make a detailed study of the manner in which the cold-neutron yield varies with the material, temperature, and dimensions of the moderator for the liquid nitrogen-cooled cold-neutron generator of the water-cooled, water-moderated IVV-2 pool-type reactor.

EXPERIMENTAL METHOD

All the measurements were carried out in the physical-simulation test-bed of the IVV-2 reactor, in which the conditions governing the formation of the real neutron spectrum at the proposed site of the

Translated from Atomnaya Énergiya, Vol.35, No.4, pp.231-234, October, 1973. Original article submitted December 6, 1972.

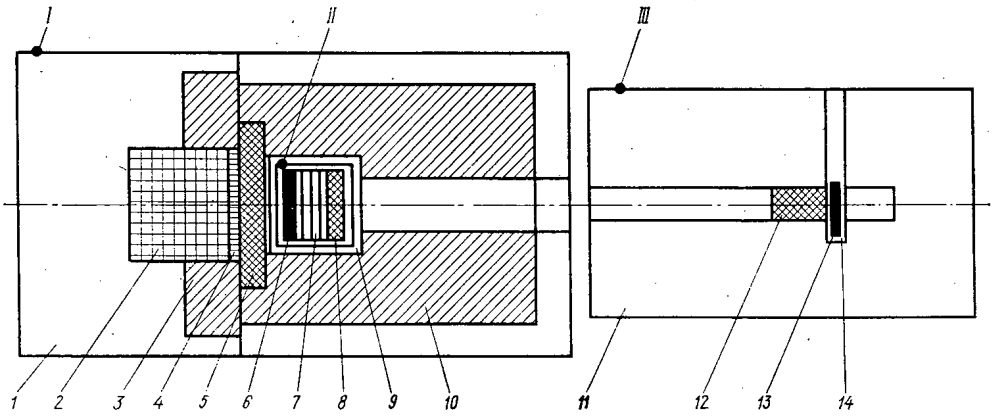

Fig. 1. Arrangement of the experimental apparatus: I) test-bed providing physical simulation of the reactor; II) cold-neutron generator; III) collimator; 1, 11) polyethylene; 2) "active zone"; 3, 10) graphite; 4) lead; 5) beryllium (graphite); 6) liquid nitrogen; 7) moderator; 8) beryllium screen; 9) vacuum thermal-insulation gap; 12) beryllium filter; 13) detector; 14) cadmium sheath.

cold-neutron generator in the reactor were closely reproduced. Figure 1 gives a general idea of the cold-neutron generator test-bed. The immediate surroundings of the cold-neutron generator, the reflector, and the graphite thermal column were reproduced on a full-scale basis. As first units of the thermal column, graphite 150 mm thick was employed instead of beryllium. In order to simulate the water surroundings, the thermal column and the reflector cassettes were provided with polyethylene blocks at least 100 mm thick. The generation of fast neutrons in the fissile material and the leakage of neutrons from the active zone were simulated by using a Po–Be source with a strength of $5 \cdot 10^7$ neutrons/sec placed in a solution of boric acid. The age of the neutrons τ and the square of the diffusion length L^2 in the solution were then close to the corresponding values in the reactor. The source was automatically held at various points of the "active zone" for a time corresponding to the calculated values of the neutron fluxes at these points in the actual reactor. The IVV-2 reactor test-bed with an analogous simulation of the active zone was used earlier in choosing the characteristics of the diffuser used for extracting the neutron beam from the tangential reactor channel [8]. The results obtained with the test-bed practically coincided with those measured in the actual reactor, thus justifying the use of the physical-simulation test-bed in the present investigation as well.

In order to cool the neutron moderators to liquid-nitrogen temperature we used a full-scale model of the cold-neutron generator with a material and construction corresponding to those of the cold-neutron generator in the reactor itself. The model consisted of two hermetically-sealed aluminum tanks placed one inside the other, with a gap of about 8 mm, the pressure in these being maintained equal to 10^{-3}–10^{-4} mm Hg, so as to ensure vacuum thermal insulation of the inner sectionalized tank. The first section was filled with liquid nitrogen in order to cool the moderator from the end surface; the remaining sections were filled with the liquid moderator, its thickness being determined by the number of sections so filled. The level of liquid nitrogen in the cold-neutron generator was monitored with level gages. The temperature of the moderator was measured at several points over the volume, using precalibrated copper– constantan thermocouples. The neutrons coming from the cold-neutron generator were recorded with a group of three He^3 counters of the SNM-16 type set in a protective collimator unit, the axis of which coincided with the axis of the physical-simulation test-bed channel (Fig. 1). The collimation was chosen so that the detector should "see" only the working surface of the cold-neutron generator. For separating the proportion of cold neutrons ($E_n \leq 0.005$ eV), a polycrystalline beryllium filter 167 mm long was placed in front of the detector in the collimator channel carrying the total flow of thermal neutrons (the extraction cross section of this filter was 10^4 times greater for thermal than for cold neutrons). The total error in measuring the neutron yield was determined by the statistical error and by the instability of operation of the time sensor; it amounted to ±3% for a measuring time of approximately 1 h. The temperature of the moderator was kept constant to ±1°C during the measurements.

Results of the Measurements and Discussion

Depending on the material, thickness, and temperature of the moderator and the other experimental conditions, the yield of cold neutrons was characterized by a quantity g equal to the ratio of the flux of cold

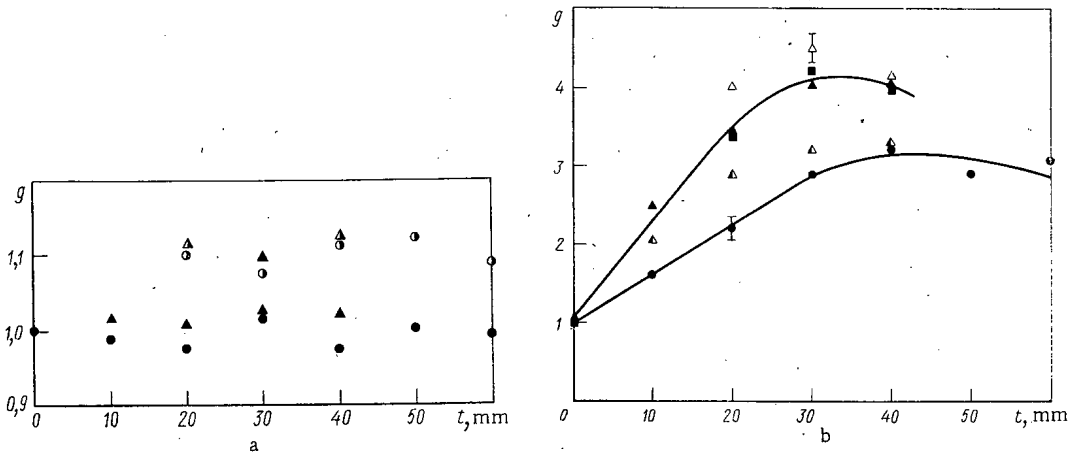

Fig. 2. Dependence of the cold-neutron yield on the thickness of the moderator t at T = 300 (a) and 78°K (b). Without the beryllium screen: ▲) C_2H_5OH; ■) C_3H_6O; ●) H_2O. With an uncooled (T = 300°K) beryllium screen: ▲) C_2H_5OH; ○) H_2O. With a cooled (T = 78°K) beryllium screen: ▲) C_2H_5OH.

TABLE 1. Maximum Values of g and Optimum Thickness of the Moderators t_{opt} at T = 78°K

Material of moderator	t_{opt}, mm	Yield of cold neutrons g	
		reflector 64 mm beryllium	reflector 80 mm graphite
Water (H_2O)	40	3,2	3,2
Ethyl alcohol (C_2H_5OH)	30	4,1	4,0
Methyl alcohol (CH_3OH)	30	—	4,1
Acetone (C_3H_6O)	30	4,2	—
Hexane (C_6H_{14})	30	—	4,0
Heptane (C_7H_{16})	30	—	4,1
Octane (C_8H_{18})	30	—	4,1

neutrons from the channel containing the cold-neutron generator to the flux of cold neutrons from the empty channel. As moderating materials we studied the following substances, which had a fairly high density relative to hydrogen: water, ethyl alcohol, methyl alcohol, acetone, hexane, heptane, and octane.

On placing the cold-neutron generator in the channel without cooling the moderator, the yield of cold neutrons remained almost constant with increasing thickness of the moderator for all the materials studied (Fig. 2a); this evidently indicates that there is only a slight perturbation of the field of thermal neutrons in the reflector and thermal column close to the cold-neutron generator. On cooling the moderator the yield of cold neutrons first increases with moderator thickness; it reaches a maximum for a certain specific thickness and then falls. Figure 2b shows the dependence of the cold-neutron yield on the thickness of the moderator at 78°K (reflector 64 mm of beryllium). Table 1 gives analogous relationships for the other materials studied.

The dependence of the cold-neutron yield on the temperature of the moderator is illustrated in Fig. 3. The measurements were made at the optimum thickness of the moderators (30 mm), corresponding to the maximum value of g at T = 78°K. We also studied the effect of the additional beryllium screen on the flux of cold neutrons. We assumed that the presence of such a screen would lead to a certain rise in the thermal-neutron flux in the moderator and hence to an increase in the cold-neutron yield. Figure 2 shows the measured values of g for the cases in which a "thermal" (T = 300°K) or "cold" (T = 78°K) beryllium screen 50 mm thick lay immediately behind the moderator (Fig. 1). We see from the curves that the beryllium screen leads to a rise of approximately 10% in g for the same temperature of the screen and the moderator. The fall in g which occurs on placing a "thermal" screen behind the cooled moderator (T = 78°K) is evidently associated with the rethermalization of the neutrons in the "thermal" beryllium and the great scattering cross section for cold neutrons at T = 300°K.

In order to examine the possibility of placing the cold-neutron generator directly in the reflector of the reactor, we measured the yield of cold neutrons obtained when the cold-neutron generator was placed tightly against the model of the active zone (without any reflector). In this case the intensity of the cold neutrons increased by approximately 25%. However, with this arrangement a thin film of water would be able to form between the outer surface of the cold-neutron generator and the end of the experimental channel in the reactor tank. In special measurements with the physical model, this layer was simulated by placing thin polyethylene plates after the cold-neutron generator along the neutron beam. The water-containing interlayers shaprly reduced the cold-neutron yield. Thus for a 2 mm thickness of the polyethylene

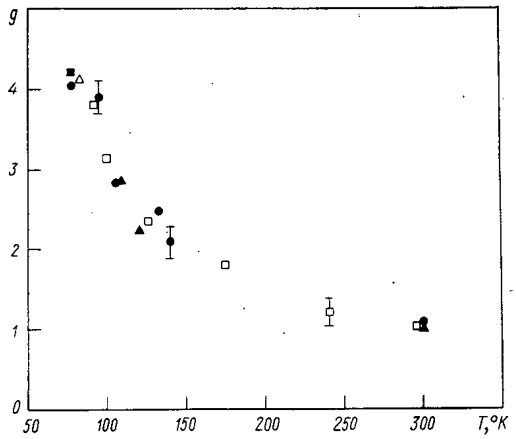

Fig. 3. Dependence of the cold-neutron yield on the moderator temperature T: ▲) C_2H_5OH; □) C_3H_6O; ●) C_6H_{14}.

plate the cold-neutron flux fell by more than a factor of two.

We see from the figures and Table 1 that the alcohols and saturated hydrocarbons cooled to the boiling point of liquid nitrogen provide approximately a fourfold, and water a threefold, increases in the cold-neutron flux. This increase occurs for a certain optimum thickness of the moderator, determined by the competition taking place between the thermilization and absorption of the neutrons in the moderator. For practical purposes it is thus better to use saturated hydrocarbons or mixtures of these, since their molecular compositions contain no oxygen, an element which may form highly-active compounds on irradiation. However, additional investigations into the radiation resistance of saturated hydrocarbons under reactor working conditions are required before making a final choice of material for the moderator.

In order to secure the maximum increase in cold-neutron flux it is essential to maintain the moderator temperature as close as possible (within some 3-5°) to the boiling point of liquid nitrogen, since in this region the temperature dependence of g(T) is very strong, as may readily be seen from Fig. 3 (a rise of 1° reduces the flux by about 1.2%). Under practical reactor conditions it is extremely important to reduce the temperature gradients in the moderator arising as a result of the fairly substantial radiative heat evolution.* The cooling of the moderator from the end surface facing the active zone provided for in the cold-neutron generator greatly increased the heat-release surface and reduced the temperature gradients. For the same purpose, additional aluminum fins occupying some 20% of the volume were introduced into the material of the moderator. Special measurements showed that a layer of liquid nitrogen in the path of the thermal-neutron beam and the additional aluminum fins in the volume of the moderator had hardly any effect on the cold-neutron yield for the optimum moderator thickness (30-40 mm). The installation of an additional beryllium screen cooled to T = 78°K should in principle increase the cold-neutron yield from the generator by some 10%. However, the use of such a screen in the actual reactor is clearly undesirable, since there would be a considerable increase in the consumption of liquid nitrogen for cooling the beryllium. The placing of the cold-neutron generator tightly against the active zone is also quite clearly undesirable in view of the much greater radiative heat evolution and the possible formation of water interlayers in the path of the cold-neutron beam, reducing the intensity of the latter.

In conclusion, the authors wish to thank Academician N.A. Dollezhal' for constant interest in the work and help in the investigations.

LITERATURE CITED

1. F. Webb, in: Optimization of Neutron Beams [Russian translation], Atomizdat, Moscow (1965), p.79.
2. H. Rauch and H. Schmidt, Atomkernenergie, 10, No. 7/8, 243 (1965).
3. P. Persson, J. Nucl. Energy, 21, No.9, 701 (1967).
4. W. Van Dingenen, Nucl. Instrum. and Methods, 16, No.1, 116 (1962).
5. E. Tunkelo and A. Palmgren, Nucl. Instrum. and Methods, 46, No.2, 266 (1967).
6. P. Ageron et al., Cryogenics, 9, No.1, 42 (1969).
7. C. Chen and R. Struss, Cryogenics, 9, No.2, 131 (1969).
8. B. N. Goshitskii et al., At. Energ., 25, No. 1, 21 (1968).
9. V.P. Gerasimenko et al., At. Energ., 31, No.1, 7 (1971).

*Preliminary measurements in the IVV-2 reactor [9] showed that the radiative heat evolution in the cold-neutron generator, on placing this behind one row of beryllium cassettes and a lead screen 20 mm thick, was approximately 0.5 W/cm^3.

RADIATION-INDUCED SWELLING OF 0Kh18N9T STEEL

V.N. Bykov, A.G. Vakhtin,
V.D. Dmitriev, L.G. Kostromin,
A.Ya. Ladygin, and V.I. Shcherbak

UDC 621.039.531:669.012.8

There have recently been a large number of papers devoted to the radiation-induced porosity of austenitic steels after irradiation in fast reactors and the ion beams of accelerators [1, 2]. The swelling of stainless steels of the 304 and 316 types has been studied the most fully. Information relating to the swelling of 0Kh18N9T steel is limited to data which have been obtained for particular temperatures and integrated doses [3]. In this paper we shall set out the results of an electron-microscope examination of radiation-induced porosity in 0Kh18N9T steel.

MATERIALS AND METHOD

The samples for electron-microscope examination were discs 3.5 mm in diameter and 0.4 mm thick cut from different fuel-element cans made of 0Kh18N9T steel and irradiated with integrated fluxes of up to $4.4 \cdot 10^{22}$ neutrons/cm^2 in the temperature range 430-590°C. The method of thinning the samples in a stream of electrolyte (60% H_3PO_4 + 40% H_2SO_4) was described in [4].

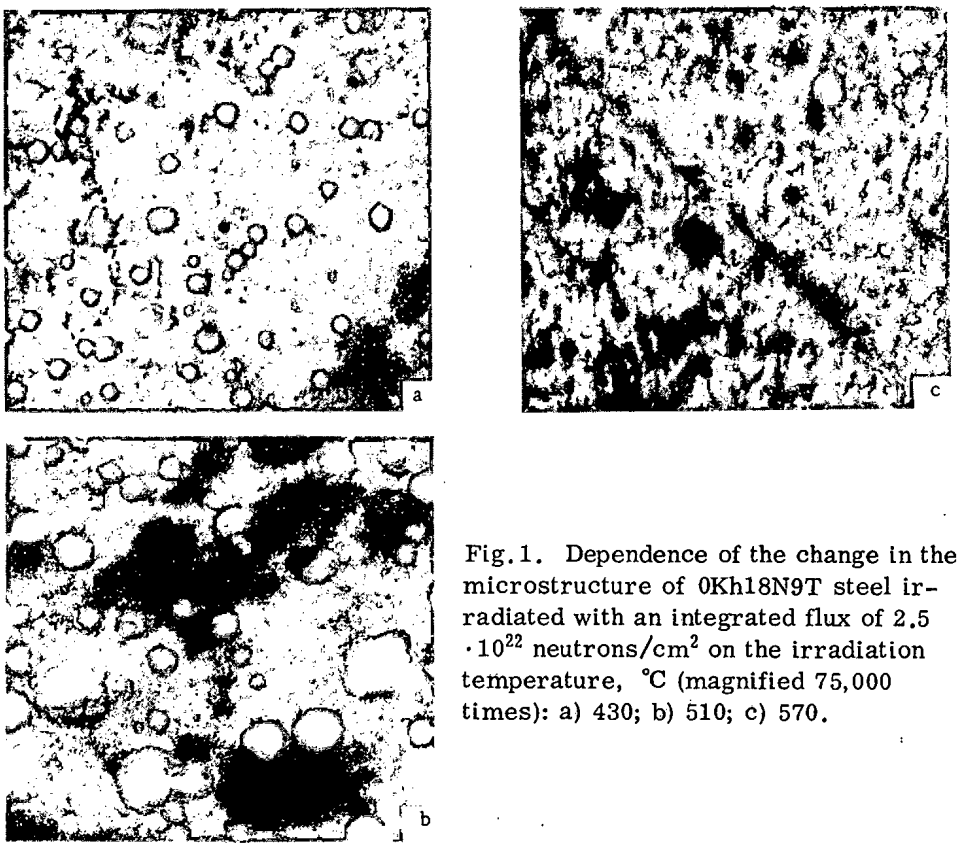

Fig. 1. Dependence of the change in the microstructure of 0Kh18N9T steel irradiated with an integrated flux of 2.5 $\cdot 10^{22}$ neutrons/cm^2 on the irradiation temperature, °C (magnified 75,000 times): a) 430; b) 510; c) 570.

Translated from Atomnaya Énergiya, Vol. 35, No. 4, pp. 235-237, October, 1973. Original article submitted January 8, 1973.

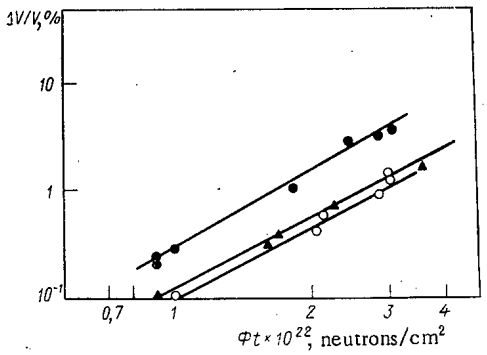

Fig. 2

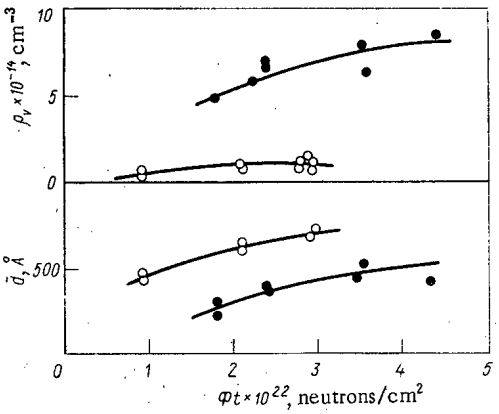

Fig. 3

Fig. 2. Dependence of the swelling of steel on the integrated flux at 460° (▲), 510° (●), and 530°C (○).

Fig. 3. Dependence of the mean diameter and concentration of the cavities in OKh-18N9T steel on the integrated flux at 460° (●) and 530°C (○).

The results were analyzed directly from the negatives using an instrumental microscope. The error in measuring the diameters of the cavities was 20 Å. The concentration of the cavities in the sample was determined by measuring not less than 600 cavities, the sample thickness being taken as 1500 Å. The total error in determining the swelling of the material was 50%; however, the spread in the values relative to the arithmetic mean was no greater than 20% for several measurements of the same sample.

Study of the Swelling of 0Kh18N9T Steel

As a result of the electron-microscope examination of the samples we found that the cavities were uniformly distributed over the main body of the grain, their concentrations and dimensions varying with the conditions of irradiation. Close to the grain boundaries there was a zone 1000 Å wide free from cavities and dislocation loops. The microstructure of some of the samples studied is shown in Fig. 1a, b, c.

Of the large number of experimental results here obtained we only used those required to plot the functional dependence of the swelling of 0Kh18N9T steel on the integrated dose and the temperature (Figs. 2-5). In the analysis we had to allow for the fact that the irradiation temperature only was known to an accuracy of ±30°C, and this clearly produced a spread in the experimental results for samples obtained from different fuel-element sheaths and cans. The spread may also be partly due to possible variations in the structure of the original material.

Some Laws Governing the Development of Radiation-Induced Porosity in 0Kh18N9T Steel

Dependence of the Swelling on the Integrated Dose. It is generally considered that the increase in the volume of material as a result of the formation of radiation-induced porosity $\Delta V/V$ is a function of the integrated flux Φt and not of the rate of creating point defects [1]. This relationship, which has been established by a number of authors, is described by a power function $\Delta V/V \sim (\Phi t)^n$; in the majority of cases $n = 1.6-1.8$ [1]. The dependence of $\Delta V/V$ on Φt for 0Kh18N9T steel (Fig. 2) also bears a power character with an index of $n = 1.7$, in agreement with the data relating to steels of the 304 and 316 types.

The total degree of swelling is of course determined by the concentration of the cavities ρ_V and the cavity size d. Figure 3 shows the dependence of ρ_V and d on Φt for 0Kh18N9T steel at 460 and 530°C. With increasing integrated flux there is a rise in the cavity concentration to 10^{15} cm^{-3}. This relationship may be closely approximated by a function $\rho_V \sim (\Phi t)^{2/3}$.

With increasing integrated dose the average diameter of the cavities $\bar{d}$ rises to 700 Å. The relationship in question may be approximately described by the function $d \sim (\Phi t)^{1/3}$. It should be noted that the rise in ρ_V and $\bar{d}$ with increasing Φt is in qualitative agreement with theoretical considerations relating to the swelling of materials [5].

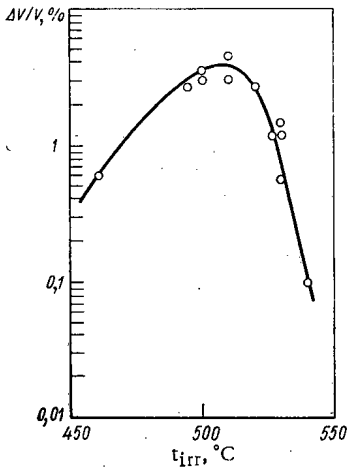

Fig. 4

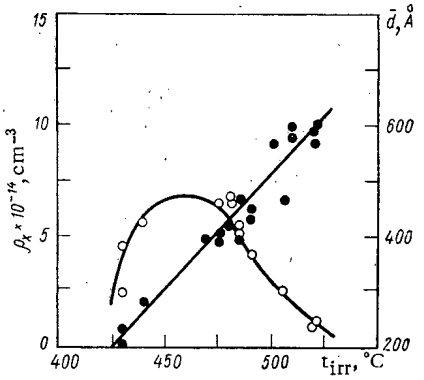

Fig. 5

Fig. 4. Dependence of the swelling of 0Kh18N9T steel irradiated with integrated fluxes of $3 \cdot 10^{22}$ neutrons/cm^2 on the irradiation temperature.

Fig. 5. Dependence of the mean diameter (●) and concentration (○) of the cavities in 0Kh18N9T steel irradiated with an integrated flux of $3 \cdot 10^{22}$ neutrons/cm^2 on the irradiation temperature.

Temperature Dependence of the Swelling. The temperature dependence of $\Delta V/V$ for 0Kh18N9T steel subject to an integrated radiation dose of $3 \cdot 10^{22}$ neutrons/cm^2 is shown in Fig. 4. With rising temperature (over the comparatively narrow temperature range of 430-550°C for the integrated fluxes studied) the swelling of the steel increases rapidly, reaching 3% at 510°C, after which it falls sharply. Figure 5 shows the way in which the concentration and mean diameter of the cavities vary with irradiation temperature for the same integrated doses. On increasing the temperature the size of the cavities increases almost linearly. It is well known that the size of the cavities is determined by the equilibrium concentration of vacancies formed as a result of the irradiation, N_V, and the self-diffusion coefficient D_V. According to [5], this relationship takes the form $d \sim (N_V D_V)^{1/2}$. With rising irradiation temperature and self-diffusion coefficient, the value of d may also increase, although the saturation of the matrix with point defects will diminish. The experimental data also indicate that the thermal dissociation of the cavities in the range of temperatures studied will certainly play a less important part. Harkness and Che-Yu Li [5] associate the temperature dependence of the cavity density with the rate of nucleation, which is proportional to the product of the difference in the diffusion fluxes of the point defects times the surface area of a critical nucleus, and to the concentration of these nuclei.

The supersaturation of the matrix with point defects diminishes with rising temperature. Hence on exceeding a certain temperature the rate of nucleation should fall, and this will lead to a reduction in cavity concentration.

It thus follows from the data presented that, on raising the irradiation temperature above 510°C, the decisive part in the swelling of 0Kh18N9T steel is played, not by the size of the cavities, but by their concentration. This result indicated that, although there may be a rise in the cavity-annealing rate with increasing temperature, yet nevertheless the mechanism associated with the fall in the rate of formation of critical nuclei would appear to be the more important. This is also indicated by the fact that the annealing of cavities in neutron-irradiated 0Kh18N9T steel only starts from temperatures above 800-900°C [3]. At the same time, no cavities are detected at temperatures of over 550°C in the irradiated steel. This difference can hardly be explained simply by virtue of the mechanism associated with the thermal dissociation of the cavities.

LITERATURE CITED

1. Proc. of Brit. Nucl. Energy Soc., European Conference on Voids Formed by Irradiation of Reactor Materials, Reading (1971).

2. Proc. of IAEA Symp. on Radiation Damage in Reactor Materials IAEA, Vienna, Vol. II (1969).
3. V.N. Bykov et al., At. Energ., 34, No. 4, 247 (1973).
4. G. Thomas, Electron Microscopy of Metals [Russian translation], IL (1963), p. 200.
5. S. Harkness et al., Nucl. Appl. and Technol., 7, 24 (1970).

RADIOLYSIS OF SOLUTIONS OF TBP IN CONTACT WITH NITRIC ACID

FORMATION OF RADIOLYSIS PRODUCTS OF THE EXTRACTION REAGENT

E.V. Barelko and I.P. Solyanina

UDC 541.15

One of the basic factors influencing the properties of an extraction system containing tributyl phosphate (TBP) as the extraction reagent, widely used in the technology of processing of nuclear fuel, is the radiation chemical decomposition of TBP with the formation of alkylphosphoric acid [1-3].

The radiolysis of individual TBP and its solutions in hydrocarbons of various compositions has been investigated in a number of studies [4-11]. It is known that an increase in the concentration of dibutyl phosphate (DBP) in the organic solution leads to a sharp increase in the distribution coefficient (K_d) of zirconium [12], when the latter is present in trace amounts. Analogous results were obtained in [10, 11] in an investigation of the radiolysis of solutions of TBP, where it was shown that the changes in K_d of zirconium depend on the nature of the diluent and are rather well correlated with the concentration of the DBP formed. Data on the radiolysis of TBP in contact with a solution of nitric acid containing zirconium and uranium nitrates were cited in [13].

Both in our studies and in other published studies, until recently the deterioration of the extraction characteristics was explained by the appearance of DBP. And yet it is clear that at sufficiently large doses of radiation, monobutyl phosphate (MBP) and phosphoric acid should also be accumulated in the system.

As was shown in [4, 8], in the radiolysis of individual TBP in the absence of an aqueous phase, the concentration of MBP is only 5-10% of the concentration of DBP. In the presence of an aqueous phase, in accord with the distribution coefficient [14], MBP should be accumulated primarily in it, and if we take into consideration the low radiation yield of MBP as well, it might seem that its influence on the extraction of zirconium should be minor. Nonetheless, there were indications of the participation of this compound in the process of extraction at relatively high concentrations of zirconium in solution [3].

In this work we discussed the formation of the basic radiolysis products of the extraction reagent – DBP, MBP, and H_3PO_4, "polymer" – and their influence on the extraction of zirconium when its concentration in solution is high.

The radiation source was ^{60}Co with an activity of the preparation equal to 200,000 gram radium equivalents. The dose was 20 W/liter, interval up to 0-100 W·h/liter. The doses were calculated according to the energy absorbed by the entire system. Irradiation was conducted in glass ampoules equipped with a mixer, supply lines for the passage of gas and collection of samples.

The ratio of the volumes of the organic and aqueous phases in the irradiated system was equal to 1:1. Composition of the phases: organic – 25% TBP + synthine; aqueous – 3 M HNO_3, 3 M $HNO_3 + 2 \cdot 10^{-2}$ $ZrO_2 \cdot (NO_3)_2$.

The experiments were conducted while bubbling oxygen through the solution under conditions of its equilibrium with air and a temperature of 18-20°C and in the presence of a "deficiency" of it, when oxygen was not bubbled through, but there was an atmosphere of air above the solution. It was shown that in this case, in the geometry of our experiments at doses ≥ 5 W·h/liter, the system was identical with deaerated systems with respect to the yield of the radiolysis products of TBP.

Translated from Atomnaya Énergiya, Vol.35, No.4, pp.239-243, October, 1973. Original article submitted February 8, 1973.

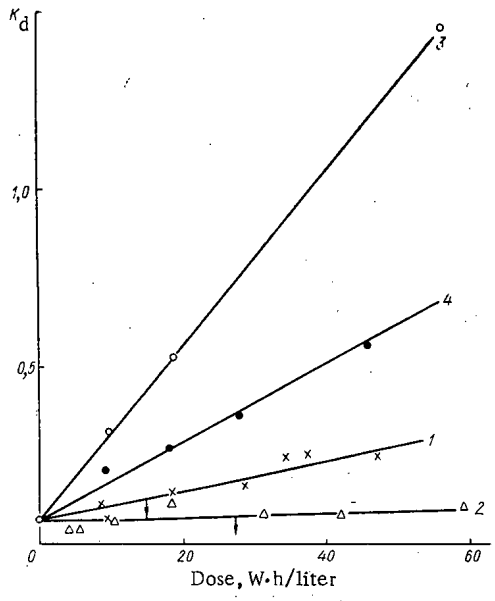

Fig. 1

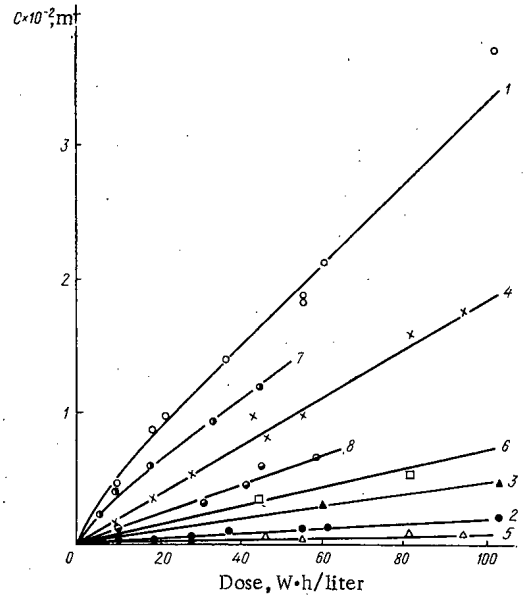

Fig. 2

Fig. 1. Dependence of the distribution coefficient of zirconium on the dose of irradiation. Irradiation in contact with a solution of 3M HNO_3 + $2 \cdot 10^{-2}$ M $ZrO_2(NO_3)_3$: 1 (×) in an atmosphere of O_2; 2 (△) in the presence of an O_2 deficiency in the system. Irradiation in contact with 3 M HNO_3 not containing Zr salt; 3 (○) in an atmosphere of O_2; 4 (●) in the presence of an O_2 deficiency in the system.

Fig. 2. Dependence of the DBP and polymer concentration on the dose of irradiation. Irradiation in contact with 3 M HNO_3: 1 (○), 4 (×) DBP in the organic phase; 2 (●), 5 (△) DBP in the aqueous phase; 3 (△), 6 (□) polymer [1-3) atmosphere solution of O_2; 4-6) deficiency of O_2 in the system]. Irradiation in contact with a solution of 3 M HNO_3 + $2 \cdot 10^{-2}$ M $ZrO_2(NO_3)_2$; 7 (◑) DBP in the organic phase in an atmosphere of O_2; 8 (◒) DBP in the organic phase under conditions of O_2 deficiency in the system.

TBP was freed of traces of acid esters by shaking with a 5% solution of potash, then redistilled at a pressure of 1 mm Hg and a temperature of 125°C. Purified oleum and synthine redistilled under vacuum were used as diluents.

The content of DBP, MBP, and H_3PO_4* was determined with the aid of the method described in [8], using colorimetric determination of the "blue" complex of phosphates with ammonium molybdate [15]. The "polymer" was determined by the method of distilling off the irradiated organic solvent [4]. A solution of zirconium with a concentration of $2 \cdot 10^{-2}$ M was prepared from ^{91}Zr nitrate, labeled with ^{96}Zr [16].

Figure 1 presents the change in the distribution coefficient of zirconium as a function of the dose in the case of radiolysis in an atmosphere of O_2 and under conditions of a deficiency of it in the irradiated system (curves 1, 2). In these experiments the formation of suspensions in the aqueous phase was detected. In Fig. 1 the doses at which the appearance of a precipitate was observed are marked by arrows. In the case of radiolysis in an atmosphere of oxygen, the precipitate appeared at doses of 15-20 W·h/liter, while in the case of an oxygen deficiency it appeared at doses of 25-30 W·h/liter. With increasing dose, the volume of the precipitate forming increased, and the zirconium content in it increased (at a dose of 50-60 W·h/liter it was 15-20% of the total zirconium content). When uranium was introduced into the aqueous phase with a concentration of 200 g/liter (with respect to the metal), in the case of irradiation of the solution in the dose range 15-170 W·h/liter, no formation of suspensions was observed.

Since the radiolysis products of synthine had no appreciable influence on K_d of zirconium and the state of the phases in the case of radiolysis at the stage of extraction [17], the observed changes can be attributed to the action of the radiolysis products of TBP. This is evidenced by experiments conducted so that there was less MBP in the organic phase. In the case of contact of a nonirradiated nitric acid solution of a

* Only the joint determination of MBP and H_3PO_4 is possible according to this method.

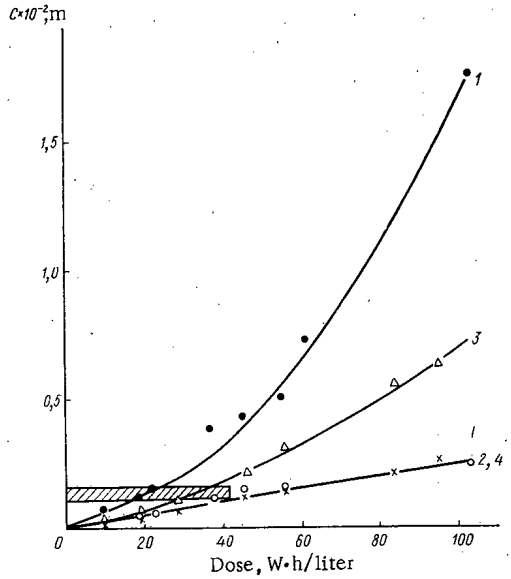

Fig. 3

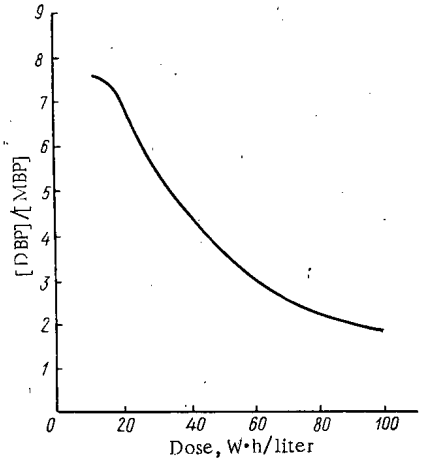

Fig. 4

Fig. 3. Dependence of the concentration of MBP and H_3PO_4 on the dose of irradiation. Atmosphere of O_2: 1 (●) aqueous phase; 2 (×) organic phase. Deficiency of O_2 in the system: 3 (Δ) aqueous phase; 4 (○) organic phase.

Fig. 4. Dependence of the ratio G_{DBP}/G_{MBP} on the dose in radiolysis of an atmosphere of O_2.

zirconium salt with an organic phase, preliminarily irradiated with 3 M HNO_3, into which the radiolytically formed MBP was transferred, higher values of K_d of zirconium are achieved (see Fig. 1, curves 3 and 4), while appreciable appearance of a precipitate is recorded at doses of 50-60 W·h/liter. These experiments showed that the formation of MBP substantially influences the extraction of zirconium.

We studied the formation of DBP, MBP + H_3PO_4, and the "polymer" as a function of the dose. The dependence of the concentration in the indicated products on the dose, obtained under conditions of oxygen deficiency in the system and in the case of its passage through the solution, is presented in Figs. 2 and 3. The distribution coefficients of the DBP and MBP formed during radiolysis, calculated from these data, are close in order of magnitude to the results obtained in model experiments in the absence of radiation [14].

In the case of radiolysis under conditions of oxygen deficiency, the yield of DBP is 0.4-0.5 molecules /100 eV. In an atmosphere of oxygen, the initial yield of DBP reaches 1.2 molecules/100 eV and as the dose is increased, it drops to 0.9 molecule/100 eV.

The rate of formation of MBP in the presence of O_2 is also higher, and when the dose increases, in contrast to DBP, it does not drop, but increases. Figure 4 shows the change in the ratio of the yields of DBP to MBP as a function of the dose in the case of irradiation in an atmosphere of oxygen. Up to a dose of 10-15 W·h/liter, the ratio G_{DBP}/G_{MBP} = 7-8; when the dose is further increased, it drops, and at doses of the order of 100 W·h/liter reaches 2-2.5.

To evaluate the yield and the origin of the "polymer," we studied its nature and chemical composition.

The elementary composition of the polymer corresponds to the atomic ratio P: C: O: H = 1: 13.4: 4.4 : 29, which is close to the ratio of the elements in TBP itself and confirms the hypothesis of a phosphate composition of the polymer [4, 6]; however, this contradicts the hypothesis of [7, 18] of its hydrocarbon structure. The presence of a P – C – O group in the polymer was also indicated by the absorption band at 1025 cm^{-1} that we detected in its IR spectrum [19]. In a calculation of the corresponding yield of the decomposition of TBP, due to the channel of "polymer" formation, we believe, assuming its molecular weight equal to 840 [4], that three molecules of TBP correspond to the formation of one molecule of the polymer. In Fig. 2 (curves 3 and 6) the concentration of the polymer was calculated on the basis of the molecular

TABLE 1. Composition of Precipitate

Dose, W·h/liter	Concentration $\cdot 10^{-3}$, M						
	Zr, precipitated	DBP				MBP (precipitated	ratio Zr: DBP: MBP in precipitate
		organic phase		aqueous phase	precipitated		
		irradiation without Zr	irradiation with Zr				
18,6	1,6	8	5,9	0,4	1,7	1,2	1 : 1,1 : 0,8
37,4	3,1	14	9,2	1	3,8	3,0	1 : 1,2 : 1
46,0	4	17,8	11,8	1	5,0	4,0	1 : 1,25 : 1

weight indicated above. In contact with the aqueous phase, in the presence of an O_2 deficiency, the value of G of the "polymer" calculated according to the number of molecules of TBP consumed, is equal to 0.5-0.6 molecule/100 eV; in the presence of O_2 this value is 1.5-2 times lower. These results agree with the data for the same systems irradiated in the absence of the aqueous phase.

New experimental results, which require explanation, are the acceleration of the formation of MBP with increasing dose in the presence of an aqueous phase. It was established that this acceleration is correlated with the drop in the yield of DBP. Within the limits of the experimental error it can be considered, for example, that when the yield of DBP decreases (in experiments in the presence of O_2) from 1.2 to 0.9 molecule/100 eV, the yield of MBP increases from 0.14 to 0.45 molecule/100 eV and, consequently, an acceleration of MBP formation occurs on account of the decomposition of DBP.

In principle the presence of an aqueous phase can have an influence on the radiolysis of the system: either as a result of the elimination of MBP from the organic phase or on account of the extraction of DBP into the aqueous phase, where its molecules are subject to the influence of active intermediate radiolysis products of water. The first factor cannot be significant, although the aqueous phase actually effectively extracts MBP, since not a slowdown of MBP formation, but an acceleration of the decomposition of DBP is observed. The second of the indicated factors is more applicable. Actually, since it is difficult to assume that DBP was decomposed in the organic phase in the presence of an approximately 100-fold excess of TBP on account of the accepting of active particles in an indirect influence,* the role of the aqueous phase in this process may be decisive (all the more in that in the absence of an aqueous phase, no increase in the yield of MBP was noted).

Actually, although at equilibrium only ~1/20 of the amount of DBP should be observed in the aqueous phase, nonetheless, at doses when the decrease in the yield of DBP becomes appreciable, its absolute concentration in the aqueous phase reaches ~10^{-3} M (see Fig. 2, curves 2 and 5), while under conditions when the concentration of other acceptors is appreciably lower, DBP may decompose on account of the indirect action of active radiolysis products of water.

Evidently we should consider the oxidative component, which agrees with the conclusions of [20], since the reductive component should be effectively accepted by HNO_3, present in solution in excess. It can be expected that when the doses are further increased, and, correspondingly, with increasing concentration of DBP in the aqueous phase, the yield of MBP will increase even more. Thus, an explanation for the influence of oxygen, especially sharply manifested in two-phase systems, should evidently be sought in analogies with other processes in which an increase in the content of molecular oxygen promotes processes that proceed through accepting of the reductive component of radiolysis of water [21].

At the first of the experimental results discussed above, we indicated the formation of a precipitate in systems containing sufficiently high concentrations of zirconium, and the role of monobutyl phosphate in this process. It is known that in the absence of neutral phosphates, dialkylphosphoric acids form a precipitate with concentrated solutions of zirconium [21, 22]. However, it was found that in model mixtures containing TBP, in the absence of MBP no precipitate is formed.

We also determined the interval of MBP (H_3PO_4) concentrations within which zirconium in a concentration of 10^{-2} M begins to precipitate on model mixtures. It is shown in the form of a band in Fig. 3, which presents the kinetic curves of the formation of MBP (H_3PO_4) during radiolysis. The point of intersection of the curves with this band corresponds to the value of the dose at which the precipitate should be formed. These results are in good agreement with the data of visual observations.

*According to the data of [4], the value of G of DBP from TBP is approximately only 1.5 times lower in comparison with G of MBP from DBP.

Since, however, it was also discovered that when a system is irradiated in the presence of zirconium there is less DBP in the organic phase (see Fig. 2, curves 7 and 8) then it follows from the data on radiolysis in the absence of zirconium (see Fig. 2, curves 1 and 4), in a consideration of the composition of the precipitate, we also considered DBP.

These results are confirmed by the decrease in the distribution coefficient of DBP in model experiments conducted with mixtures of DBP and MBP in the organic phase in contact with a nitric acid solution of zirconium. On the basis of the results obtained, we suggested that the DBP removed from the organic phase, as well as all of the MBP formed during radiolysis, are components of the precipitate.

Table 1 presents data according to which we calculated the molar ratios of the components contained in the precipitate. Analogous ratios of the components were obtained at the same concentrations of DBP, MBP, and zirconium in a model experiment.

LITERATURE CITED

1. J. Goode, Nucleonics, 15, No. 2, 68 (1957).
2. A. Bathelier, Bull. Docum. et Inform. Sci. and Technol., 127, 35 (1968).
3. G. Lefort and P. Miquel, ibid., p. 43.
4. L. Wagner et al., Indstr. and Engng. Chem., 51, 45 (1959).
5. L. Burger and E. MacClanachan, Indstr. and Engng. Chem., 50, 159 (1958).
6. J. Burr, Radiation Res., 8, 214 (1958).
7. V.P. Shvedov and S.N. Rosyanov, Zh. Fiz. Khim., 35, 561 (1961).
8. R. Wilkinson and T. Williams, J. Amer. Chem. Soc., 4, 4098 (1961).
9. J. Canva and M. Page, Radiochim. Acta, 4, 88 (1965).
10. E.V. Barelko, I.P. Solyanina, and Z.N. Tsvetkova, At. Energ., 21, 281 (1966).
11. E.V. Barelko, I.P. Solyanina, and Z.N. Tsvetkova, Khim. Vys. Energ., 4, 229 (1970).
12. V.B. Shevchenko and V.S. Smelov, in: Extraction [in Russian], Vol. 2, Gosatomizdat, Moscow (1962), p. 257.
13. A. Huggard and B. Warner, Nucl. Sci. and Engng., 17, 638 (1963).
14. A.P. Ilozhev, I.V. Poddubskaya, and A.M. Rozen, Sm. [12], 71.
15. A.S. Solovkin, P.G. Krutikov, and A.N. Panteleeva, Zh. Neorg. Khim., 24, 3376.
16. R.I. Shamaev, Radiokhimiya, 10, 479 (1968).
17. I.P. Solyanina and E.V. Barelko, At. Energ., 32, 395 (1972).
18. A.A. Vashman, Radiokhimiya, 12, No. 1, 12 (1970).
19. L. Bellamy, Infrared Spectra of Complex Molecules [Russian translation], IL, Moscow (1963).
20. C. Sonntag et al., Z. Naturforsch, 276, 471 (1972).
21. I.V. Vereshchinskii and A.K. Pikaev, Introduction to Radiation Chemistry [in Russian], Izd-vo AN SSSR, Moscow (1963).
22. V.V. Fomin and S.A. Potapova, Zh. Neorg. Khim., 12, 530 (1967).

AGING OF IMPREGNATED CARBONS FOR TRAPPING RADIOACTIVE IODINE

I.E. Nakhutin, N.M. Smirnova,
G.A. Loshakov, and V.N. Vezirov

UDC 628.543

Impregnated carbons are fairly widely used to remove radioactive iodine and its compounds from gases, both in continuous extraction apparatus and in devices for operation in an emergency. However, little work has been done on the so-called aging of impregnated carbons (in this article, we shall understand this term to mean a loss of efficiency with respect to methyl iodide). One difficulty of this type of research is the long time required for aging experiments.

In this article we give some results obtained in an investigation of aging of impregnated carbons in a current of ordinary atmospheric air. We used carbons impregnated with PbI_2, CuI, and AgI [1], since no information was available on the aging of these compounds.

EXPERIMENTAL METHOD

We investigated three columns, each of which contained one of the above impregnated carbons. The columns were connected in parallel, and equal linear gas flow rates were maintained in all three. They were divided into 1 cm sections. Transfer of dust between sections was prevented by aerosol filters. The activity of ^{131}I in each section was measured by means of a scintillation-type γ-ray counter with a collimator.

Dust-free atmospheric air was passed through the column for a long time (with interruptions at night); the absorptive capacity of the column was then measured section by section. For this purpose, every 48 h, radioactive methyl iodide was briefly passed through the column in a mixture with air, and the activity of each section was then measured. To accelerate aging, the experiment was performed at high gas flow rates (up to 120 cm/sec). It was assumed that aging does not depend on time as such or on the quantity of air passing through the carbon. As we shall show, this assumption is adequately justified.

After the first measurement we continued to pass air, and made the last measurement when the ^{131}I accumulated in the columns had practically completely decayed.

RESULTS AND DISCUSSION

Instead of the usual monotonically falling curve, the distribution of gamma activity along all three columns shows a curve with a clearly-marked maximum. This means that the earlier sections have reduced absorptive capacity. As the amount of air passed increases, the maxima on the curves shift further from the initial sections of the columns towards the outlets.

Figure 1 plots the absorptive capacity of the first section of the PbI_2 column vs the amount of air which has been passed. After passage of $8 \cdot 10^5$ liters/cm^2 of air, the absorptive capacity of the first section was reduced by 60%. In the second section, the reduction in similar conditions was 46%, and in the third section, 26%. This phenomenon cannot be attributed to erosion by the gas current, because we should then expect to find uniform changes along the whole column. It is natural to suppose that the air contains some sort of impurities which are absorbed in the column and which reduce the absorptive capacity of the carbon for methyl iodide. These impurities move along the column in the form of a chromatographic front.

Translated from Atomnaya Énergiya, Vol.35, No.4, pp.245-246, October, 1973. Original article submitted November 9, 1972.

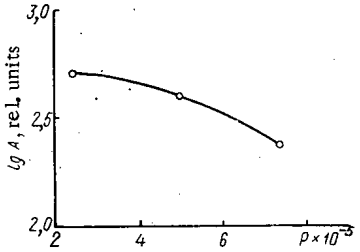

Fig. 1. Absorptive capacity A of first section of column containing PbI_2 vs quantity of air passed, P.

The very slow movement of the distribution curve maximum along the column (only 6-7 cm in the course of the entire experiment) shows that the impurity is present in the air in very small amounts.

On the basis of the above data, the observed effect of change in the absorptive capacity can be quite confidently attributed to poisoning of the impregnated carbons.

Similar results on poisoning of impregnated carbons were obtained by Acklej and Adams [2]. However, they used carbons with different impregnating agents, and therefore only a qualitative comparison can be made with our results. They also observed a change in the purification efficiency; the change was greater in the first layer of impregnated carbon than in the second. These observations are also consistent with the hypothesis that harmful microimpurities are absorbed from the air.

Substances which might cause this effect include oxides of nitrogen which are always present in air in small amounts. It is known that they react with iodides of metals forming nitroso compounds. For example, complete neutralization of the lead iodide in one section of the column requires about 5 mg of nitrogen peroxide, which agrees with the quantity of nitrogen peroxide in the air passed through the column, i.e., $2.5 \cdot 10^{-5}\%$. This figure is of the same order of magnitude as the nitrogen oxides contained in atmospheric air $(1.5\text{-}2.9) \cdot 10^{-5}\%$ [3].

Account must also be taken of the influence of SO_2 and SO_3 which are always present in the air, especially in large towns. These substances can also poison impregnated carbons by reacting with iodides.

Regardless of the cause of the aging, these values can give some idea of the service lives of impregnated carbons in a current of atmospheric air.

The amounts of oxides of nitrogen and other microimpurities in gaseous discharges from nuclear power stations may differ markedly from the amounts in atmospheric air. In particular there may be radiation synthesis of oxides of nitrogen in the air. This process is the subject of additional investigation. However, even from the data at present available, we can conclude that the service life of impregnated carbons is shorter than that of nonimpregnated carbons, which are also used to remove iodine.

Impregnated carbons are sensitive to microimpurities and other chemically-active substances in the gas phase, and therefore their service lives in different purification apparatus may be very varied.

Thus we can draw the following conclusions. The absorptive capacities of carbons impregnated with PbI_2, CuI, and AgI towards methyl iodide decrease after prolonged passage of a current of atmospheric air through a layer of the carbon. This is due to microimpurities contained in atmospheric air which act on the impregnants: this is confirmed by the nature of the variation of absorptive capacity.

LITERATURE CITED

1. I.E. Nakhutin et al., Fourth Geneva Conference (1971), report 49/P/703 (USSR).
2. R. Acklej and R. Adams, Tenth AEC Air Cleaning Conference, New York (1968).
3. A. Altschuller, Anal. Chem., 41, No. 5 (1969).

INSTRUMENTAL NEUTRON ACTIVATION ANALYSIS OF ROCKS AND ROCK-FORMING MINERALS BY USING Ge(Li) DETECTORS AND A COMPUTER

E.M. Lobanov, Yu.A. Levushkin, and S.P. Vlasyuga

UDC 543.53:539.107.5

The practical and theoretical necessity of more complete knowledge of the chemical elements in natural formations and the widespread introduction of mathematical statistics methods and the interpretation of the results of geochemical research [1, 2] require increasing the sensitivity and accuracy of analytic procedures [3]. In this respect the most reliable and promising is neutron activation analysis [4]. The simultaneous determination of several elements in a single specimen and the elimination of contamination of the samples in the instrumental version of neutron activation analysis permit the preservation of the similarity of the natural ratios of chemical elements in the objects being studied [5].

The use of Ge(Li) detectors, which have a resolving power an order of magnitude larger than that of sodium iodide scintillization crystals, in an instrumental version of neutron activation analysis of geological objects offers the best solution of the problem of the simultaneous determination of a large group of chemical elements contained in the specimen without destroying it. Gordon et al. [6] determined the elemental composition of the US geological standards by an instrumental method of neutron activation analysis using Ge(Li) detectors.

We present the results of our practical procedure of instrumental neutron activation analysis for the simultaneous determination of several chemical elements in rocks and basic rock-forming minerals.

Gross samples of rocks (granitoids) and basic rock-forming minerals (plagioclase, potassium feldspars, biotites, muscovites, and quartzes) extracted from them were selected for analysis. Five-hundred mg test specimens, crushed to pass through a 200 mesh screen, were packed in aluminum foil with standards and monitors and irradiated in a reactor by a flux of $1.8 \cdot 10^{13}$ neutrons/cm^2 sec for 10 h.

The γ-spectra of the irradiated specimens, kept for 8-30 days, were measured on a γ-spectrometer consisting of a coaxial Ge(Li) detector, a high-performance stabilization circuit, and an Ai-4096 pulse-height analyzer. The detectors had volumes of 8.5, 10.5, 25.5, and 50.5 cm^3, and their resolutions at the Cs^{137} photopeak (E_γ = 661.65 keV) were 0.59, 0.74, 0.95, and 1.48%, respectively.

Figure 1 shows a typical γ-spectrum of plagioclase measured on the spectrometer with a Ge(Li) detector. The large volume and the complexity of the information contained in the spectral measurements require a new methodical approach to the processing of spectrometric data [7-17]. It is practically impossible to extract all the information from the spectra without using a computer.

We present below a brief description of a program for the computer processing of γ-spectra measured with Ge(Li) detectors in an instrumental neutron activation analysis of geological samples.

The spectra were analyzed in four stages: 1) preparation of the initial data for the calculation; 2) search in the γ-spectrum of regions containing single photopeaks or groups of closely spaced peaks; 3) tabulation of the photopeaks found in the spectrum and the calculation of their energies and intensities; 4) identification of the isotopes in the spectrum and the calculation of the amounts of the chemical elements in the spectrum.

Translated from Atomnaya Énergiya, Vol.35, No.4, pp.247-252, October, 1973. Original article submitted November 23, 1972.

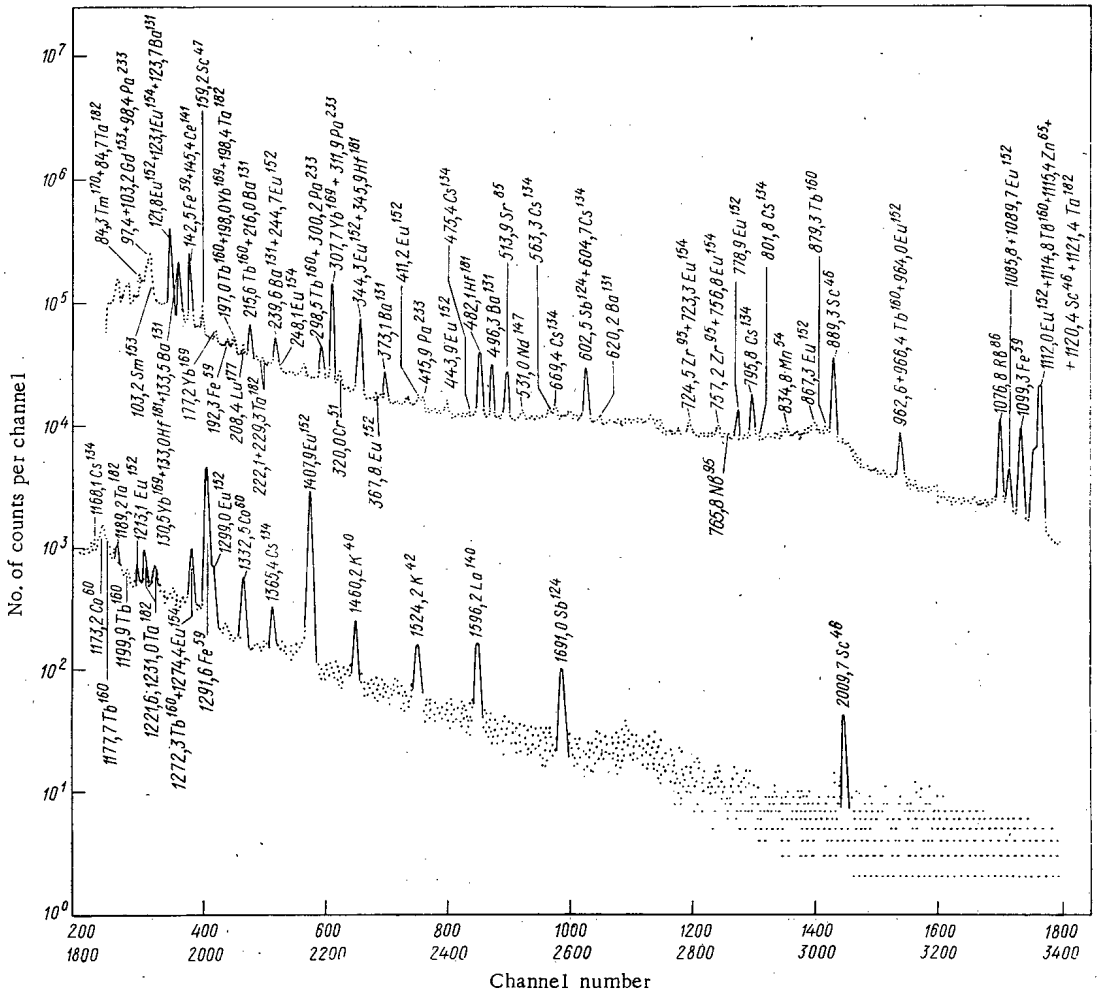

Fig. 1. Typical γ-spectrum of plagioclase measured on a spectrometer with a 10.5 cm^3 semiconductor Ge (Li) detector.

The catalog of standard data includes: E_{rkl}, the energies of photopeaks in the spectra of the standard isotopes (k = 1-32 is the index of the isotope: l = 1-15 is the index of the photopeak of the given isotope); S_{rkl}, the intensities of the photopeaks in the spectra of the standard isotopes; ΔS_{rkl}, the errors in the values of the intensities of the photopeaks; η_k, the shielding factors of the elements in the specimen during irradiation; m_k, the masses of the standards; $T^k_{1/2}$, the half-lives of the standard isotopes; $\Delta T^k_{1/2}$, the errors in the values of the half-lives; I^s_m, the intensity of the photopeak of the monitoring isotope irradiated with the standards.

The constants used in the analysis of the γ-spectrum of a specimen are: E^ξ_γ, the values of the energies of the reference photopeaks in the spectrum of a specimen for calculating the coefficients of internal energy calibration of the spectrum (ξ = 1-16); x^ξ, the approximate values of the centers of the reference photopeaks in the spectrum of the specimen; Δx^ξ, the limiting deviations from the approximate values of the centers of the reference photopeaks for identification of internal references of the energy calibration of the spectrum; α and β, coefficients for scaling the γ-spectrum of the specimen to take account of the dead time of the spectrometer; φ, a coefficient for scaling the intensities of the photopeaks to take account of the geometry of the measurement; K_ω, coefficients for calculating the smoothed out spectrum of the specimen (ω = 0-4); F_ω, coefficients for calculating the spectrum of first derivatives (ω = (0-3); ν_0 and ν_1, coefficients describing the dependence of the resolution of the detector on the γ-energy.

Control numbers which are fed into one computer with the γ-spectrum of the specimen are T_{cool}, the "cooling" time of the specimen; T_{meas}, the time the γ-spectrum was measured; m_0, the mass of the specimen, Z_j, the photopeak of the monitoring isotope irradiated with the specimen (j = 1-32 is the channel number), h, the geometry factor of the measurement.

Block diagram of the program:

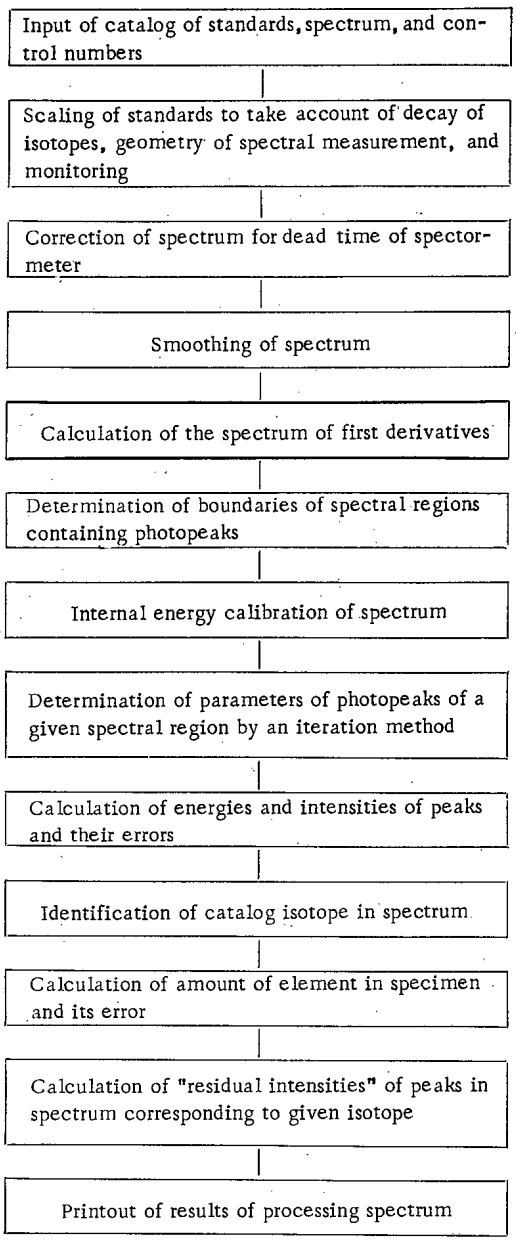

The catalog of standard data and constants, the initial γ-spectrum of the specimen y_i^{in} ($i = 1$–3200 is the channel number in the spectrum), and the control numbers are fed into the computer with punchcards or magnetic tape. The standard data are modified to correspond to the irradiation and cooling of the specimen and the measurement of its γ-spectrum. The processed γ-spectrum is smoothed by the method of least squares using nine adjacent channels with a second degree parabola approximation [18, 19]:

$$y_i^{in} = \left(\sum_{\omega=0}^{4} K_\omega\right)^{-1} \left\{\sum_{\omega=0}^{4} K_\omega (y_{i+\omega} + y_{i-\omega})\right\}. \quad (1)$$

The results of the smoothing are used to calculate the spectrum of first derivatives:

$$\delta_i = F_0 \sum_{\omega=1}^{3} F_\omega (y_{i+\omega}^{cr} - y_{i-\omega}^{in}). \quad (2)$$

Preliminary values of the centers m_γ of the photopeaks in the spectrum and their boundaries n_γ are determined by the changes in sign of the first derivative [11, 18, 20]:

$$i = \begin{cases} m_\gamma, & \text{if} \quad \delta_i > 0, \ \delta_{i+1} < 0; \\ n_\gamma, & \text{if} \quad \delta_i < 0, \ \delta_{i+1} > 0. \end{cases} \quad (3)$$

The values found for the centers of the peaks are used in the identification of the reference photopeaks for internal energy calibration of the spectrum. A search is carried out among the values of the m_γ given in the catalog of constants of reference photopeaks with centers in channels x^ξ corresponding to energies E_γ^ξ. The values of m_γ satisfying the condition

$$|m_\gamma - x^\xi| < \Delta x^\xi, \tag{4}$$

and the corresponding values of the energies of the reference photopeaks E_γ are used to determine the coefficients a, b, c, d, and f in the calibration relation

$$E_\gamma = ax^4 + bx^3 + cx^2 + dx + f. \tag{5}$$

The pseudopeaks not statistically represented in the spectrum are eliminated by using the inequality

$$y(m_\gamma) - y(n_\gamma) < \varepsilon \sqrt{y(n_\gamma)}, \tag{6}$$

where $y(m_\gamma)$ is the value of the spectrum at the center of the photopeak; $y(n_\gamma)$ is the value of the spectrum at the left boundary point of the peak. The value of the coefficient ε is determined by the value of the confidence interval. The values of the centers of closely spaced peaks in the spectrum are combined into groups. Twice the width of the peaks at half-height is taken as a criterion of closeness of neighboring peaks with centers in channels m_γ and m_{r+1}. This is a function of the γ-energy:

$$m_\gamma - m_{\gamma+1} < 2\sigma(E_\gamma). \tag{7}$$

The boundaries of a spectral region containing several photopeaks are determined by the boundary channels of the outside peaks.

The expression [9]

$$y_i = Ai + B + \sum_{p=1}^{4} R_p \exp\{-4 \ln 2 (i - x_p)^2 \sigma_p^{-2}\} \tag{8}$$

is a mathematical model of a spectral region with photopeaks. The initial values of the parameters A and B are calculated as coefficients of the straight line passing through the boundary points of the region. To determine the initial values of the centers x_p of the photopeaks the values of the energies $E_{\gamma kl}$ from the catalog of standard data are converted to the values of the channels of the spectrum by Eq. (5), after which a search is carried out among the values thus obtained which fall in the given spectral region. The initial value of the width of the photopeak at half-height σ_p is determined by using the given dependence of this quantity on the γ-energy:

$$\sigma_p = \nu_0 + \nu_1 E_\gamma(x_p). \tag{9}$$

The initial value of the height of the photopeak R_p is calculated by the formula

$$R_p = y(x_p) - (Ax_p + B). \tag{10}$$

A value of the height R_p which does not satisfy the condition

$$R_p > \varepsilon \sqrt{Ax_p + B}, \tag{11}$$

is eliminated from the parameters of the spectrum along with the corresponding values of x_p and σ_p.

The parameters of the photopeaks x_p, R_p, and σ_p are refined by the method of nonlinear least squares [9]. The result is achieved in a prescribed number of iterations. After each iteration the refined parameters are analyzed and the incorrect values are eliminated from the calculation. The refined values of the parameters of a photopeak are used to calculate its energy by Eq. (5) and its intensity by

$$S_\gamma = \sum_i R \exp\{-4 \ln 2 (i - x)^2 \sigma_p^{-2}\}. \tag{12}$$

The error in the values of the intensity is given by

$$\Delta S_\gamma = \left\{ \sum_{j=1}^{3} \left(\frac{\partial S_\gamma}{\partial \omega_j} \right) \operatorname{var} \omega_j + \sum_{j=1}^{3} \sum_{\substack{k=1, \\ k \neq 1}}^{3} \left(\frac{\partial S_j}{\partial \omega_j} \right) \left(\frac{\partial S_j}{\partial \omega_k} \right) \operatorname{covar} (\omega_j \omega_k) \right\}^{1/2}, \tag{13}$$

where $\omega_1 = R$, $\omega_2 = x$, and $\omega_3 = \sigma$.

TABLE 1. Sensitivity (in wt. %) of the Simultaneous Determination of the Chemical Elements in Various Geological Objects by Instrumental Neutron Activation Analysis Using Semiconductor Ge(Li) Detectors and a Computer

Element	Radioisotope	Granitoids		Plagioclase		Potassium feldspars		Biotites		Quartzes		Muscovites	
		A	B	A	B	A	B	A	B	A	B	A	B
Sc	^{46}Sc	$6{,}3\cdot10^{-6}$	$1{,}2\cdot10^{-6}$	$5{,}4\cdot10^{-7}$	$1{,}0\cdot10^{-7}$	$6{,}0\cdot10^{-7}$	$1{,}1\cdot10^{-7}$	$1{,}1\cdot10^{-5}$	$2{,}2\cdot10^{-6}$	$4{,}1\cdot10^{-7}$	$7{,}8\cdot10^{-8}$	$2{,}1\cdot10^{-5}$	$3.9\cdot10^{-6}$
Cr	^{51}Cr	$3{,}4\cdot10^{-4}$	$9{,}4\cdot10^{-5}$	$1{,}6\cdot10^{-4}$	$4{,}4\cdot10^{-5}$	$2{,}7\cdot10^{-4}$	$7{,}3\cdot10^{-5}$	$2{,}0\cdot10^{-3}$	$5{,}4\cdot10^{-4}$	$1{,}3\cdot10^{-4}$	$3{,}6\cdot10^{-5}$	$5{,}4\cdot10^{-3}$	$1{,}5\cdot10^{-3}$
Fe	^{59}Fe	$2{,}4\cdot10^{-4}$	$4{,}2\cdot10^{-5}$	$1{,}1\cdot10^{-2}$	$2{,}0\cdot10^{-3}$	$9{,}3\cdot10^{-4}$	$1{,}7\cdot10^{-4}$	$2{,}0\cdot10^{-1}$	$3{,}6\cdot10^{-2}$	$9{,}3\cdot10^{-3}$	$1{,}7\cdot10^{-3}$	$2{,}7\cdot10^{-1}$	$5{,}1\cdot10^{-2}$
Co	^{60}Co	$2{,}1\cdot10^{-5}$	$3{,}4\cdot10^{-6}$	$7{,}4\cdot10^{-6}$	$1{,}2\cdot10^{-6}$	$7{,}6\cdot10^{-6}$	$1{,}3\cdot10^{-6}$	$1{,}5\cdot10^{-4}$	$2{,}4\cdot10^{-5}$	$6{,}1\cdot10^{-6}$	$1{,}0\cdot10^{-6}$	$2{,}0\cdot10^{-4}$	$3{,}2\cdot10^{-5}$
Zn	^{65}Zn	$7{,}3\cdot10^{-4}$	$1{,}3\cdot10^{-4}$	$2{,}3\cdot10^{-4}$	$4{,}1\cdot10^{-5}$	$2{,}2\cdot10^{-4}$	$4{,}0\cdot10^{-5}$	$1{,}8\cdot10^{-3}$	$3{,}2\cdot10^{-4}$	$1{,}6\cdot10^{-4}$	$2{,}9\cdot10^{-5}$	$6{,}2\cdot10^{-3}$	$1{,}1\cdot10^{-4}$
Rb	^{86}Rb	$6{,}5\cdot10^{-4}$	$1{,}2\cdot10^{-4}$	$3{,}2\cdot10^{-4}$	$5{,}7\cdot10^{-5}$	$1{,}9\cdot10^{-4}$	$3{,}4\cdot10^{-5}$	$4{,}2\cdot10^{-3}$	$7{,}6\cdot10^{-4}$	$2{,}3\cdot10^{-4}$	$4{,}2\cdot10^{-5}$	$5{,}1\cdot10^{-3}$	$9{,}2\cdot10^{-4}$
Sr	^{85}Sr	$6{,}8\cdot10^{-3}$	$1{,}6\cdot10^{-3}$	$3{,}9\cdot10^{-3}$	$8{,}9\cdot10^{-4}$	$4{,}9\cdot10^{-3}$	$1{,}1\cdot10^{-3}$	$6{,}7\cdot10^{-3}$	$1{,}5\cdot10^{-3}$	$1{,}2\cdot10^{-2}$	$2{,}8\cdot10^{-3}$	$3{,}4\cdot10^{-2}$	$7.8\cdot10^{-3}$
Zr	^{95}Nb	$7{,}6\cdot10^{-3}$	$1{,}5\cdot10^{-3}$	$9{,}2\cdot10^{-3}$	$1{,}8\cdot10^{-3}$	$7{,}9\cdot10^{-3}$	$1{,}6\cdot10^{-3}$	$1{,}9\cdot10^{-2}$	$3{,}8\cdot10^{-3}$	$6{,}2\cdot10^{-3}$	$1{,}2\cdot10^{-3}$	$8{,}2\cdot10^{-2}$	$1{,}7\cdot10^{-2}$
Sb	^{124}Sb	$2{,}0\cdot10^{-5}$	$3{,}1\cdot10^{-6}$	$3{,}8\cdot10^{-6}$	$5{,}8\cdot10^{-7}$	$5{,}4\cdot10^{-6}$	$8{,}2\cdot10^{-7}$	$6{,}1\cdot10^{-5}$	$9{,}3\cdot10^{-6}$	$4{,}1\cdot10^{-6}$	$6{,}2\cdot10^{-7}$	$1{,}2\cdot10^{-4}$	$1{,}8\cdot10^{-5}$
Cs	^{134}Cs	$2{,}9\cdot10^{-5}$	$5{,}6\cdot10^{-6}$	$9{,}1\cdot10^{-6}$	$1{,}7\cdot10^{-6}$	$1{,}8\cdot10^{-5}$	$3{,}4\cdot10^{-6}$	$1{,}5\cdot10^{-4}$	$3{,}0\cdot10^{-5}$	$5{,}3\cdot10^{-6}$	$1{,}0\cdot10^{-6}$	$3{,}4\cdot10^{-4}$	$6{,}5\cdot10^{-5}$
Ba	^{131}Ba	$5{,}2\cdot10^{-3}$	$1{,}2\cdot10^{-3}$	$2{,}9\cdot10^{-3}$	$6{,}8\cdot10^{-4}$	$2{,}5\cdot10^{-3}$	$5{,}8\cdot10^{-4}$	$4{,}4\cdot10^{-2}$	$1{,}0\cdot10^{-2}$	$2{,}8\cdot10^{-3}$	$6{,}5\cdot10^{-4}$	$6{,}7\cdot10^{-2}$	$1{,}5\cdot10^{-2}$
La	^{140}La	$1{,}5\cdot10^{-3}$	$2{,}3\cdot10^{-4}$	$1{,}8\cdot10^{-3}$	$2{,}8\cdot10^{-4}$	$1{,}8\cdot10^{-4}$	$2{,}9\cdot10^{-5}$	$3{,}0\cdot10^{-3}$	$4{,}6\cdot10^{-4}$	$9{,}3\cdot10^{-2}$	$1{,}4\cdot10^{-2}$	$2{,}7\cdot10^{-3}$	$4{,}3\cdot10^{-4}$
Ce	^{141}Ce	$1{,}2\cdot10^{-4}$	$4{,}5\cdot10^{-5}$	$1{,}0\cdot10^{-5}$	$3{,}6\cdot10^{-6}$	$1{,}2\cdot10^{-4}$	$4{,}2\cdot10^{-5}$	$2{,}4\cdot10^{-4}$	$8{,}8\cdot10^{-5}$	$6{,}0\cdot10^{-5}$	$2{,}2\cdot10^{-5}$	$2{,}3\cdot10^{-3}$	$8{,}3\cdot10^{-4}$
Nd	^{147}Nd	$3{,}7\cdot10^{-3}$	$8{,}4\cdot10^{-4}$	$1{,}9\cdot10^{-3}$	$4{,}2\cdot10^{-4}$	$7{,}0\cdot10^{-4}$	$1{,}6\cdot10^{-4}$	$1{,}8\cdot10^{-3}$	$4{,}1\cdot10^{-4}$	$8{,}9\cdot10^{-4}$	$2{,}0\cdot10^{-4}$	$3{,}6\cdot10^{-5}$	$8{,}2\cdot10^{-4}$
Sm	^{153}Sm	$2{,}2\cdot10^{-4}$	$8{,}3\cdot10^{-5}$	$4{,}7\cdot10^{-5}$	$1{,}8\cdot10^{-5}$	$6{,}1\cdot10^{-6}$	$2{,}4\cdot10^{-6}$	$5{,}0\cdot10^{-5}$	$1{,}9\cdot10^{-5}$	$5{,}7\cdot10^{-4}$	$2{,}2\cdot10^{-4}$	$1{,}2\cdot10^{-4}$	$4{,}4\cdot10^{-5}$
Eu	^{152}Eu	$7{,}4\cdot10^{-5}$	$1{,}5\cdot10^{-5}$	$3{,}5\cdot10^{-5}$	$7{,}0\cdot10^{-6}$	$4{,}4\cdot10^{-5}$	$8{,}8\cdot10^{-6}$	$1{,}7\cdot10^{-4}$	$3{,}5\cdot10^{-5}$	$1{,}3\cdot10^{-5}$	$2{,}7\cdot10^{-6}$	$2{,}7\cdot10^{-4}$	$5{,}4\cdot10^{-5}$
Gd	^{153}Gd	$7{,}8\cdot10^{-6}$	$1{,}0\cdot10^{-6}$	$1{,}5\cdot10^{-5}$	$6{,}2\cdot10^{-6}$	$1{,}8\cdot10^{-6}$	$7{,}4\cdot10^{-7}$	$1{,}6\cdot10^{-5}$	$6{,}5\cdot10^{-6}$	$5{,}1\cdot10^{-7}$	$2{,}1\cdot10^{-7}$	$2{,}3\cdot10^{-5}$	$9{,}3\cdot10^{-6}$
Tb	^{160}Tb	$1{,}5\cdot10^{-4}$	$2{,}9\cdot10^{-5}$	$6{,}2\cdot10^{-5}$	$1{,}2\cdot10^{-5}$	$3{,}8\cdot10^{-5}$	$7{,}2\cdot10^{-6}$	$4{,}2\cdot10^{-4}$	$8{,}1\cdot10^{-5}$	$2{,}6\cdot10^{-5}$	$4{,}9\cdot10^{-6}$	$7{,}3\cdot10^{-4}$	$1{,}4\cdot10^{-4}$
Tm	^{170}Tm	$2{,}1\cdot10^{-6}$	$8{,}3\cdot10^{-7}$	$1{,}5\cdot10^{-6}$	$6{,}1\cdot10^{-7}$	$1{,}7\cdot10^{-7}$	$6{,}9\cdot10^{-8}$	$2{,}6\cdot10^{-6}$	$1{,}0\cdot10^{-6}$	$4{,}7\cdot10^{-8}$	$1{,}9\cdot10^{-8}$	$2{,}1\cdot10^{-5}$	$8{,}6\cdot10^{-6}$
Yb	^{169}Yb	$1{,}5\cdot10^{-5}$	$5{,}2\cdot10^{-6}$	$6{,}9\cdot10^{-6}$	$2{,}3\cdot10^{-6}$	$6{,}6\cdot10^{-6}$	$2{,}2\cdot10^{-6}$	$1{,}0\cdot10^{-4}$	$3{,}7\cdot10^{-5}$	$4{,}2\cdot10^{-6}$	$1{,}4\cdot10^{-6}$	$1{,}5\cdot10^{-4}$	$5{,}2\cdot10^{-5}$
Lu	^{177}Lu	$8{,}7\cdot10^{-6}$	$2{,}8\cdot10^{-6}$	$4{,}0\cdot10^{-6}$	$1{,}3\cdot10^{-6}$	$3{,}9\cdot10^{-6}$	$1{,}3\cdot10^{-6}$	$3{,}6\cdot10^{-5}$	$1{,}2\cdot10^{-5}$	$5{,}4\cdot10^{-6}$	$1{,}8\cdot10^{-6}$	$3{,}6\cdot10^{-5}$	$1{,}2\cdot10^{-5}$
Hf	^{181}Hf	$2{,}1\cdot10^{-5}$	$5{,}1\cdot10^{-6}$	$7{,}8\cdot10^{-6}$	$1{,}9\cdot10^{-6}$	$1{,}2\cdot10^{-5}$	$2{,}8\cdot10^{-6}$	$1{,}4\cdot10^{-4}$	$3{,}4\cdot10^{-5}$	$4{,}6\cdot10^{-6}$	$1{,}1\cdot10^{-6}$	$1{,}0\cdot10^{-4}$	$2{,}5\cdot10^{-5}$
Ta	^{182}Ta	$1{,}2\cdot10^{-6}$	$2{,}2\cdot10^{-6}$	$5{,}1\cdot10^{-6}$	$9{,}4\cdot10^{-7}$	$2{,}0\cdot10^{-6}$	$3{,}7\cdot10^{-6}$	$9{,}9\cdot10^{-5}$	$1{,}8\cdot10^{-5}$	$2{,}6\cdot10^{-6}$	$4{,}7\cdot10^{-7}$	$9{,}8\cdot10^{-5}$	$1{,}8\cdot10^{-5}$
Th	^{233}Pa	$2{,}7\cdot10^{-5}$	$7{,}4\cdot10^{-6}$	$1{,}1\cdot10^{-5}$	$3{,}1\cdot10^{-6}$	$1{,}4\cdot10^{-5}$	$3{,}9\cdot10^{-6}$	$1{,}1\cdot10^{-4}$	$3{,}0\cdot10^{-5}$	$8{,}9\cdot10^{-6}$	$2{,}4\cdot10^{-6}$	$3{,}0\cdot10^{-4}$	$8{,}2\cdot10^{-5}$

Note: Confidence coefficient 98%; time of measurement of gamma spectra one hour; volume of detectors: A = 10.5 cm^3; B = 50.5 cm^3.

The isotopes in the spectrum of a specimen are identified in the following way. From the set of calculated values of E_γ there is determined the energy of the photopeak with the highest intensity which agrees within half the resolution of the detector at that energy with one value of $E_{\gamma kl}$ from the catalog of standard data. The amount of the corresponding element in the specimen is calculated by the formula

$$M_k = \eta_k \frac{S_\gamma}{S_{\gamma kl}} \cdot \frac{m_k}{m_0} \cdot 100\%, \tag{14}$$

The error in the value of the amount of the element is given by [21]

$$\Delta M_k = \frac{\eta_k m_k}{S_{\gamma kl} m_0} \left(\Delta S_\gamma - \frac{S_\gamma}{S_{\gamma kl}} \Delta S_{\gamma kl} \right) \cdot 100\%. \tag{15}$$

The sensitivity of the determination of a chemical element in the specimen is found from the expression

$$M_k^{\min} = \frac{\varepsilon \sqrt{R_\Phi}}{R_\gamma} \cdot \frac{m_k}{m_0} \cdot 100\%, \tag{16}$$

where R_γ is the height of the corresponding photopeak, and R_Φ is the "pedestal" of the photopeak at its center.

The values of the energies $E_{\gamma j}$ ($j \neq l$) of the photopeaks of a given isotope in the catalog of standard data are compared with the energies E^*_γ ($E^*_\gamma \neq E_\gamma$) found in the spectrum of the photopeaks, and if the values of E^*_γ and $E_{\gamma j}$ agree within the limits of half the resolution of the detector the "residual intensity" of the photopeak with energy E^*_γ is calculated

$$\overline{S}^*_\gamma = S^*_\gamma - S_{\gamma j} \frac{S_\gamma}{S_{\gamma kl}}. \tag{17}$$

If the residual intensity of the photopeak is less than the error in the initial intensity the photopeak is not considered further. The next isotope is identified by using the rest of the set of energies and intensities of the photopeaks in the spectrum and the catalog of standard data with the exception of the values of the energies and intensities of the photopeaks of the identified isotope.

The processing of a 3200 channel γ-spectrum of a specimen and the quantitative determination of the amounts of 15–30 chemical elements require from five to ten minutes on an M-220 computer, depending on the complexity of the spectrum being analyzed. After the computer has processed a spectrum it prints out the symbols of the identified isotopes, the energies of the photopeaks by means of which these isotopes were identified, the amounts of the corresponding elements in the specimen and their errors, the sensitivity of the determination of the elements, and the residual spectrum of energies and intensities of the unidentified photopeaks in the spectrum of the specimen.

Table 1 lists the experimentally determined sensitivies for the simultaneous determination of 24 chemical elements in various geological objects. It is clear from the table that the minimum determinable concentrations of elements in most cases are an order of magnitude smaller than those which can reliably be determined by Klarkov [22].

The accuracy of determining the amounts of chemical elements in samples is 8-12% for Sc, Cr, Fe, Co, Zn, Rb, Sr, Cs, Ba, Ce, Eu, Yb, Lu, Hf, Ta, and Th, and 12-18% for Sb, La, Nd, Sm, Gd, Tm, Zr, and Tb.

The amounts of elements found by the method described above are in good agreement with those determined by chemical and quantitative spectral analysis, within the limits of their sensitivities and accuracies.

LITERATURE CITED

1. B.I. Bolov, in: Mathematical Methods of Geochemical Research [in Russian], Nauka, Moscow (1966), pp. 99-105.
2. L.N. Ovchinnikov and N.F. Chelitsev, Geokhimiya, 11, 1328-1335 (1967).
3. M.V. Limonova and I.N. Nyuberg, Geologiya i Geofizika, 11 (1970).
4. I.P. Alimarin and Yu.V. Yakovlev, in: Nuclear Physics Methods of Analysis of Matter [in Russian], Atomizdat, Moscow (1971), pp. 5-14.
5. D.M. Shou, Geochemistry of Trace Elements in Crystalline Rocks [in Russian], Nedra, Leningrad (1969), pp. 44-45.
6. G. Gordon, Geochim. et Cosmochim. Acta, 32, 369 (1968).
7. V. Gadzhokov, Preprint OIYaI, P10-5035, Dubna (1970).
8. R. Arl't et al., Preprint OIYaI, P6-6227, Dubna (1972).
9. R. Helmer and R. Heath, Nucl. Instrum. and Methods, 57, 46 (1967).
10. M. Mariscotti, Nucl. Instrum. and Methods, 50, 309 (1967).
11. V. Barness, IEEE Trans. Nucl. Sci., 15, 437 (1968).
12. J. Routti and S. Prussin, Nucl. Instrum. and Methods, 72, 125 (1969).
13. J. Phillipot, IEEE Trans. Nucl. Sci., 17, 446 (1970).
14. A. Connely and W. Black, Nucl. Instrum. and Methods, 82, 141 (1970).
15. J. Slavic and S. Bingulac, Nucl. Instrum. and Methods, 84, 261 (1970).
16. G. Borchardt et al., J. Radioanal. Chem., 6, 241 (1970).
17. F. Adams and R. Dams, J. Radioanal. Chem., 7, 329 (1971).
18. A. Savitzky and M. Golay, Anal. Chem., 36, 1627 (1964).
19. H. Yule, Nucl. Instrum. and Methods, 54, 61 (1967).
20. H. Yule, Anal. Chem., 38, 103 (1966).
21. G.V. Sukhov and V.I. Firsov, in: Nuclear Physics Methods of Analysis of Matter [in Russian], Atomizdat, Moscow (1971), pp. 52-60.
22. S.P. Salov'ev, Chemism of Magnetic Rocks and Some Problem of Petrochemistry [in Russian], Nauka, Leningrad (1970), pp. 32-33.

PLASMA LOSSES IN THE RING GAP OF AN ELECTROMAGNETIC TRAP

Yu.I. Pankrat'ev, N.A. Tulin,
E.F. Ponomarenko, and V.A. Naboka

UDC 533.9

In electromagnetic traps [1, 2] it is necessary to make the magnetic gaps narrow in order to increase the confined plasma density. Narrow gaps are needed to minimize the space-charge potential of the electrons oscillating through the gaps. Theoretical analyses [2] show that the thickness of the electron layer in the ring gap must be on the order of a millimeter for confinement of a thermonuclear plasma. However, the theory of electron beams in crossed electric and magnetic fields predicts instability of thin layers [3].

For electromagnetic plasma confinement the ion lifetime is determined by the duration of the negative potential well inside the trap, that is, by the electron lifetime. The additional plasma losses caused by instability of the electron layer in the magnetic gap prevent increasing the plasma density in the trap by simply narrowing the gaps without taking precautions to suppress the instability. The results of an experimental study of the diocotron instability in the ring gap were presented in [4]. The present work is a continuation of this research.

Plasma was produced in an electromagnetic trap (Fig. 1) by ionization of neutral gas by an electron beam with 100 mA at up to 3 keV and confined by a cusped magnetic field produced by coils 1 and 2. The width of the ring gap and the diameter of the axial openings were 1 cm. The ions inside the trap were also confined by the negative potential well of the space charge of the electrons injected from the gun 5. The losses of electrons leaving the trap along the magnetic field lines were suppressed by the retarding electric fields of the electrodes 7, 8, which were maintained at negative potentials exceeding the energy of the injected electrons. The ring electrode 7 was cut into eight sections. The particle current from each sector, produced by loss of plasma from the trap, was recorded on a separate channel of an oscillograph. Plasma loss across the magnetic field was measured by means of small collectors 3 located on each side of the ring gap. The plasma density inside the trap was measured by a microwave interferometer 4. With

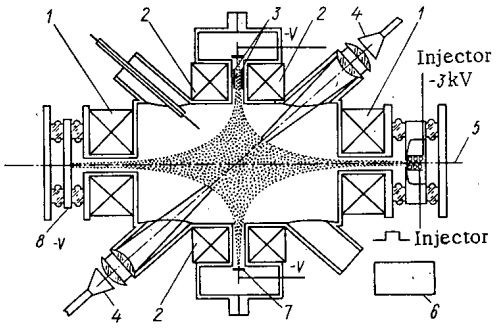

Fig. 1

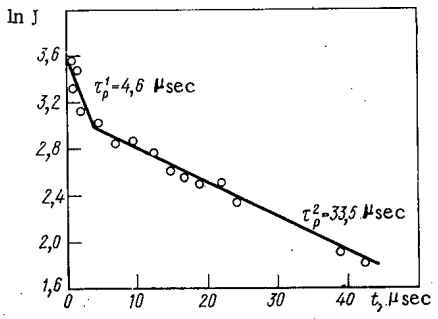

Fig. 2

Fig. 1. Diagram of electromagnetic trap.

Fig. 2. Plasma decay in the trap. (H = 3000 Oe, $n_e = 10^9$ cm^{-3}, τ_p^1 = 4.6 μsec and τ_p^2 = 33.5 μsec.)

Translated from Atomnaya Énergiya, Vol. 35, No. 4, pp. 253-257, October, 1973. Original article submitted May 30, 1972. Revision submitted February 6, 1973.

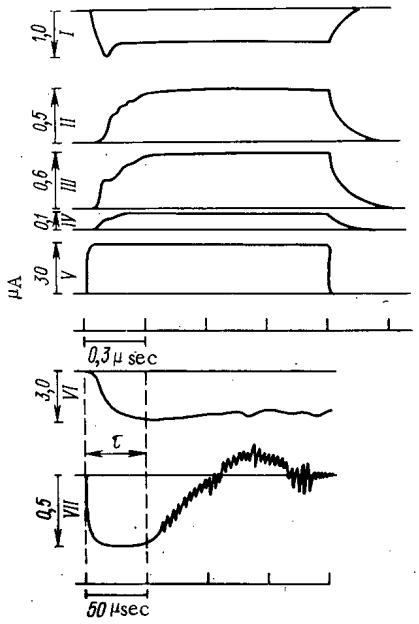

Fig. 3

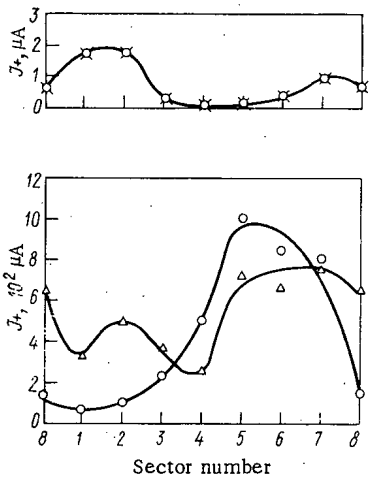

Fig. 4

Fig. 3. Oscillograms of plasma losses from the trap. (H = 3000 Oe, p = 10^{-5} torr). I) electron current across the magnetic field in the gap; II-IV) ion current into the ring gap at three sectors of the retarding electrode; V) injection current; VI, VII) electron current across and through the ring gap with no applied voltage on the ring electrode.

Fig. 4. Distribution of ion losses around the ring gap. (⋈) p = $5 \cdot 10^{-6}$ torr; △) p = $4 \cdot 10^{-5}$ torr; ○) p = 10^{-4} torr.

an 8 mm interferometer the electron gun was pulsed by the modulator 6. (Other regimes of operation of electromagnetic traps are described in [1, 4, 5].)

Plasma was produced in the trap by ionization of neutral gas by an injected electron beam. The plasma density grew only during the initial stages of injection. Plasma accumulation ceased when a density around 10^8-10^9 cm^{-3} was reached. Since the plasma density is determined by the balance of two processes (the plasma formation rate and loss rate), an attempt was made to raise the plasma density by increasing the ionization rate. However, neither an increase of neutral gas pressure nor an increase of injected electron beam current lead to an increase of plasma density inside the trap.

The decay of plasma density after the end of injection is shown in Fig. 2. Immediately after the cessation of injection the decay time is $\tau_p^1 \approx 4$-5 μsec. Then, with a lower plasma density in the trap, the decay rate decreases. The slower decay time $\tau_p^2 \approx 30$-100 μsec and is inversely proportional to neutral gas density. Since τ_p^1 determines the decay at higher densities, more attention was paid to studying how this decay time varied with the conditions of plasma accumulation in the trap.

The variation of the experimental ion lifetime τ_p^1 with neutral gas density n_0 was found to fit the empirical relation [1]

$$1/\tau_i \approx 1/\tau_0 + 1.3 \cdot 10^{-7} n_0.$$

The presence of the $1/\tau_0$ term indicates that in addition to losses caused by collisional processes with neutral gas, other loss processes are active. The magnitude of $1/\tau_0$ depends on conditions in the trap: magnetic field strength, injected electron current, position of the electron layer in the ring gap, and the plasma density. Measurements with the collectors on the chamber walls indicated that anomalous losses were maximum in the ring gap, and that these losses are caused by plasma instability.

The development of the instability is shown in Fig. 3. The amount of ion current is different to different sectors. The azimuthal variation of ion loss rates is shown in Fig. 4. The curves were taken at different pressures. At low pressures (p ≈ $5 \cdot 10^{-6}$ torr) the inhomogeneity of the current is still weak.

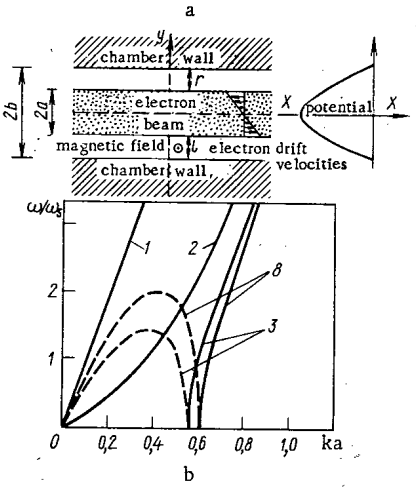

Fig. 5

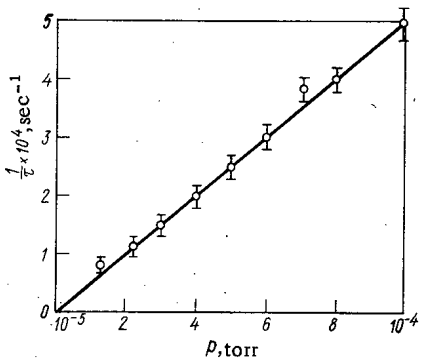

Fig. 6

Fig. 5. Unperturbed situation of the electron cloud in the ring gap (a) and the dispersion relation for the diocotron oscillations (b). Numbers on the curves indicate the ratio b/a. Dashed curves) Im(ω/ω_s).

Fig. 6. Variation of instability growth rate with residual gas pressure.

With an increase in pressure the flow loses its azimuthal symmetry, and when p = 10^{-4} torr the losses occur mainly at an azimuthal angle ~90–120°. Measurements of electron losses across the gap indicated that their distribution is similar to the ion loss distribution.

The azimuthal inequality of plasma losses was also observed for plasma confinement in the usual magnetic trap regime. Oscillograms VI and VII (Fig. 3) show the variation of electron current across and through the ring gap when the potential of the electrode ring was zero. At low injection currents (2–5 mA) and low pressures the current of electrons leaving the trap along the magnetic field was independent of azimuthal angle. With an increase of either injection current or gas pressure the azimuthal symmetry was lost at some time τ after the beginning of injection. Oscillograms VI and VII (Fig. 3) show a decrease of electron current along the magnetic field and an increase of losses across the field. With a transition to the regime of electromagnetic plasma confinement, that is, with a gradual increase in negative voltage on the ring electrode, the electron losses along the magnetic field finally were suppressed. However, a simultaneous increase of electron losses across the field in the gap prevented increasing the plasma density in the trap.

These data provide basis for supposing that the initially thin layer of electrons in the ring gap buckles or becomes thicker during the development of the instability to the point where the electrons touch the walls of the gap.

It should be noted that the azimuthal distribution of plasma losses did not vary with the interchange of the direction of the magnetic field and the rotation of the electron beam around its own axis. If a negative potential two or three times the energy of the injected electrons was applied to the collectors on the wall of the ring gap where the losses were a maximum, then the angular loss distribution was shifted by about 180°.

DISCUSSION OF RESULTS

Increasing the plasma density in the trap by increasing the ionization rate was prevented by the onset of an instability in the ring gap. An expanded view of the ring gap is shown in Fig. 5, with notation defined. The electron layer undergoes a drift along the X axis in the electric field E of the space charge layer and perpendicular magnetic field H (out of the paper). The drift speed increases towards the outer boundary of the electron layer. The "slipping" of the flow, defined by the quantity

$$\omega_s = |\operatorname{rot} v| = \frac{d}{dy} \cdot \frac{cE}{H} = \frac{4\pi cne}{H}, \qquad (1)$$

causes the onset of diocotron oscillations [3, 4], running in opposite directions along the two boundaries of the flow. The distance of the conducting walls from the flow boundary can exert a significant influence on the development of the oscillations. The dispersion equation from [6]

$$\left(\frac{\omega}{\omega_s}\right)^2 = \{ka - [(\mathrm{ch}\, 2kb - \mathrm{ch}\, 2ka)/2\,\mathrm{sh}\, 2kb]\}^2 - \{[\mathrm{sh}^2 k(b-a)]/\mathrm{sh}\, 2kb\}^2, \quad (2)$$

is shown in Fig. 5. It is evident that the conducting walls can provide a stabilizing effect when they are close to the boundary of the flow. Large values of the electron layer's half-thickness a should cause instabilities at wavelengths 10a in the region between the electron beam and the wall.

Because of the finite dimensions of the ring gap the wave vector k can only take on discrete values. Thus, $ka = ma/R$, where m = 1, 2, 3, ... is the mode number of the oscillations; R is the radius of the ring gap; and a is the half-thickness of the electron layer. The size of a depends on the conditions of the electrom beam injection: on the electron beam radius and on the magnetic flux at the electron gun cathode. In the present experiments $2a \approx 0.4$ cm, 2b = 1 cm, and R = 10 cm, so $b/a > 2$. In the instability region waves with m from 1 to 30 grow, and the maximum growth increment is for $m \approx 15$. The experimental data give information only on the nonlinear stages of the instability. As can be seen in Fig. 4, only one or two periods are located within the circumference of the ring gap, so m = 1 or 2. This does not contradict the results of [6], where it was shown that an initial kink perturbation leads to the formation of a vortex with m = 1. Evidently, modes with finer scale (higher mode numbers) fall into the region with $ka > 0.6$ after the onset of the instability.

The growth rate of the diocotron instability is

$$\gamma \equiv Im\omega \approx \frac{1}{4}\omega_s ka = \frac{1}{4}\frac{4\pi cne}{H}. \quad (3)$$

This growth rate is a function of time in an electromagnetic trap, because the electron density in the gap varies during accumulation of plasma in the trap. Therefore only a qualitative comparison of theory and experiment is possible. With a small or zero retarding potential on the ring electrode, the rate of plasma accumulation in the trap is significantly less (by a factor of 1000) than during electromagnetic confinement [1, 7]. The time τ, during which the electron current onto the ring electrode is azimuthally symmetric, is inversely proportional to residual gas pressure, as shown in Fig. 6. Thus, the growth rate of the instability is proportional to the electron density

$$n_e'' \approx n_e' n_0 \langle \sigma_i v \rangle = n_e' \cdot 6 \cdot 10^9 p\tau. \quad (4)$$

The quantity $p\tau$, determined from the slope of the straight line of Fig. 6, is equal to $2 \cdot 10^{-9}$ torr sec. From this it follows that at the moment of the onset of the instability the density of secondary electrons n_e'' (produced by ionization) exceeds the density of the primary (beam) electrons n_e' by approximately an order of magnitude.

The time required for development of the instability increases linearly with magnetic field H at small field strengths (H < 1500-2000 Oe), in accordance with theory, but then τ saturates.

In the regime of electromagnetic confinement the instability occurred with greater speed, since the retarding electric field eliminates losses along the field lines not only of the primary beam electrons but also of the secondary electrons.

Thus, the accumulation of cold electrons formed by ionization of neutral gas in the magnetic gaps causes the long-wavelength diocotron instability to develop. The onset of the instability ends the accumulation of plasma in the trap, since the rate of plasma generation is balanced by the rate of plasma loss in the ring gap. The particle lifetime defined by the initial decay of plasma density after the termination of injection is approximately $1/\gamma = (I/Im\omega) \approx H/0.9$ nm, calculated from Eq. (3). For example, for the conditions indicated in Fig. 2, $1/\gamma \approx 3.3$ μsec, and $\tau_i \approx 4.5$ μsec. This indicates that the particle lifetime in the trap is mainly determined by the loss rate of electrons across the magnetic field of the gap in the azimuthal electric field of the developing instability:

$$\frac{dn_e}{dt} = n_e' n_0 \langle \sigma_i v \rangle - \frac{n_e' S c E_\varphi}{VH}, \quad (5)$$

where V is the volume of the plasma in the trap; S is the effective loss area; E_φ is the average magnitude of the electric field of the instability. An estimation of E_φ from Eq. (5) gives a value of about 10 V/cm.

The diocotron instability is caused by the growth of waves on the surfaces of the electron layer in the magnetic gaps of the trap. In [3] it is shown that for small ka, that is, for large wavelengths, the layer must be stable if $a^2 > rl$ (where r and l are the distances from the edge of the electron layer to a conducting surface). In other words, for stability it is sufficient to have not two, but just one conducting surface,

in order to "short circuit" the electric field of one of the surface waves. By varying the magnetic fields in the two halves of the trap, the electron layer may be moved across the ring gap. The instability was suppressed when the electron layer grew near to either side wall of the gap. The suppression of the instability was accompanied by an increase of plasma density in the trap from 10^8 up to $2\text{-}5 \cdot 10^{11}$ cm^{-3}.

The second method for accumulating plasma in an electromagnetic trap – the gradual buildup of plasma at low neutral gas pressures ($p = 10^{-7}$ torr) – was described in [4, 5].

In conclusion the authors express deep gratitude to K.N. Stepanov, O.A. Lavrent'ev, and A.A. Kalmykov for valuable advice and discussion of the results.

LITERATURE CITED

1. O.A. Lavrent'ev, in: Magnetic Traps [in Russian], Vol.3, Naukova Dumka, Kiev (1968), p.77.
2. A. Ware and J. Faulkner, Nucl. Fusion, 9, 953 (1969).
3. O. Buneman et al., J. Appl. Phys., 37, 3209 (1966).
4. Yu.I. Pankrat'ev et al., At. Energ., 31, No.3, 274 (1971).
5. Yu.I. Pankrat'ev et al., At. Energ., 32, No.2, 131 (1972).
6. R. Levy and R. Hockey, Phys. Fluids, 11, 766 (1968).
7. W. Strijland, Physica, 47, 617 (1970).

BOOK REVIEWS

V. I. Vladimirov

PRACTICAL PROBLEMS IN THE OPERATION OF NUCLEAR REACTORS*

Reviewed by M. A. Chepovskii

Despite the extensive materials available in the literature on nuclear reactors at the present time, one lack clearly felt in the literature is on engineering aspects of heat transfer and heat physics.

This three-chapter text, covering and surveying the basic problems encountered in work with nuclear reactors in a consistent manner, discusses the physical processes occurring in a reactor with power on and in a shutdown reactor, bringing a power reactor up to criticality, reactor performance at the rated power output level, reactor cooldown, and also various problems pertaining to reactor safety and radiation safety. Special attention is reserved for how to calculate reactor startup characteristics (critical position of absorber rods) in a variety of situations.

The first chapter deals with procedures for estimating exposure doses, dose rates, and residence times for different sets of conditions affecting the radiation situation, and offers a presentation of the physical meaning of breeding factor and reactivity.

The second chapter is devoted to the physical processes accompanying reactor operation (release of energy in the core, reactor power output, burnup, poisoning, reactor poisoning by fission products), and the temperature effect of reactivity. A procedure for calculating samarium poisoning and xenon poisoning of a reactor is described in detail. The effect of the temperature coefficient of reactivity on stable reactor performance and on reactor on-power lifetime is also treated.

The third chapter takes up reactor control from startup and until cooldown. Procedures for calculating the critical (starting) position of reactor control rods and compensation rods are presented. Problems concerning the choice of a feasible reactor startup program and schedule are covered along with problems dealing with changes in power level up to the point of shutdown and cooldown of the reactor. The chapter ends with a very important section reflecting various aspects of reactor safety under normal operating conditions, and when malfunctions arise in reactivity control and compensation equipment. Close attention is given to variable reactor operating conditions.

The book encompasses virtually the entire range of questions that can arise in the operation of a nuclear reactor. Nevertheless, we feel it advisable to make some further demands on the author:

1. Fuel breeding is almost totally left out of account in the discussion of burnup calculations. While that is allowable when dealing with reactors burning highly enriched fuel, it cannot be left out of a treatment of reactors burning weakly enriched uranium.
2. The reader's attention should have been directed to such a phenomenon as a possible reactor reactivity increase that might occur after the reactor has been shut down, on account of a buildup of plutonium from decaying neptunium. This is typical of reactors burning natural fuel or weakly enriched fuel.
3. Problems involving calculations of the remaining on-power lifetime in the case of reactors with burnable poisons are not discussed in the text.
4. It would have been helpful in a text of this kind to include some problems left to the reader to solve in each section.

*Atomizdat, Moscow (1972).

Translated from Atomnaya Énergiya, Vol.35, No.4, pp.257-258, October, 1973.

In conclusion, we may point out that this book will be of interest and value to those directly involved in the operation of nuclear reactors, and also to students majoring in related areas.

Yu. V. Gott and Yu. N. Yarlinskii

INTERACTION OF SLOW PARTICLES WITH MATTER AND PLASMA DIAGNOSTICS*

Reviewed by Yu. V. Martenko

This book deals with interactions of slow particles (energy range extending from hundreds of electron-volts to tens of kiloelectron-volts) with solids. While this is a somewhat narrow topic, it is of the utmost timeliness.

The first two chapters offer a survey of theoretical and experimental research on stopping of particles in matter, the charge state of the particles interacting with solids, and scattering of particles by a solid target. The third chapter describes experimental techniques for measuring energy losses in thin films.

The fourth chapter handles applications of phenomena observed as particles traverse thin films. This chapter is based primarily on research findings arrived at by the book's authors. These topics are of great interest, particularly in that they are not reflected in any of the monographs that have appeared to date on this topic.

The book assembles a wealth of material. The authors strove not only to provide a detailed presentation of theoretical and experimental techniques, but also to facilitate ready use of those techniques and of the results obtained with them. The formulas are presented in the most convenient way, their range of error and validity are clearly delineated, and hence the text can be useful as a reference work. Different ways of investigating the iteraction of slow particles and matter are treated in detailed fashion and are evaluated critically.

The book will be of value both to experimental physicists working on plasma diagnostics, ionic alloying of semiconductors, the structure of solids, field emission electrons, and to specialists in other fields of science and industry.

D. Bedenig

GAS-COOLED HIGH-TEMPERATURE REACTORS†

Reviewed by B. Yashma

This book is the 44th volume in a series of pocket editions published by the West German firm.

The book is in nine chapters, with appendices and a subject index. Each chapter ends with a list of reference literature that may be of interest to a reader wishing to acquaint himself with some particular aspect of the topic.

*Atomizdat, Moscow (1973).

†Verlag K. Thiemig, Munich (1972).

The introduction lists the basic features of the design and technology of high-temperature reactors (HTR) as compared to reactors of other types, and goes into detail on the development of HTR in other countries.

The second chapter is devoted to the reactor primary loop. The choice of helium as coolant is validated, the design of prestressed reinforced concrete pressure vessels is discussed. A description is given of the gas cleanup system, steam generators, and gas blowers. The design of HTR is elucidated by examples such as the Fort St. Vrene and THTR reactors.

The third chapter renders a very concise account of the ancillary systems, and discusses specifically the possible formation of tritium in the secondary loop.

The fourth chapter, which goes into adequate detail on the subject of nuclear fuel and breeding materials for HTR, and their physical and radiation properties, as well as coated fuel particles, the design of fuel elements for the AVR, THTR, Peach Bottom, Dragon, and Fort St. Vrene reactors, as well as the results of in-pile and out-of-pile fuel testing, is of great interest. There is also a discussion of reprocessing and reuse of irradiated fuel (with particular emphasis on recycling of thorium-containing fuel).

Fuel reloading (to which the fifth chapter is devoted) centers mainly around the example of the West German AVR reactor, and the THTR reactor now being built.

Breeding of secondary nuclear fuel, various fuel cycles, nuclear physics characteristics and heat transfer characteristics of HTR are discussed in the next chapter, which also touches on the dynamics of that type of reactor.

The seventh chapter deals with the safety of HTR reactors in any accident situation (up to and including rupture of the concrete pressure vessel), and formulates requirements and specifications for the HTR control system and its instrumentation.

The next two chapters deal with the current state of HTR development. These chapters describe designs and present results of operating experience with reactors already in operation or now being built. The highly intriguing developmental outlook for high-temperature reactors, and their prospective use in combination with gas turbines, are discussed, as well as applications of high-temperature reactors in the chemical process industry and in the metallurgical industry, and in MHD generators. Summarized information is given on fast gas-cooled reactors, and the place open for HTR in the nuclear power development picture extrapolated to the year 2020 is analyzed.

An appendix presents the basic characteristics of all gas-cooled high-temperature reactors now in operation or now under construction.

This book is a unique publication on HTR. The text reviews and analyzes a host of data taken from different journals and the periodical literature. It is written in straightforward laconic language, and presents a fairly complete characterization of all aspects of HTR. The text is fully deserving of translation into Russian.

ARTICLES

ELECTROMAGNETIC FIELDS IN A PLASMA HEATED NEAR THE LOWER HYBRID RESONANCE

Yu. V. Skosyrev, N. A. Krivov, and V. M. Glagolev

UDC 621.039.643:533.951

Theory shows that the ions of a plasma can be heated when electromagnetic waves retarded along the magnetic field are excited in the plasma. Conditions were found in [1] under which an electromagnetic wave propagating across the magnetic field in a plasma with an increasing density is reflected at a certain point in the form of a plasma wave. A detailed review of the transformation of electromagnetic waves into plasma waves is given in [2].

The strong absorption of a plasma wave due to Cerenkov interaction with the plasma must result in the heating of the ions. Experimental studies of the hybrid resonance are reported in [3, 4].

Paper [5] reports the heating of a plasma initially produced by means of a microwave injector [6]. In these experiments the plasma propagates along the lines of force of the magnetic field and enters a high-frequency resonator resonating at a frequency $\omega/2\pi = 140$ Mc/sec. This frequency is close to the frequency of the lower hybrid resonance, which corresponds to the condition $\omega^2 = \omega_{He}\,\omega_{Hi}\,(1 + \omega_{He}^2/\omega_0^2)^{-1}$ of a plasma with a density $\sim 10^{12}$ cm^{-3} situated in a magnetic field ~3 kOe. Here ω_{He}, ω_{Hi} are the electron and ion cyclotron frequencies and ω_0 is the plasma frequency. The resonator was located in the magnetic field of an adiabatic trap with a mirror ratio 1.4. The resonator was formed by a two-conductor line coupled to a ~100 kW high-frequency generator. At the end of the line a turn of diameter 150 mm and width 200 mm encompassed the plasma column of diameter 60 mm. The plasma was heated in this manner to $nT = 2 \cdot 10^{14}$ eV·cm^{-3}. The transverse energy of the plasma was measured in terms of its diamagnetism. Probe measurements established that the ion temperature was in excess of 150 eV. The plasma density increased during heating. The initial plasma density produced by the microwave injector was $\sim 7 \cdot 10^{11}$ cm^{-3}. In proportion to the heating the signal from the sensor measuring the plasma diamagnetism increased enormously more rapidly than the density. However, when the density increased to $\sim 5 \cdot 10^{12}$ cm^{-3} the diamagnetism signal decreased, despite continued operation of the high-frequency generator. The cessation of heating was explained by the displacement, with increasing density, of the region where electromagnetic waves are transformed into plasma waves along the radius to the periphery of the plasma column, and on the other hand by a diminution in the energy input per particle. A reduction in the absorption of high-frequency power as the singular point shifts towards the plasma boundary, when the wavelength is comparable to the dimensions of the systems, was noted in [7]. The singular point corresponded to equality of the radial component of the dielectric tensor to zero. If the theoretical ideas on the nature of the heating are correct, one would expect the wavelength in the radial direction to decrease in proportion to the density increase. Further, electromagnetic fields must have been able to exist in the plasma during the time the density was varying over a definite range (from the density at which wave propagation is first possible to the density at which absorption occurs). Since the conditions of the experiment are consistent with the possibility of magnetoacoustic resonance, the heating of the plasma may perhaps be explained by an increase in the fields as a result of geometric magnetoacoustic resonance [4, 8]. In this connection it would be interesting to establish how electromagnetic waves behave in a plasma whose density is increasing as a result of heating.

Description of the Experiment

The fields were measured using electric and magnetic probes introduced into the plasma column in glass tubes. The probes were used to measure the spatial distribution of the field and for phase

Translated from Atomnaya Énergiya, Vol. 35, No. 4, pp. 259-262, October, 1973. Original article submitted January 15, 1973.

measurements. In the phase measurements use was made of a standing-wave line supplied, through decoupling attenuators, with a signal from the measuring probe and with a reference signal from a loop located in the jacket of the heating resonator. The attenuation of the reference and measured signals introduced by these attenuators was ~10 dB. The signal from a probe moving in the slot of the standing-wave line is fed through a detector to an oscilloscope. This signal was photographed simultaneously with the diamagnetism signal and the density. The oscillograms were used to determine the position of the standing-wave minimum in the line at different moments of heating. The phase variation of the signal was calculated from the ratio of the displacement of the minimum in the field distribution along the line, Δl, to the free-space wavelength λ: $\Delta\varphi = 2\pi(2\Delta l/\lambda)$. The sign of the phase change was found from the direction in which the minimum shifts when the probe is moved along the radius.

Figure 1 shows the measured amplitude distribution of the fields along an axis coincident with the chamber axis and the axial magnetic field. The half-width of the H_z distribution equals l (200 mm), which corresponds to the width of the turn. This sort of distribution guaranteed the necessary retardation of the wave, since the main harmonic in the Fourier expansion of the magnetic field structure has a wavelength $\lambda = 2l$. The outermost peaks in the E_r and E_z distributions are probably connected with field distortions near the ends of the metal jacket. Theory indicates that the best conditions for wave transformation occur when E waves (the boundary wave) having a component E_z are excited on the plasma surface, since E waves have a greater refractive index than H waves. Excitation of H-mode fields is preferable, however, since a field H_z which increases away from the center of the plasma column can exert a stabilizing influence on the plasma [6]. With our method of energy insertion an H wave was excited in the plasma. However, E waves could thereby be excited in the plasma by virtue of the coupling between E and H waves implicit in the equations for wave propagation in a gyrotropic unbounded medium.

The plasma formed by the microwave injector decayed with a time constant of a few hundred microseconds. By varying the delay of the high-frequency pulse relative to the end of the injection pulse it is possible to find out how the plasma density n_0 at the moment the high-frequency generator is switched on affects the magnitude of the electromagnetic field in the plasma. If $n_0 < 1.2 \cdot 10^{12}$ cm^{-3} heating (recorded in terms of the diamagnetism signal) was not observed. If the high-frequency generator was switched on at a moment of time when $n_0 > 10^{10}$ cm^{-3}, the electric field of the wave E_z at the center increased by a factor of 4 and the magnetic field H_z by a factor of ~1.5 in comparison with the field values in the absence of plasma. If $n_0 > 1.2 \cdot 10^{12}$ cm^{-3} the electromagnetic fields are a few times smaller than the vacuum values. Finally, when $n_0 > 5 \cdot 10^{12}$ cm^{-3}, E_z was reduced by an order of magnitude and H_z disappeared completely. The "skinning" of the fields occurs because with increasing density the transformation point shifts outwards from the center of the plasma column. The diamagnetism signal stops increasing after the density increased to $5 \cdot 10^{12}$ cm^{-3}. There are probably two reasons for this: reduction in introduced energy per particle, and reduction in heating efficiency as the transformation point approaches the wall. The radial distributions of the fields E_r and H_z measured by displacing the probes are shown in Fig. 2.

At moment of time t_1 (Figs. 2 and 3) the field E_r at the center is greater than at the periphery, while at t_2 it falls somewhat towards the center. The magnetic field is diminishing by the skin effect at this moment and at the periphery does not exceed the vacuum value. The heating of the plasma thus cannot be explained by geometric magnetoacoustic resonance of the plasma column. The radial field distributions shown in Fig. 2 demonstrate that there is no large-amplitude reflected wave. In this case the phase of the electromagnetic fields in the plasma must vary smoothly along the radius.

The phase measurements were performed as described above. The results (Fig. 4) show that at moment t_1 the phase variation corresponded to an increase of phase velocity of the wave in the radial direction. At this time the radial electric field of the wave, E_r, exceeded the field value in the absence of plasma (see Fig. 3a).

The increase in the phase velocity and amplitude of the electromagnetic wave can be explained by the reduction to zero of the radial component of the wave vector k_r of the extraordinary (H) wave at some value of the plasma density. The theory of wave propagation in an unbounded plasma can be used to estimate the plasma density corresponding to this condition. The estimates give $\omega_{oe}^2 \sim \omega\omega_{He}$. Under the conditions of the experiment this corresponds to $n \sim 10^{10}$ cm^{-3}. It can be seen from Fig. 3 that the plasma density at moment t_1 is appreciably less than 10^{12} cm^{-3}. It follows from Maxwell's equations that, for a given H_z and $(\tilde{E}_\varphi/\tilde{H}_z) \sim (k_0/k_r)$, i.e., $k_r \to 0$, the azimuthal electric field $E\varphi$ increases in an unbounded manner. Here $k_0 = \omega/c$. The increase of E_φ is accompanied by an increase in the radial drift of the electrons, and the radial polarization electric fields accordingly also increase. This can explain the experimentally observed

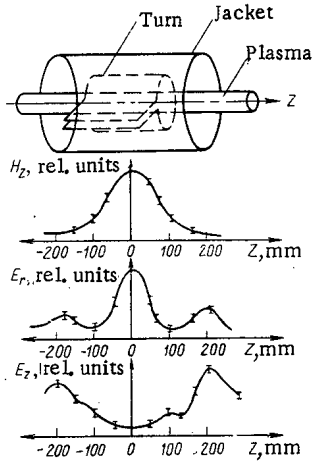

Fig. 1

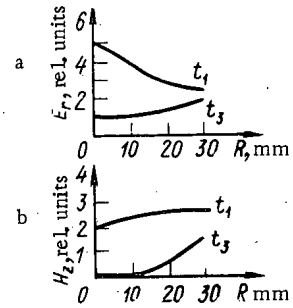

Fig. 2

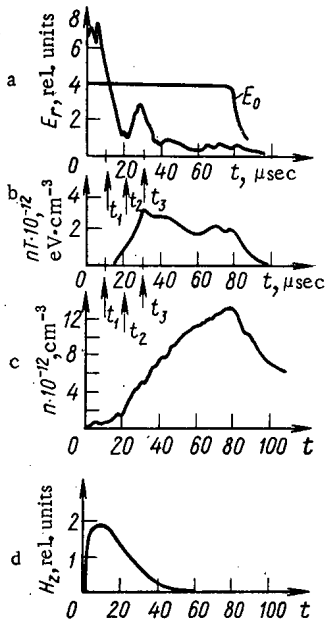

Fig. 3

Fig. 1. Distribution of electromagnetic fields along axis of device.

Fig. 2. Radiation distributions of: a) electric; b) magnetic field of wave. The time values t_1 and t_3 are specified in Fig. 3.

Fig. 3. Time variation during high-frequency pulse of: a) radial electric field E_r on discharge axis (E_0 is field in absence of plasma); b) diamagnetism signal; c) plasma density; d) magnetic field; H_z) of wave in plasma.

rise of E_r at moment t_1. The radial phase variations of the fields at moments t_2 and t_3 corresponded to a slowing down of the wave along the radius. At these moments a rise was observed in the amplitude of the radial field and the diamagnetism signal increased. These facts demonstrate that the heating is connected with the appearance of a retarded wave. Such a wave probably occurred through the transformation of the electromagnetic wave into a plasma wave. The maximum radial variation of phase was observed at moment t_2, i.e., when the diamagnetism signal (plasma heating) is increasing most rapidly, at a radius 5-10 mm. At moment t_3 maximum phase variation was observed at a larger radius. This sort of behavior of the maximum phase variation can be explained by the displacement of the transformation point towards the outer region of the plasma column as the plasma density increases. This accords with the "skinning" of the electric fields at moment t_3 (see Fig. 2).

Regimes in which a hotter plasma was obtained corresponded to larger variations of phase. The local refractive index can be calculated from $N_r(r) = (c/\omega)(d\varphi/dr)$ [5], where ω is the wave frequency, c is the velocity of light, and r is the radius of the plasma column. Maximum $N_r = 100$ and corresponded to a radius r = 7-10 mm. For a Cerenkov mechanism of energy accumulation the ion velocity must not exceed the velocity of the retarded wave. The wave velocity corresponding to the maximum measured refractive index and equal to $3 \cdot 10^8$ cm/sec is comparable with the maximum ion velocity observed experimentally (ion energy ~2 keV). The accuracy of the N_r determinations was limited by the dimensions of the probe, since the efficiency of recording waves of wavelength smaller than the dimenions of the probe is low. Similar measurements were carried out with a magnetic probe in the plasma. The magnitude of the H_z phase variation was 3-5 times smaller than for the electric field (see Fig. 4b). This confirms that E waves have a larger refractive index than H waves. With increasing axial magnetic field the phase variation of the electromagnetic wave after traversal through the plasma increased almost in proportion to the magnetic field.

The measurements reported above lead to the following conclusions:

1. The method of energy insertion used in our experiments assured the excitation and penetration into the plasma of H and E.

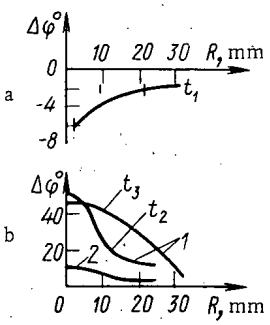

Fig. 4. Radial phase variation of wave in plasma. The wave is slowed down for a positive phase and speeded up for a negative phase. a) Radial phase variation of E_r at moment t_1; b) radial phase variation of E_r at moments t_2 and t_3 (curves 1) and of H_z (curve 2).

2. As the ion component of the plasma heated up (to ~100 eV) there was an accompanying increase in the amplitude of the electric fields in the plasma and decrease in the phase velocity of the electromagnetic wave.
3. During heating the substantial increase in the magnetic field of the wave characteristic of magnetoacoustic resonance was not observed.
4. Volume resonances of the plasma column were not observed. The heating of the ion component of the plasma must accordingly be ascribed to the collisionless Cerenkov mechanism of absorption of slow plasma waves.

LITERATURE CITED

1. V.M. Glagolev, "Propagation and absorption of ion hybrid waves in a weakly inhomogeneous plasma layer" [in Russian], Preprint Institut Atomnoi Energii (1970). See also: V.M. Glagolev, Plasma Physics, 14, 301-314 (1972).
2. V.E. Golant and A.D. Piliya, Usp. Fiz. Nauk, 104, No.3 (1971).
3. V.F. Tarasenko et al., Zh. Tekh. Fiz., 42, No.9, 1996 (1972).
4. I.A. Kovan et al., At. Energ., 25, 503 (1968).
5. V.M. Glagolev, N.A. Krivov, and Yu.V. Skozyrev, Proc. Fourth International Conference on Plasma Physics and Controlled Thermonuclear Fusion Magate [in Russian], Report CN-28/L-6.(1971).
6. V.M. Glagolev, I. N. Khromkov, and N.S. Cheverev, At. Energ., 20, 401 (1966).
7. Yu. N. Dnestrovskii, D.N. Kostomarov, and G.V. Pereverzev, International Conf. on Phenomena in Ionized Gases, Oxford (1971), p.343.
8. N.V. Ivanov, I.A. Kovan, and E.V. Los', At. Energ., 32, 389 (1972).

ABSTRACTS

OPTIMIZATION OF THE CYCLICITY OF OPERATION OF A RESEARCH REACTOR

K. A. Konoplev and Yu. P. Semenov

UDC 621.039

Nuclear reactors as tools for physical investigations are very common devices, their power and cost of operation have been increasing; therefore, the question of the most economical operation of the reactors acquires very significant importance [1, 2].

In the present paper we attempt to optimize the cyclicity of reactor operation (without solving the questions of the refinement of the physical parameters and reprocessing of fuel) and we determine the parameters of the cycle for which the cost per unit thermal energy developed is a minimum. We consider cores that permit cassette reloading to be made.

By the cycle of operation of a reactor we shall mean the time interval from a start-up to the following start-up, i.e., the sum of the times of operation of the reactor (α days) and its station (β days).

The cost of 1 MW·day of thermal energy developed by a reactor is

$$A=\frac{\gamma(\alpha+\beta)+\beta_q}{W\alpha}+\frac{ag}{y}+\frac{Q}{W}, \quad (1)$$

where γ is the cost of maintaining a reactor neglecting the cost of the fuel, electrical energy, and materials consumed during the operation, rubles/day; g is the cost of fuel in the fuel assembly, rubles/g; W is the power of the reactor, MW; y is the mean depletion of the fuel assemblies unloaded from the reactor at the end of each operating cycle; Q is the consumption of electrical energy and materials when the reactor is producing power, rubles/day; q is the consumption of electrical energy and materials when the reactor is shut down, rubles/day; a is the amount of fissionable material needed to develop 1 MW·day, which weakly depends on the type of fuel and the neutron spectrum, taken equal to 1.3 g U^{235}/(MW·day).

To analyze the cost A as a function of a we must give the dependence of the mean depletion of the unloaded fuel y on the mean depletion of the fuel in the zone $\varkappa$. We assume that

$$y=\frac{2k}{k+n}\varkappa,$$

where k is the number of fuel assemblies that form the core; n is the number of fuel assemblies reloaded at the end of the cycle, where

$$n=\frac{aW\alpha}{by}.$$

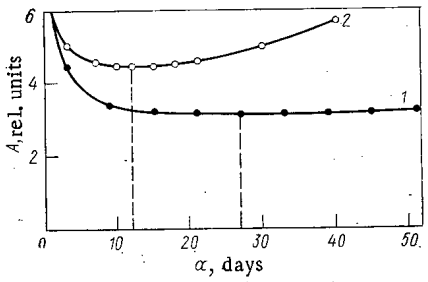

Fig. 1. The function $A = f(\alpha)$ (α_{1opt} = 27 days; α_{2opt} = 12.3 days): 1) $\varkappa$ = 0.27; k = 78; 2) $\varkappa$ = 0.14; k = 62.

Translated from Atomnaya Énergiya, Vol. 35, No. 4, pp. 263-266, October, 1973. Original article submitted July 21, 1972.

We can show that there exists an optimal value α_{opt}, for which the cost for the operation of the reactor is a minimum, and that

$$\alpha_{opt} = -\frac{2bk\varkappa\beta}{aW\left(\frac{gbk}{\gamma+q}-\beta\right)} + \sqrt{\left[\frac{2bk\varkappa\beta}{aW\left(\frac{gbk}{\gamma+q}-\beta\right)}\right]^2 + \frac{4b^2k^2\varkappa^2\beta}{a^2W^2\left(\frac{gbk}{\gamma+q}-\beta\right)}}, \quad (2)$$

where b is the number of grams of U^{235} in one fuel assembly.

The dependence of A on α for $\beta = 3$ for the VVR-M reactor of the Leningrad Nuclear-Physics Institute is presented in Fig. 1. Similar dependencies are shown for a number of values of the parameters appearing in Eq. (2).

For reactors of type VVR-M the quantity A varies most significantly for increase in cycle length in the limits up to two weeks. If we extend the operating period from four to eleven days under specified conditions the cost of the thermal energy can be decreased by 20%.

LITERATURE CITED

1. A.S. Kochenov, At. Energ., 21, No. 2, 97 (1966).
2. V.A. Tsykanov, At. Energ., 31, No. 1, 15 (1971).

SPECIAL FEATURES ON THE RESONANCE ABSORPTION OF NEUTRONS FOR INTERMEDIATE LEVELS

A.P. Platonov and A.A. Luk'yanov

UDC 539.125.5.173.162.3:539.125.5.162.3

The value of the effective resonance integral is a quantitative characteristic of the resonance escape probability. In determining this quantity various approximations are commonly made for the energy dependence of the neutron spectrum in the resonance region. The straightforward way of estimating the accuracy of the approximate calculations is to compare them with accurate results. We use a numerical procedure for solving the equation for the slowing down of neutrons in an infinite homogeneous medium developed in [1] to determine the spectrum of the neutron flux in the neighborhood of two intermediate U^{238} resonances at 189.6 and 208.6 eV for the systems U – H, U – O, U – Fe, and U – Pb (Fig. 1). The spectra obtained were used to calculate the effective U^{238} resonance integrals for various values of the scattering cross section of a nonresonance moderator σ_m and various temperatures of the medium.

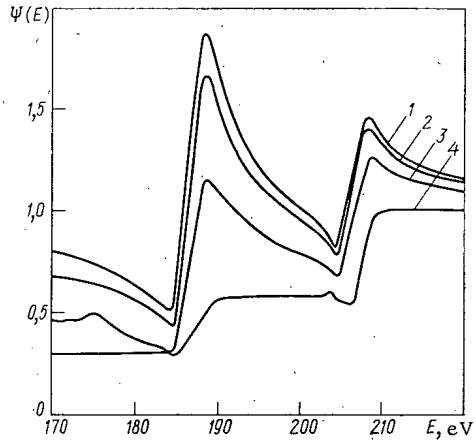

Fig. 1. Neutron collision density $\psi(E)$ in homogeneous mixtures of U^{238} with H, O, Fe, and Pb (curves 1-4, respectively) for $\sigma_m = 10b$ and the medium at 300°K.

Original article submitted November 9, 1972; abstract submitted May 21, 1973.

The values of the resonance integrals for the U^{238} levels mentioned above calculated by using the familar approximations differ from the results of numerical calculations for concentrated media by up to 25-30%. The effective resonance integrals for the moderators studied vary with the concentration and temperature of the medium, taking account of the fine structure of the collision density spectrum in the same way as in the NR-approximation, taking account of the interference of resonance and potential scattering [2]. For media with the same concentrations and temperatures the resonance integral is found to depend strongly on the atomic weight of the nonresonance moderator. The "intermediacy" of selected U^{238} levels was investigated for parameters of the IR-approximation scheme [3]. The significant differences in the values of these parameters determined from the numerical calculation and by the analytic method for concentrated media are due to a detailed accounting of the energy dependence of the cross sections and the collision density spectrum in the neighborhoods of the resonances.

LITERATURE CITED

1. A.P. Platonov, Zh. Vychisl. Matem. i Matem. Fiz., 12, 1325 (1972).
2. L.P. Abagyan et al., Byull. Inform. Tsentra Yadernykh Dannykh. Prilozhenie, Atomizdat, Moscow (1968).
3. R. Goldstein and E. Cohen, Nucl. Sci. and Engng., 13, 132 (1962).

USE OF SUPERPOSITION IN CALCULATING THE TEMPERATURE OF A REACTOR CORE COOLED BY A LIQUID METAL

A.A. Sholokhov and V.E. Minashin

UDC 621.039.5:536.24

The steady-state temperature distribution in a reactor core is adequately described by the linear equation [1]

$$w(x, y)\, c(x, y)\, \gamma(x, y) \frac{\partial t(x, y, z)}{\partial z} - \nabla\lambda(x, y)\, \nabla t(x, y, z) = q_v(x, y, z).$$

The temperature which results from many sources is equal to the sum of the temperatures due to the individual sources, and therefore the temperature at an arbitrary point in the core can be calculated by the formula

$$t(x, y, z) = \sum_{k=1}^{m} C_k \sum_{i=1}^{N_k} n_{k,i} A_{k,i} \int_0^z \eta_k'(\xi)\, t^*_{k,i}(x, y, z-\xi)\, d\xi,$$

where $t^*_{k,i}$ is a particular solution for the release of heat in the k-th fuel element of the i-th group; $\eta(z)$ is the distribution along the fuel element. For liquid metals molecular heat conduction makes a large contribution to heat transfer, and the coefficients in the equation vary slowly with velocity. Under these conditions temperature for a varying velocity w can be calculated in terms of the Green's functions $t^*_{k,i}$ found for a previous velocity w_0:

$$t(x, y, z) = \sum_{k=1}^{m} C_k \sum_{i=1}^{N_k} n_{k,i} A_{k,i} \int_0^z \eta_k'(\xi)\, t^*_{k,i}[\beta(z-\xi)]\, d\xi,$$

where $\beta = w_0/w$.

The nonstationary temperature distribution in the core is described by the equation

$$wc\gamma \frac{\partial t}{\partial z} + c\gamma \frac{\partial t}{\partial \tau} - \nabla\lambda\nabla t = q_v(x, y, z, \tau).$$

Original article submitted November 15, 1972; abstract submitted June 11, 1973.

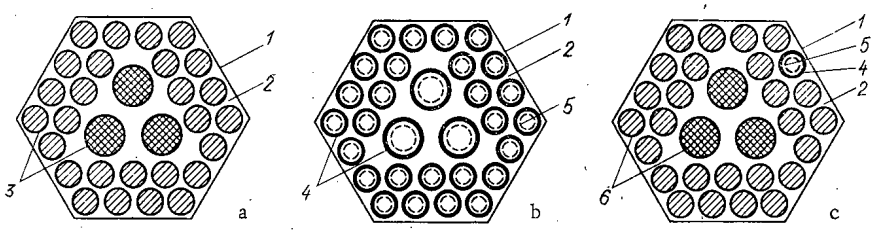

Fig. 1. Experimental and simulated reactor cells: a) a fuel rod assembly; b) tubes containing electric heaters to mock up fuel elements; c) solid rod mock-ups; 1) shell; 2) coolant; 3) fuel elements; 4) tubular heater; 5) helix; 6) fuel elements or mock-ups of them.

Let $q_V = q_{V,0} f(x, y) \eta(z)(1 + \varphi(\tau))$. Then the time-dependent temperature distribution is given by

$$t(x, y, z, \tau) = \sum_{k=1}^{m} C_k \sum_{i=1}^{N_k} n_{k,i} A_{k,i} \int_0^z \eta_k'(\xi) \left\{ t^*_{k,i}[\beta(z-\xi), \tau=0] + \int_0^\tau \varphi'(\tau')\, t^*_{k,i}[\beta(z-\xi), \tau-\tau'] \right\} d\xi\, d\tau',$$

where $t^*_{k,i}$ is an elementary Green's function given by

$$wc\gamma \frac{\partial t^*}{\partial z} + c\gamma \frac{\partial t^*}{\partial \tau} - \nabla\lambda\nabla t^* = q_{v,0} f(x, y)\, \eta^*(z)\, \varphi^*(\tau).$$

Here $\eta^*(z)$ and $\varphi^*(\tau)$ are unit functions.

The Green's functions are found experimentally by a substitution method [2]. For example, in order to investigate a subassembly of the core (Fig. 1a) a model must be constructed with electric heaters as shown in Fig. 1b. It is sufficient to perform a series of experiments with one heater (Fig. 1c), putting it in place of a mock-up or a fuel element whose Green's function is to be determined. In this way the accuracy of the simulation is increased.

LITERATURE CITED

1. V.E. Minashin, A.A. Sholokhov, and Yu.I. Gribanov, Thermophysics of Liquid Metal Cooled Reactors and Methods of Electric Simulation [in Russian], Atomizdat, Moscow (1971).
2. V.E. Levchenko, V.E. Minashin, and A.A. Sholokhov, Byull. Izobret., 35, 67 (1968).

BUILDUP OF SCATTERED RADIATION BEHIND A SHADOW SHIELD

V.L. Generozov, V.A. Sakovich, and V.M. Sakharov

UDC 621.039.78:539.12.172

The Monte Carlo method has been used to calculate doses of scattered radiation at various distances from the surface of a shield of finite transverse dimensions for monodirectional and cosine disk sources of neutrons and γ-rays.

The same programs were used in the calculations as in [1-3]. The source and the adjoining cylindrical shield had diameters d = 50 cm. The biological dose produced by neutrons with a reactor spectrum was calculated at points behind slab shields of polyethylene (ρ = 0.92 g/cm^3) 10, 20, 30, and 40 cm thick. The energy flux of γ radiation was calculated at points behind tungsten slab shields of thicknesses 2, 4, 6, and 8 mean free paths at the source energy E_0 for E_0 equal to 0.5, 1.25, and 5 MeV.

Original article submitted November 23, 1972; revision submitted May 4, 1973; abstract submitted May 21, 1973.

The calculations were performed for a detector placed on the axis of symmetry on the surface of the shield and at distances of 0.2, 0.5, 2.0, and 5.0 m from it. The statistical error was estimated by the method of successive distributions; in simulating 6000 histories it was 2-10%.

From the results obtained we can recommend the following formulas for the dose behind a finite shield in terms of data for an infinite shield:

$$D(t, R)=\begin{cases} D^{S}(t) & \text{for } R \ll d; \\ D^{S}(t)\dfrac{\xi(t, E_0)}{R^2} & \text{for } R \gg d, \end{cases}$$

where t is the shield thickness, R is the distance from the shield in meters, D^S is the radiation dose at the surface behind an infinite slab shield and $\xi(t, E_0)$ is a scale factor depending on the angular distribution of the source, the kind of radiation, and the shield thickness.

For the neutron dose behind a polyethylene shield for a cosine source with a reactor spectrum the value of $\xi(t, E_0)$ for t = 20-40 cm is 0.093-0.1. For γ rays with energies E_0 equal to 0.5, 1.25, and 5 MeV from a cosine source the values of ξ behind a tungsten shield are the following: for a thickness of one mean free path ξ = 0.13-0.15; for 6 mfp ξ = 0.17-0.26, and for 8 mfp ξ = 0.2-0.4.

We have not calculated ξ for a large number of materials or for other angular distributions of the source, but the results obtained show clearly that the range of ξ values is rather narrow.

LITERATURE CITED

1. V.L. Generozov and V.A. Sakovich, At. Energ., 28, 175 (1970).
2. V.L. Generozov and V.A. Sakovich, At. Energ., 30, 536 (1971).
3. Yu.A. Vakarin et al., in: Dosimetry and Radiation Shielding Problems [in Russian], L.R. Kimel' (editor), Atomizdat, Moscow, No.12, p.117.

LETTERS TO THE EDITOR

THERMODYNAMIC PROPERTIES AND MUTUAL DIFFUSION IN THE SYSTEM UC – ZrC

G.B. Fedorov, V.N. Gusev,
V.N. Zagryazkin, and E.A. Smirnov

UDC 539.219.3:669.822

This article continues our work on the diffusion properties of the system UC – ZrC [1]. To calculate the coefficients of mutual diffusion we used the results of an analysis of diffusion in three-component systems with one interstitial element [2]. With certain approximations, the relation between the coefficients of mutual diffusion and the coefficients of diffusion of radioactive atoms of the components of the system and the thermodynamic properties is as follows:

$$\left.\begin{aligned}
&\tilde{D}_{11}=\tilde{D}_{22}=N_2D_1^*g_{11}+N_1D_2^*g_{22};\\
&\tilde{D}_{13}=-\tilde{D}_{23}=\frac{N_1N_2}{N_3}(D_1^*g_{13}-D_2^*g_{23});\\
&\tilde{D}_{33}=D_3^*g_{33}-(N_1D_1^*g_{13}+N_2D_2^*g_{23});\\
&\tilde{D}_{31}=\frac{N_3}{N_1}D_3^*g_{31}-N_3(D_1^*g_{11}-D_2^*g_{22}),
\end{aligned}\right\} \quad (1)$$

where

$$g_{ij}=\delta_{ij}+\frac{\partial \ln \gamma_i}{\partial \ln N_j}; \quad (2)$$

δ_{ij} is the delta function, N_i is the ratio of the number of atoms of species i in a local volume to the number of lattice γ_i is the coefficient of thermodynamic activity of the i-th component, and D_i^* is the coefficient of diffusion of radioactive atoms of the i-th component. Here and below, N_1 and N_2 refer to the elements of substitution (uranium and zirconium, respectively), and N_3 to the interstitial element; $N_1 + N_2 = 1$.

In Eqs. (1), as D_i^* we used the previously-measured diffusion coefficients of the components of the system UC – ZrC [1]. The values of the thermodynamic factors g_{ij} were determined by means of models of the thermodynamics of the system [3].

The monocarbides $U_{1-x}C_x$ and $Zr_{1-x}C_x$ form a solid solution in accordance with the reaction

$$(1-z)\,U_{1-x}C_x+zZr_{1-x}C_x \rightleftharpoons U_{(1-z)(1-x)}Zr_{z(1-x)}C_x, \quad (3)$$

where x is the atomic fraction of carbon, $x < 0.5$, and z is the molar fraction of monocarbide, $0 \leq z \leq 1$.

The activities of the components in this solution can be represented [3] in the form

$$\ln a_U^{III}=\ln a_U^{I}+\frac{xz}{1-x}[\ln a_C^{I}-\ln a_C^{II}]-z^2\frac{\Delta L}{RT}+\ln(1-z); \quad (4)$$

$$\ln a_{Zr}^{III}=\ln a_{Zr}^{II}+\frac{x(1-z)}{1-x}[\ln a_C^{II}-\ln a_C^{I}]-(1-z^2)\frac{\Delta L}{RT}+\ln z; \quad (5)$$

$$\ln a_C^{III}=(1-z)\ln a_C^{I}+z\ln a_C^{II}, \quad (6)$$

where the index I denotes reference to the monocarbide $U_{1-x}C_x$, index II denotes reference to the monocarbide $Zr_{1-x}C_x$, and index III denotes reference to the three-component solid solution; ΔL is the energy of interexchange, used in the theory of regular solutions.

To calculate the activities of the components in the monocarbides we used the methods of statistical thermodynamics [4]. In contrast to the work described in [5, 6], in which a statistical approach was also used, in our present work the ensemble of particles formed by the atoms of the monocarbides is regarded

Translated from Atomnaya Énergiya, Vol. 35, No. 4, pp. 267-269, October, 1973. Original article submitted December 6, 1972.

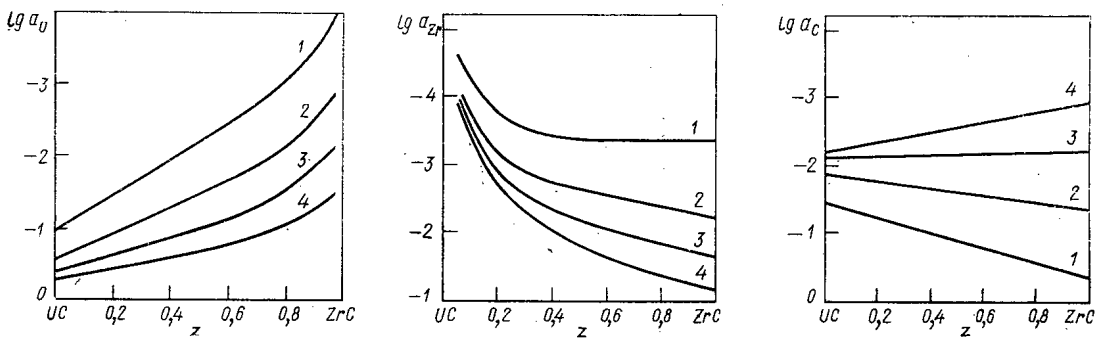

Fig. 1. Concentration dependences of activities of uranium, zirconium, and carbon in system $U_{(1-z)(1-x)}Zr_{z(1-x)}C_x$ at 2200°C: 1) x = 0.49; 2) x = 0.47; 3) x = 0.45; 4) x = 0.43.

TABLE 1. Values of Parameters E_{ij} (kcal/g-atom) and S_{ij} (cal/(g-atom · deg))

Carbide	$E_1+0.5E_{11}$	E_{22}	$E_{22}+E_{12}$	$S_1+0.5S_{11}$	S_{22}	S_2+S_{12}
UC	−37±3	−100±10	60,5±6	−15,8±2	−38,2±3	37,2±3
ZrC	56±8	−191±25	−197±30	15±3	39±6	−35±6

as "united." The grand statistical sum Q of this ensemble [5] takes the form

$$Q=\sum_{M_1}\sum_{M_2}\frac{M_1!}{(M_1-M_2)!\,M_2!}a^{N_1}a^{N_2}\exp\left[-\frac{F(M_1,\ M_2,\ T,\ V)}{kT}\right], \qquad (7)$$

where M_1 and M_2 are the numbers of metal and carbon atoms, a_1 and a_2 are the activities of the metal and carbon, and $F(M_1, M_2, T, V)$ is the Helmholtz free energy, equal to the sum of the changes in the free energies of the atoms for the formation of the compound from standard components. The free energy is a function of the number of atoms, the temperature, and the volume V of the system. As the standard states we take pure metal and graphite. The free energy of the system can be written as

$$F(M_1,\ M_2,\ T,\ V)=M_1(F_1+0.5F_{11})+\frac{M_2^2}{2M_1}F_{22}+M_2(F_2+F_{12}), \qquad (8)$$

where F_1 and F_2 are the free energies necessary for transfer of atoms of the substance from the standard state to the NaCl structure, and F_{11}, F_{12}, and F_{22} are the free energies of interaction between the atoms. By means of the relation F = E − TS relating the Helmholtz free energy with the energies E and the entropies S, for each value F_{ij} (i = 1, 2; j = 0, 1, 2) we can choose corresponding values of F_{ij} and S_{ij}. For a regular ensemble the entropy of pairwise interaction is S_{ij} = 0 [4] (this means that the internal degrees of freedom do not depend on the atomic environment). The grand statistical sum for a regular ensemble was used in [6, 7] to estimate the energies of pairwise interaction in nitrides and carbides. However, the question of the applicability of the regular approximation to refractory compounds of transition metals has not yet been investigated.

In the usual way [4], converting from Eq. (7) to activities, we get

$$RT\ln a_1=E_1+0.5E_{11}-0.5\left(\frac{x}{1-x}\right)^2E_{22}-T\left[R\ln\frac{1-x}{1-2x}+S_1+0.5S_{11}-0.5\left(\frac{x}{1-x}\right)^2S_{22}\right]; \qquad (9)$$

$$RT\ln a_2=E_2+E_{12}+\left(\frac{x}{1-x}\right)E_{22}-T\left[R\ln\frac{1-2x}{x}+S_2+S_{12}+\left(\frac{x}{1-x}\right)S_{22}\right], \qquad (10)$$

where $\ln a_1$ corresponds to $\ln a_U^I$ or $\ln a_{Zr}^{II}$, and $\ln a_2$ to $\ln a_C^I$ or $\ln a_C^{II}$ in Eqs. (4)-(6).

Analysis of the experimental data in [8] on the activity of niobium in the region of homogeneity of its monocarbide on the basis of Eqs. (9) and (10) enabled us to explain the observed experimental concentration dependence of the partial excess entropy of formation of niobium in its monocarbide.

The values of E_{ij} and S_{ij} in Eqs. (9) and (10) (Table 1) were estimated on the basis of experimental data on the activities of uranium and carbon in uranium monocarbide [9, 10] and also from the results of an analysis of the phase diagram of zirconium – carbon [10].

The value of the energy of interaction in Eqs. (4)-(6) for the system UC – ZrC is equal to 6000 cal/g · mole [11].

Figure 1 shows the concentration dependences of the activities of the components in the system UC – ZrC at 2200°C for various values of x. On the basis of these results we calculated the thermodynamic

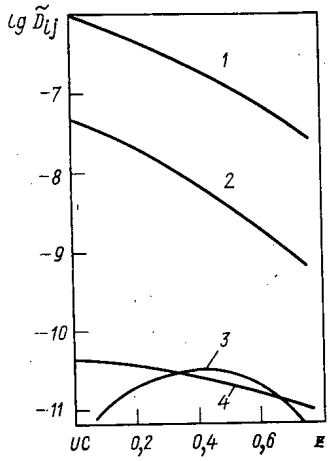

Fig. 2. Concentration dependences of coefficients of mutual diffusion in the system $U_{(1-z)(1-x)}Zr_{z(1-x)} \cdot C_x$ at 2200°C (x = 0.46). 1) D_{33}; 2) D_{31}; 3) D_{13}; 4) D_{11}.

TABLE 2. Values of g_{ij} for Some Compositions of the System $U_{(1-x)(1-x)}Zr_{z(1-x)}C_x$ at x = 0.46 (t = 2200°C)

g_{ij}	z			
	0	0,23	0,51	0,72
g_{11}	2,85	2,4	1,4	1,2
g_{22}	1,0	1,5	1,5	1,5
g_{33}	6,5	9,8	14,7	19,2
g_{13}	−6,0	−9,5	−13,2	−16,5
g_{23}	6,0	−9,5	−13,3	−16,6
g_{31}	0,4	0,29	0,17	0,15

factors (2) of the quasibinary cross section of the system x = 0.46 (Table 2), for which we investigated the diffusion of radioactive atoms of the components [1]. We assumed that $N_1 = 1 - z$, $N_2 = z$, and $N_3 = x/(1-x)$. Similar calculations for the systems ZrC – NbC and TiC – ZrC were made in [12].

From the results, with the aid of Eq. (1) we calculated the coefficients of mutual diffusion, the concentration dependences of which are shown in Fig. 2. The coefficients $\tilde{D}_{11}$, $\tilde{D}_{22}$, $\tilde{D}_{13}$, and $\tilde{D}_{23}$ in Eqs. (1) are expressed purely in terms of the diffusion coefficients of radioactive atoms of the elements of substitution ($\tilde{D}_{11}$ corresponds to the ordinary coefficient of mutual diffusion in the binary system). The difference is due to the fact that D_1^*, D_2^*, g_{11}, and g_{22} in Eqs. (1) depend on N_3. The coefficients $\tilde{D}_{13}$ and $\tilde{D}_{23}$ characterize the influence of the force field due to the interstitial atoms on the displacement of the atoms of substitution; therefore they are also expressed only in terms of D_1^* and D_2^*.

The equations for $\tilde{D}_{33}$ and $\tilde{D}_{31}$ involve all three diffusion coefficients of the components, owing to involvement of interstitial atoms in mechanical motion of a nondiffusive nature associated with the difference between D_1^* and D_2^* (the Kirkendall effect).

As we see from Fig. 2, the coefficients $\tilde{D}_{11}$, $\tilde{D}_{33}$, and $\tilde{D}_{31}$ are monotonic functions of composition; they decrease rapidly as uranium monocarbide is diluted with zirconium monocarbide. This decrease in the coefficients of mutual diffusion is due to a decrease in D_i^* [1]. Note that the marked decrease in D_i^* and $\tilde{D}$ in binary systems as the concentration of the more refractory component increases was previously observed for a number of metallic systems, including zirconium – niobium [13], uranium – niobium [14], etc.

The concentration dependence of $\tilde{D}_{13}$ is a parabola, which is mainly due to the factor N_1N_2/N_3. We must remember that this coefficient is determined with the lowest degree of accuracy because it involves a difference of comparable quantities. Whereas in the calculation of $\tilde{D}_{11}$, $\tilde{D}_{33}$, and $\tilde{D}_{31}$ the errors are 30-40%, $\tilde{D}_{13}$ is determined only to within an order of magnitude. A considerable contribution to the errors in the $\tilde{D}_{ij}$ may be made by inaccurate determination of the chemical composition of the alloy, which is particularly bad in the calculation of the g_{ij} for the given system with a narrow region of homogeneity.

If we regard the coefficients of mutual diffusion in a multicomponent system as diffusion-thermodynamic criteria of heat resistance [15], we can suppose that as zirconium carbide is added the strength of the interatomic bonds in the solid solutions of the system UC – ZrC increases. This is confirmed by the results of a previous investigation of the diffusion of the components in the system [1].

LITERATURE CITED

1. G.B. Fedorov et al., At. Energ., 32, No. 7, 584 (1972).
2. K.P. Gurov and R.A. Andrievskii, Fiz. Metallov i Metallovedenie, 29, 757 (1970).
3. G. de Poorter and T. Wallace, Fundamentals of Refractory Compounds, H. Housner and M. Bowmon (editors), Plenum Press, New York (1968), pp. 1-16.

4. R. Fowler and E.A. Guggenheim, Statistical Thermodynamics [in Russian], IL, Moscow (1949).
5. V.N. Zagryazkin et al., Zh. Fiz. Khim., 47, No.8, 1946 (1973).
6. M. Hooch, in: Phase Stability in Metals and Alloys [Russian translation], Mir (1970), p.356.
7. G. de Poorter, J. Amer. Ceram. Soc., 52, 311 (1969).
8. E. Storms et al., High Temper. Sci., 1, 430 (1969).
9. E. Storms, Thermodynamics, Vol.1, IAEA, Vienna (1966), p.309.
10. E. Storms, Refractory Carbides [Russian translation], Atomizdat, Moscow (1970), p.234.
11. R.A. Andrievskii, V.N. Zagryazkin, and R.A. Lyutikov, Thermodynamics of Nuclear Materials, IAEA, Vienna (1968), p.449.
12. R.A. Andrievskii, Poroshkovaya Met., No.2 (122), 76 (1973).
13. G.B. Fedorov et al., in: Metallurgy and Physical Metallurgy of Pure Metals [in Russian], Atomizdat, Moscow (1971), 9th Edn., p. 37.
14. G.B. Fedorov, E.A. Smirnov, and V.N. Gusev, At. Energ., 32, No.1, 11 (1972).
15. G.B. Fedorov and E.A. Smirnov, in: Structure and Properties of Heat-Resistant Metallic Materials [in Russian], Nauka, Moscow (1973), p.171.

AN APPARATUS FOR STUDYING THE KINETICS OF THE LIBERATION OF INERT GASES FROM MATERIALS DURING ISOTHERMAL ANNEALING

D.M. Skorov, A.I. Dashkovskii,
A.G. Zaluzhnyi, and O.M. Storozhuk

UDC 621.039.548.343

The mechanical properties of a number of construction materials undergo a change under the action of neutron radiation. Several investigators connect this with the formation of helium in the materials as a result of nuclear reactions [1, 2]. The mechanism of this phenomenon can undoubtedly be clarified by studying the behavior of inert gases in the materials.

The present article contains a description of an apparatus for use in studying the kinetics of the liberation of inert gases from materials during the process of isothermal annealing. Figures 1 and 2 show the basic scheme of the proposed apparatus and a diagram of the vacuum system. The apparatus consists of a stainless steel high-vacuum chamber with a heater made of molybdenum or tungsten wire wound on an insulating tube in which the sample to be studied is placed. Since the insulating tube was made of quartz, the maximum temperature in this investigation was 1000-1100°C. Since the heater used in this apparatus has a very slow action, and is supplied by a regulated voltage, the sample temperature stays practically constant within the interval ±(2 + 3)°C during a prolonged isothermal annealing process. A molybdenum thermal shield cuts down the dissipation of the energy which is evolved. A sputter-ion pump is connected to the chamber (see Fig. 2) through a high-vacuum valve. A manometer tube is used to measure the vacuum. The active volume is connected via a flange to an RMO-4S omegatron tube placed between the poles of the permanent magnet of the omegatron. The chamber and magnet are rigidly fastened to a stand.

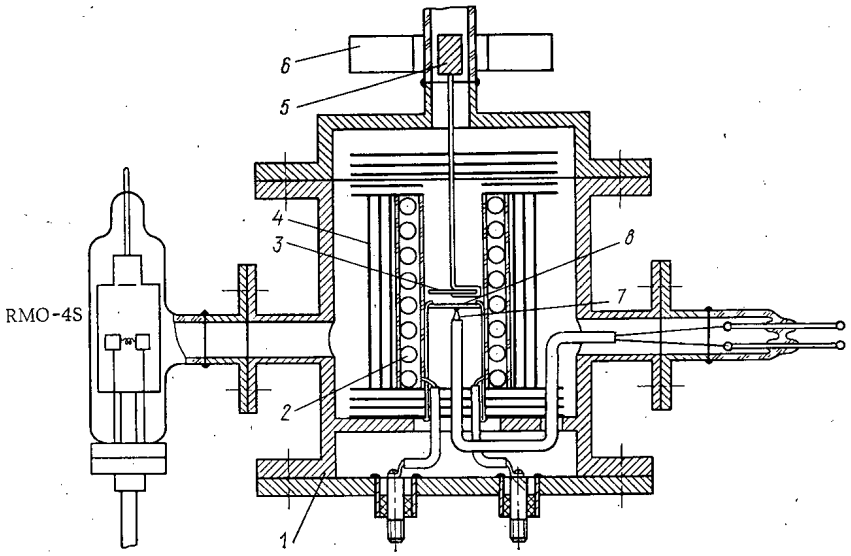

Fig. 1. Diagram of the apparatus: 1) high-vacuum chamber; 2) heater; 3) sample being studied; 4) thermal shield; 5) magnetic rod; 6) magnet; 7) thermocouple; 8) control sample.

Translated from Atomnaya Énergiya, Vol. 35, No. 4, pp. 269-271, October, 1973. Original article submitted December 18, 1972.

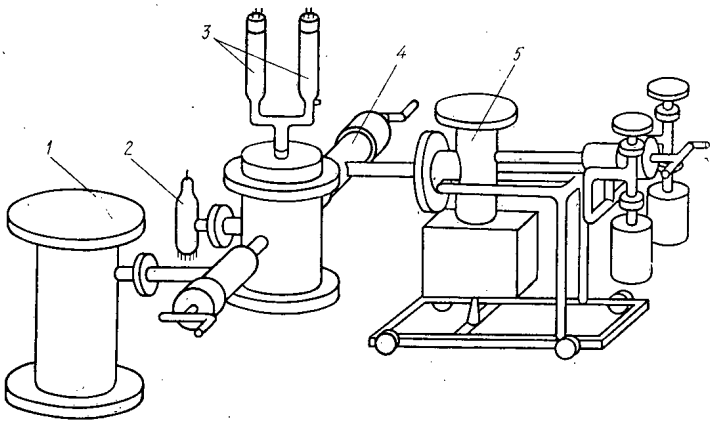

Fig. 2. Diagram of the vacuum system: 1) getter-ion pump; 2) omegatron tube; 3) manometer tubes; 4) high-vacuum valve; 5) sputter-ion pump.

The sample being studied, which is fastened to the magnetic rod by a magnet positioned on the outside of a glass tube connected via a Kovar inlet to the upper flange of the chamber, can shift in the vertical direction within the chamber. The magnitude of the shift corresponds to two positions of the sample within the chamber: in the center of the effective space of the heater, and outside the zone of heating. A thermocouple in contact with the control sample is used to measure the temperature of the sample. The sample being studied in the annealing process is located 1-2 mm from the control sample. The temperatures of the control sample and the sample being studied are the same, since the distance between them is very small compared to the size of the heater (the length of the heater is ~140 mm), and the samples in the annealing process are located at the center of the heater where there is no vertical gradient of the temperature. The accuracy of the measurement of the temperature of the sample being studied is determined by the accuracy of the thermocouple. A getter-ion pump is attached to the annealing chamber via a lateral flange.

The vacuum system of the apparatus is evacuated beforehand to a residual pressure of 10^{-7}-10^{-8} mm Hg, and the functioning subassemblies of the apparatus are outgassed by using external heaters to heat them to 450°C. The outgassing of the subassemblies of the apparatus is finished by bringing the heater up to the assigned temperature, with the sample located outside the heating zone. The volume of the annealing chamber is then evacuated by a getter-ion pump operating in the sorption mode, the sputter-ion pump is shut off from the chamber by using the high-vacuum valve, and the sample studied drops down into the heating zone. The getter-ion pump, operating in the sorption mode, evacuates only the chemically active gases [3], so that inert gases evolved from the sample in the annealing process accumulate in the active volume. The quantity of gas in the active volume is measured with an IPDO-1 instrument (measurement accuracy 10%, sensitivity $3 \cdot 10^{-10}$ mm Hg) [4]. The annealing of the samples can be carried on in a vacuum of the order of 10^{-7} mm Hg by continuously operating the getter-ion pump.

LITERATURE CITED

1. D.J. Harries, J. Brit. Nucl. Soc., 5, No.1, p.74 (1966).
2. R. Barnes, Nature, 206, No.4991, 1307 (1965).
3. A.F. Frensio and R.N. Dzhensen, in: Residual Gases in Electron Tubes [in Russian], Energiya, Moscow (1967), pp.196-205.
4. A.P. Averina, Pribory i Tekh. Eksperim., No.3, 123 (1962).

EFFECT OF ELECTRON-BEAM REMELTING ON THE HIGH-TEMPERATURE DUCTILITY OF STEEL 1Kh18N10T IRRADIATED WITH AN INTEGRATED FLUX OF $2.7 \cdot 10^{21}$ NEUTRONS/CM^2

A.N. Vorob'ev, V.N. Bykov,
Yu.S. Belomyttsev, V.D. Dmitriev,
and M.E. Smelova

UDC 621.039.531:669.14.018.8

It is well known that the irradiation of steels and alloys with austenitic structures leads to high-temperature embrittlement, which appears as a reduction in ductility at temperatures of around 0.5 T_m (°K) or over [1-6]. The majority of research workers regard helium, formed as a result of reactions of the (n → α) type as the main cause of this embrittlement. In a paper read by Soviet scientists at the Fourth Geneva Conference, the factors affecting high-temperature embrittlement were set out in detail [1]. One of the factors reducing the tendency of metals toward high-temperature embrittlement is purity [1, 4].

However, other authors [5] found that purity had no marked effect on the ductility of irradiated steels. Thus existing data provide no unambiguous conclusion as to the influence of purity on the high-temperature properties of irradiated steels.

In the present investigation we studied the effect of neutron irradiation on the high-temperature ductility of 1Kh18N10T steel produced by electric-arc and electron-beam melting. The chemical composition of the steel samples under consideration is given in Table 1 (principal constituents). The steel obtained by electron-beam melting contains much less manganese than that obtained in the usual manner. As regards the other alloying elements, the composition of each kind of steel differs in no way from the standard. In the steel produced by electron-beam melting there are 2-5 times less impurities than in that produced in the traditional way.

Plane samples 0.5 × 2 mm in cross section, with a working length of 7.5 mm, were cut from strips rolled with a 60% reduction and annealed for 0.5 h at 850°C. Then the samples were irradiated in a BR-5 reactor at 450-500°C to an integrated flux of $2.7 \cdot 10^{21}$ neutrons/cm^2. Neutrons with energies over 1 MeV made up 30% of the total flux. Tensile tests were carried out in vacuum at 550-850°C with an initial strain rate of 2.2×10^{-3} sec^{-1}. The results of tests on irradiated and unirradiated samples are shown in Fig. 1.

It was found that with increasing test temperature the relative elongation of the unirradiated steel of both melts increased continuously, the elongation depending little on the method of steel production. After irradiation the ductility of the steel produced in the ordinary manner increased with rising test temperature above 550°C, but remained lower in magnitude than that of the unirradiated steel. A similar change in the ductility of irradiated steels was observed earlier [7, 8]. For the 1Kh18N10T steel produced by electron-beam melting, irradiation had no effect on the high-temperature ductility up to 850°C.

TABLE 1. Chemical Composition of the Steel Studied

Method of producing the steel	Concentrations of elements, % wt.						
	C	Si	Mn	Cr	Ni	Ti	Fe
Electric-arc melting	0,12	0,24	1,10	17,0	10,8	0,57	Base
Electron-beam-melting	0,12	0,40	0,12	16,0	10,3	0,86	Base

Thus the results show that the high-temperature ductility of irradiated metals largely depends on their method of production (chemical composition and purity

Translated from Atomnaya Énergiya, Vol. 35, No. 4, pp. 271-272, October, 1973. Original article submitted January 8, 1973.

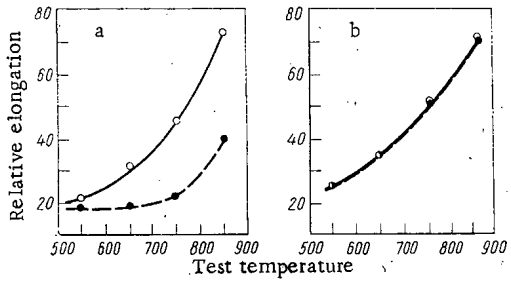

Fig. 1. High-temperature ductility of 1Kh18N10T steel: a) electric-arc melting; b) electron-beam melting; ——) before irradiation; – – –) after irradiation at 450-500°C with an integrated neutron flux of $2.7 \cdot 10^{21}$ neutrons/cm^2.

in the original state); similar conclusions were reached in [1, 4].

Thus 1Kh18N10T steel may be obtained in a state in which it is not subject to high-temperature embrittlement on irradiation with an integrated neutron flux of $2.7 \cdot 10^{21}$ neutrons/cm^2. The quantity of nuclear reaction products (helium, lithium, hydrogen, etc.) formed in electrom-beam melted 1Kh18N10T steel by irradiation with an integrated neutron flux of $2.7 \cdot 10^{21}$ neutrons/cm^2 is insufficient to produce high-temperature embrittlement.

LITERATURE CITED

1. N.P. Agapova et al., Fourth Geneva Conference (1971), paper 49/P/453 (USSR).
2. H. Bahm et al., Metallkunde, 57, 352 (1966).
3. D. Harries, J. Brit. Nucl. Energy, 5, 74 (1966).
4. J. Andre et al., Tenth Colloquium of Metallurgy, Brittleness and the Effects of Irradiation, Saclay (1968), p.199.
5. F. Garzarolli et al., J. Nucl. Materials, 28, 280 (1968).
6. S.N. Votinov et al., in: Solid-State Radiation Physics and Science of Reactor Materials [in Russian], Atomizdat, Moscow (1970), p.82.
7. Sh.Sh. Ibragimov and I.M. Voronin, At. Energ., 20, 137 (1966).
8. E. Bloom and J. Steigler, Trans. Amer. Nucl. Soc., 14, 557 (1971).

APPROXIMATION FOR TIME RELATIONSHIPS IN PULSED GAMMA – GAMMA LOGGING

I.G. Dyad'kin, B.N. Krasil'nikov, and V.N. Starikov

UDC 550.835

Pulsed $\gamma-\gamma$ logging (PGGL) is based on measurement of the time distribution of γ radiation from a pulsed source scattered by rock; it increases the reliability of determinations of rock density because it decreases the effect of neighboring zones considerably [1].

This paper presents formulas for the determination of the time distribution of γ rays scattered in rock for probes of various lengths and demonstrates the good agreement obtained with the results of Monte Carlo calculations. These expressions were obtained by transformation of the well-known time-dependent solutions for the neutron transport equation.

In calculating γ-ray fields in geophysics, one often uses for a stationary case the diffusion approximation [2, 3], which is borrowed from neutron transport theory and which makes it possible to estimate the nature of the dependence of the measurements on rock density and drill-hole diameter.

There is justification for considering the time distributions of γ rays from a pulsed source and neutrons in hydrogenous media to be similar. We have in mind the scattering of ^{60}Co γ rays in rock of densities to 3 g/cm^3 and the moderation of neutrons from ~5 MeV to ~100 eV in the same rock.

This is confirmed in the following way:

1. On the average, emitted ^{60}Co γ rays undergo more than 10 collisions before their energy is reduced to 0.05 MeV when they are practically absorbed because of the photoeffect. In highly hydrogenous media, the neutrons also undergo 10 collisions.
2. The neutron range decreases as the energy decreases because of the increase in scattering cross section in hydrogen. For γ rays, the first free path also plays the most important part because of the increase in cross section with (decreasing) energy.
3. The scattering kernels for γ rays and neutrons are different; however, predominantly forward scattering is characteristic of both.
4. The spatial distribution of neutrons in hydrogenous media, like that for γ rays, is almost purely exponential.
5. Although the velocity of a photon is constant and the neutron velocity falls during migration, the "final" velocity $V = \sqrt{2E/M}$ plays a fundamental part in the distribution of neutrons with energy E [4-6].

In PGGL, therefore, one should expect the same type of time dependence as with epithermal neutrons in pusled neutron logging (but with different parameters).

Pulsed neutron logging is well described by a Poisson distribution [5, 6]:

$$J(t)=\left(\frac{vt}{l}\right)^{\frac{2}{\xi}} e^{-\frac{vt}{l}}, \quad (1)$$

where v is the neutron velocity, l is the range, t is time, and ξ is the mean logarithmic energy loss.

Translated from Atomnaya Énergiya, Vol.35, No.4, pp.272-273, October, 1973. Original article submitted December 6, 1972; revision submitted March 3, 1973.

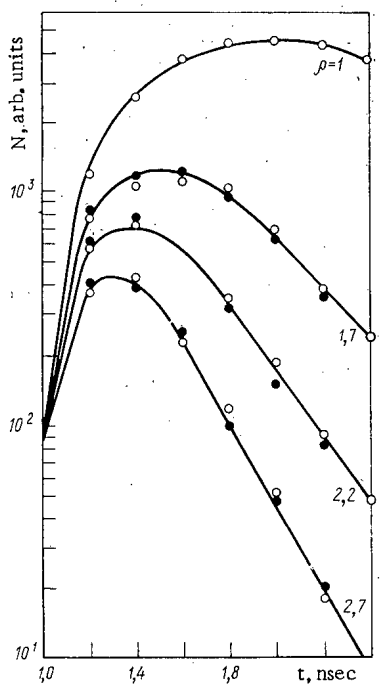

Fig. 1. Time distribution of scattered γ radiation in rock of various densities ρ for a probe length of 25 cm: ○) calculated from Eq. (2); ●) Monte Carlo calculation.

Thus the time dependence in PGGL can be represented in the form of Eq. (1) with the following differences taken into account.

The γ-ray velocity is the velocity of light c and therefore it can occur in an expression for a scale factor; the Compton scattering coefficient μ_k should be substituted for l^{-1}, and photons generally do not reach the detector before the time $t_0 = Lc^{-1}$ (L is the source-detector distance). The coefficient μ_k is proportional to rock density.

$$J(t) = A\left[\frac{\rho(t-t_0)}{b}\right]^a_{t>t_0} e^{-\frac{\rho(t-t_0)}{a}}. \qquad (2)$$

The parameters a, b, and t_0 may depend on the probe length L and, to a lesser extent, on the recorded energy. We let $t - t_0 = t_1$. Then t_{1max}, the time of arrival of the radiation maximum ($dJ(t_1)/dt_1 = 0$), and the moments

$$\bar{t}_1^k = \frac{\int_0^\infty t_1^k J(t_1)\, dt_1}{\int_0^\infty J(t_1)\, dt_1}; \quad k = 1, 2$$

are connected with a and b by the relations

$$t_{1max} = \frac{ab}{\rho}; \quad \bar{t}_1 = \frac{(a+1)b}{\rho}; \quad \bar{t}_1^2 = \frac{(a+2)(a+1)b^2}{\rho^2}.$$

Hence the constants a and b can be defined as:

$$a = \frac{\bar{t}_1^2}{\bar{t}_1^2 - \bar{t}_1^2} - 1; \quad b = \frac{\rho \bar{t}_1}{a+1}. \qquad (3)$$

Figure 1 shows a comparison of curves calculated by the Monte Carlo method with those obtained from Eq. (2) for a probe length L = 25 cm. The correct nature of the displacement of the maximum of the distribution with increasing ρ and the excellent agreement of the curves is clear.

In making comparison with experimental data, one should take into account the fact that Eq. (2) has the form of a differential distribution with respect to t_1 and in real apparatus the measurements are carried out for a time not less than the resolving time; this can be taken into account approximately by changing the value of the time dispersion in the constant a by the quantity Δ which is proportional to the square of the experimentally determined resolving time:

$$a = \frac{\bar{t}_1^2}{\bar{t}_1^2 + \Delta - \bar{t}_1^2} - 1.$$

LITERATURE CITED

1. E.M. Kadisov et al., "Pulsed gamma–gamma logging," in: Pulsed Neutron Logging [in Russian], Izd. VNIIYaG (1968), pp.184–189.
2. I.G. Dyad'kin, "Theory of borehole logging," Izv. AN SSSR, Ser. Geofiz., No.4 (1965).
3. G.M. Voskoboinikov, "The question of accuracy and limitations of applicability of the diffusion approximation in the solution of problems of γ-ray propagation," Zh. Tekh. Fiz., 30, No.1, 90–95 (1960).
4. R. Marshak, "On the theory of the slowing down of neutrons," Rev. Mod. Phys., 19, 185 (1947).
5. I.G. Dyad'kin and E.P. Batalina, "Time variation of the spatial and energy distribution of neutrons from a pulsed source," At. Energ., 10, No.1, 5–12 (1961).
6. V.F. Zakharchenko, "Applicability of approximate schemes for neutron transport in a homogeneous moderator," Ural. Fil., AN SSSR, Tr. In-ta Geofiziki, No.2, pp.17–45 (1962).

GAMMA-RAY ATTENUATION IN APPLIED SCINTILLATION SPECTROMETRY

V. I. Polyakov and Yu. V. Chechetkin

UDC 539.122.164

Scintillation γ spectrometry is widely used in the determination of the activity of isotopes with relatively simple γ spectra and in control devices in technical processes using radioisotopic methods for measuring the absorptive properties of materials.

In determining the activity of point sources in containers, the specific radioactivity of isotopes in pipes and tanks, and in the solution of a number of other problems, it is necessary to realize that γ photons scattered in shielding or material at small angles may be recorded in the photopeak corresponding to the initial energy because of the finite energy resolution of spectrometers [1, 2]. The amount of scattered radiation which is recorded in the photopeak depends on the shield (medium) material and thickness, on the energy resolution of the spectrometer, and on the method of determining the area of the photopeak.

Measurements with shielded cylindrical sources and collimated scintillation spectrometers showed that for shielding thicknesses up to 3-5 mean free paths, the γ-ray attenuation law is described by an exponential with an attenuation coefficient μ_{eff} which is less than the theoretical narrow-beam attenuation coefficient μ_0. It was experimentally found that $\mu_{eff} = 0.52 \pm 0.02$ cm^{-1} ($\mu_0 = 0.57$ cm^{-1}) for cylindrical sources with a γ-ray energy $E_0 = 0.662$ MeV and iron shielding. In first approximation, the effective γ-ray attenuation coefficient is independent of source and collimator dimensions. Similar experiments with cylindrical and point sources of ^{141}Ce and ^{60}Co behind shields of water, aluminum, iron, and lead showed that the differences between μ_{eff} and μ_0 increase at low energies and for light absorbers.

For the theoretical calculation of μ_{eff}, we considered a parallel beam of γ rays having a flux density Φ_0 sec^{-1} . cm^{-2} incident on a slab of thickness t.

Depending on the spectrometer resolution $\eta = \Delta E_{1/2}/E_0$ and the method used for determining the area under the photopeak, pulses will be counted for γ rays scattered into an energy range from E_0 to $E_1 = E_0 - \alpha\eta E_0$ where $\alpha \leq 1$.

The effective γ-ray attenuation coefficient is defined by

$$\Phi_0 e^{-\mu_0 t} + \Phi_1 = \Phi_0 e^{-\mu_{eff} t}, \tag{1}$$

where Φ_1 is the flux density of singly-scattered γ rays outside the shield.

Using the Klein–Nishina–Tamm formula, one can determine the angular distribution of singly scattered γ rays outside a shield. Integrating the resultant expression over shield thickness, including the attenuation of scattered γ rays, and over energy between the limits of the photopeak area assumed in the calculation, we obtain

$$\mu_{eff} = \mu_0 - \frac{1}{t} \ln \left\{ 1 + \frac{0.15dz}{A} \cdot \frac{m_e c^2}{E_0} \cdot \frac{\alpha\eta}{(1-\alpha\eta)} \times \left[1 + (1-\alpha\eta)^2 - \frac{2m_e c^2}{E_0} \alpha\eta + \frac{m_e^2 c^4}{E_0^2} \cdot \frac{\alpha^2\eta^2}{(1-\alpha\eta)} \right] \frac{1}{\mu_1 - \mu_0} (1 - e^{(\mu_0 - \mu_1)t}) \right\}, \tag{2}$$

where d is density, g/cm^3; z and A are respectively the atomic number and atomic weight of the shielding material; $m_e c^2$ is the rest energy of the electron, MeV; E_0 is the energy of the incident γ-ray beam, MeV; μ_1 is the attenuation coefficient for scattered γ rays of energy E_1.

According to the calculations, μ_{eff} is independent of shield thickness with an error less than 3% for shield thicknesses up to five mean free paths; consequently, one can set t = 1 cm in Eq. (2).

Translated from Atomnaya Énergiya, Vol. 35, No. 4, pp. 274-275, October, 1973. Original article submitted January 15, 1973.

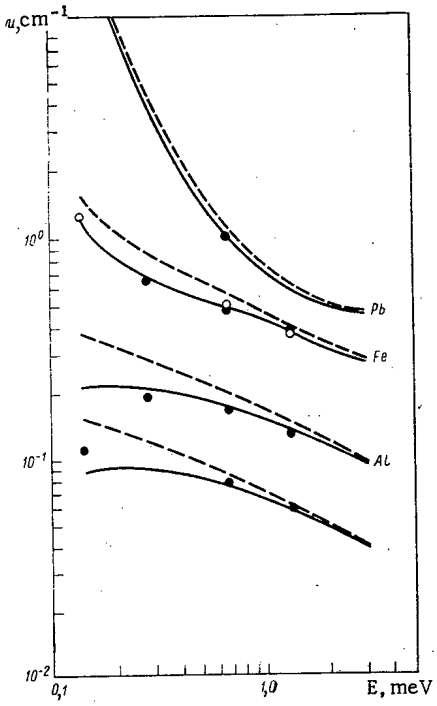

Fig. 1. Energy dependence of γ-ray attenuation coefficient (η = 10% for E_0 = 0.662 MeV): ——) calculated with Eq. (2); – – –) calculated without consideration of scattered radiation [5]; ○,●) experimental points for cylindrical and point sources respectively.

Only single scattering is taken into account in Eq. (2). Using the results of [3], one can show the contribution from double scattering is less than 8% of that from single scattering even in an infinite water medium for 1-MeV γ rays and a spectrometer resolution of 10%; consequently, it need not be considered.

Figure 1 shows that calculation of the effective γ-ray attenuation coefficient by means of Eq. (2) yields results that are in good agreement with experimental values obtained from measurements of the activity of cylindrical and point sources (in the calculation, it was assumed $\eta \sim 1/\sqrt{E_0}$).

The possibility of using Eq. (2), which was obtained for a plane source, in the calculation of self-absorption and absorption in shielding for radiation from other types of sources (point and volume) can be explained by the small differences between the scattered γ-ray spectra [4].

Thus in measurements with NaI(Tl) crystals, γ-ray attenuation can be taken into account by means of an exponential law; the effective attenuation coefficient depends little on measurement geometry and is well described by Eq. (2).

LITERATURE CITED

1. V.M. Kodyukov et al., in: Radiation Technology [in Russian], No. 1, Atomizdat, Moscow (1967), p. 215.
2. V.I. Polyakov and Yu.V. Chechetkin, At. Energ., 31, No. 2, 139 (1971).
3. V.V. Pavlov, in: Problems in Dosimetry and Radiation Shielding [in Russian], V.I. Ivanov (editor), No. 2, Atomizdat, Moscow (1963), p. 66.
4. E.L. Stolyarova, in: Problems in Dosimetry and Radiation Shielding [in Russian], L.R. Kimel' (editor), No. 7, Atomizdat, Moscow (1967), p. 54.
5. L.R. Kimel' and V.P. Mashkovich, Handbook for Shielding against Ionizing Radiation [in Russian], Atomizdat, Moscow (1966).

NATURAL γ-RAY BACKGROUND MEASURED WITH Ge(Li) DETECTOR

L.M. Mosulishvili, N.E. Kharabadze, and T.K. Tevzieva

UDC 543.54

In activation analysis, semiconductor Ge(Li) detectors are often used which have high resolution for the detection of γ rays with energies ranging from several keV to 4-5 MeV [1-3]. An exact determination of the energy and intensity of each line is necessary in studies of γ-ray spectra from multicomponent media and particularly in the identification of various radioisotopes. As is well known, this procedure is most difficult and very important in the activation analysis of complex multicomponent objects. In addition, an exact determination of the photopeaks belonging to the natural background is necessary in the identification of radioisotopes producing radiation of low intensity. The natural background results from many factors of which one should mention radiation from natural radioactive isotopes in the Earth's crust and in structural materials of laboratory buildings, cosmic rays, and radiation from the radioactive isotopes in nuclear reactors if measurements are made in the neighborhood of one.

The background radiation is of low intensity; however, the counting time is long, as a rule, when Ge(Li) detectors are used and many resolved lines appear in the spectrum when counting times are long.

This paper is devoted to a detailed study of the spectral composition of the natural background at the nuclear reactor of the Institute of Physics, Academy of Sciences, Georgian SSR during 1971-1972.

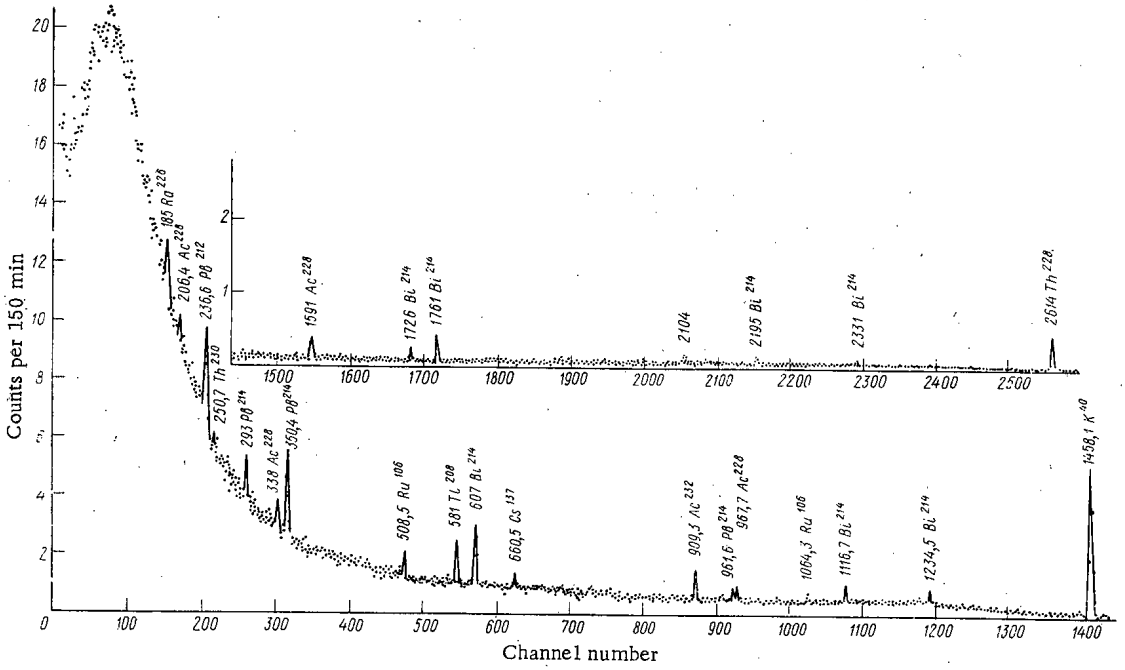

Fig.1. γ-Ray spectrum of natural background measured with a Ge(Li) semiconductor spectrometer.

Translated from Atomnaya Énergiya, Vol.35, No.4, pp.275-276, October, 1973. Original article submitted February 7, 1973.

TABLE 1. Set of Radioisotopes Identified in γ-Ray Background by Means of a Ge(Li) Detector

γ-ray energy, keV*	Line intensity (total counts per 150 min)	Identified radioisotope *	γ-ray energy [4]	γ-ray energy, keV*	Line intensity (total counts per 150 min)	Identified radioisotope *	γ-ray energy [4]
185	690	^{226}Ra	186,2	909	330	^{228}Ac	911
207	290	^{228}Ac	209	962	50	^{214}Pb	965
237	860	^{212}Pb	238,6	968	110	^{228}Ac	968,8
250	260	^{230}Th	250	1064	45	^{106}Ru	1061
293	430	^{214}Pb	295,4	1117	110	^{214}Bi	1120
338	700	^{228}Ac	338	1235	80	^{214}Bi	1238
351	780	^{214}Pb	352	1458	1740	^{40}K	1460,7
509	360	^{106}Ru	511,9	1591	80	^{228}Ac	1588,3
581	310	^{208}Tl	583,1	1726	30	^{214}Bi	1731
608	640	^{214}Bi	609,3	1761	80	^{214}Bi	1765
660	60	^{137}Cs	661,6	2201	35	^{214}Bi	2204
664	50	^{214}Bi	665	2332	25	^{214}Bi	2340
805	50	^{214}Bi	806	2612	200	^{228}Th	2614

* This work.

The natural background was measured over a period of 2.5 h with a DGL-4E Ge(Li) detector made by the French company SAIP connected to a "Tridak-S" 4096-channel analyzer. The detector resolution is 2.5 keV for 1332 keV γ rays. There are numerous photopeaks in the spectrum (Fig. 1) including some very weak ones. Photopeak energies were determined by means of careful calibration with various isotopes having γ rays of known energies.

Knowing the energy of each line with a given accuracy and establishing that the intensity of the radiation remained constant in time, a set of radioisotopes which produced one or more lines in the background spectrum was determined. The experimentally deterined γ-ray energies at 185, 250, 293, 351, 608, 664, 805, 962, 1117, 1235, 1726, 1761, 2201, and 2332 keV are in good agreement with the values given [4] for the most intense lines from the radioactive isotopes ^{226}Ra, ^{214}Pb, ^{230}Th, ^{214}Bi, which, in turn, are decay products of ^{238}U (Table 1). The lines with energies of 207, 237, 338, 581, 909, 968, and 1591 keV are produced by the most intense γ rays from the isotopes ^{228}Ac, ^{212}Pb, ^{208}Tl, and ^{228}Ra, which are in the ^{232}Th family.

In addition, lines from the isotopes ^{137}Cs and ^{106}Ru, which are fission products, are clearly observed in the spectrum as well as the line at 1458 keV from ^{40}K.

Background radiation was measured in the radiochemistry building near the nuclear reactor. Although lines produced by artificial radioactive isotopes can be observed in the spectrum, the main contribution to the background spectrum is made by radiation from natural radioactive isotopes in the Earth's crust, in structural materials, and in the atmosphere. This conclusion should be considered perfectly natural if one considers that the average concentration of ^{238}U and ^{232}Th in the crust is $\sim 10^{-4}\%$.

Background radiation should be taken into account particularly carefully in those cases where work is carried on close to the limit of sensitivity of the equipment during activation determination of an element.

LITERATURE CITED

1. E. Steinnes et al., J. Radioanal. Chem., 9, 267 (1971).
2. Z. Randa et al., J. Radioanal. Chem., 11, 305 (1972).
3. K. Pillay and C. Thomas, J. Radioanal. Chem., 7, 107 (1971).
4. R. Dams and F. Adams, J. Radioanal. Chem., 7, 127 (1971).

DETERMINATION OF A HAFNIUM IMPURITY IN ZIRCONIUM AND ITS ALLOYS BY A NEUTRON ACTIVATION METHOD

V. V. Ovechkin and V. S. Rudenko

UDC 543.54

Two variations of a method based on irradiation of samples with thermal reactor neutrons and measurement of the γ radiation of the active products were proposed in [1] for the determination of low concentrations of hafnium in zirconium and alloys based on it. In one case the γ radiation of the short-lived isotope ^{179m}Hf ($T_{1/2}$ = 19 sec, E_γ = 0.217 MeV) was used, while in the other the activities of the long-lived isotopes ^{175}Hf ($T_{1/2}$ = 70 days) and ^{181}Hf ($T_{1/2}$ = 46 days) were used. In a comparison of these variations of analysis as applied to zirconium concentrates, it was found that the first ensures higher sensitivity, rapidity, and better reliability of the results [2]. However, in both cases a reactor is required, which to some degree hinders the possibility of practical application of such analysis.

A measurement of the hafnium content in the presence of zirconium according to the induced activity of ^{179m}Hf can also be performed by irradiation of the samples with a neutron flux with an energy of 14 MeV from a low voltage generator [3].

In the interaction of neutrons with an energy of 14 MeV with the nuclei of stable isotopes of hafnium, the 19-second isomer ^{179m}Hf is formed in the following nuclear reactions: ^{180}Hf (n, 2n) and ^{179}Hf (n, n').

However, the irradiation of zirconium with 14 MeV neutrons creates a strong interfering background in the region of measurement of the γ spectrum of ^{179}Hf, due to the harder γ radiation of the isotopes ^{89m}Zr ($T_{1/2}$ = 4.2 min, E_γ = 0.59 and 1.51 MeV) and ^{89m}Y ($T_{1/2}$ = 16 sec, E_γ = 0.91 MeV), which are formed in the

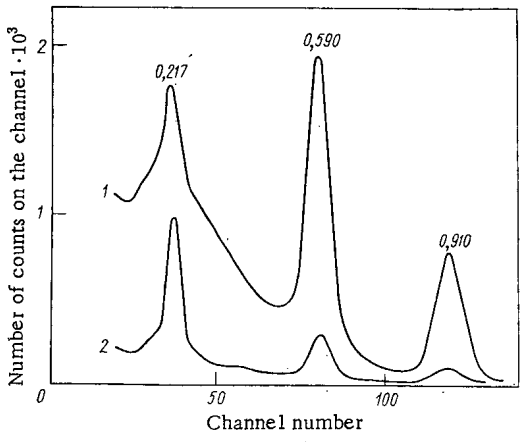

Fig. 1

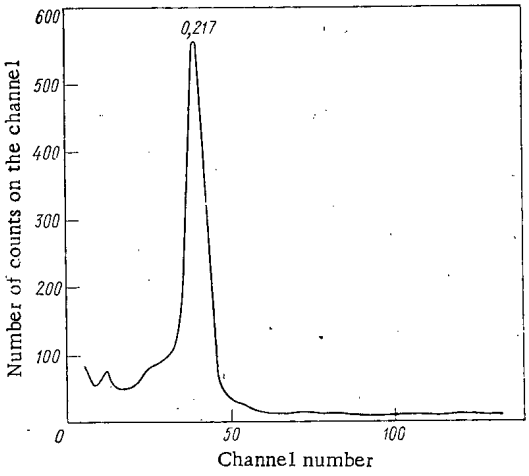

Fig. 2

Fig. 1. Apparatus γ spectra of a sample of zirconium containing ~0.3% by weight hafnium, obtained on a neutron generator.

Fig. 2. Apparatus γ spectrum of a sample of zirconium containing ~0.3% by weight hafnium, irradiated with the neutrons of an isotope source.

Translated from Atomnaya Énergiya, Vol. 35, No. 4, pp. 277-278, October, 1973. Original article submitted March 7, 1973.

TABLE 1. Hafnium Content in Zirconium Samples, % by Weight

Material	Activation method	Spectral method
Zirconium	$6{,}7\cdot10^{-2}$	$6{,}3\cdot10^{-2}$
"	$5{,}0\cdot10^{-2}$	$4{,}8\cdot10^{-2}$
Zirconium alloy	$4{,}6\cdot10^{-2}$	$4{,}4\cdot10^{-2}$
The same	$3{,}7\cdot10^{-2}$	$3{,}7\cdot10^{-2}$
" "	$5{,}3\cdot10^{-2}$	$5{,}6\cdot10^{-2}$
" "	$2{,}9\cdot10^{-2}$	$2{,}7\cdot10^{-2}$

reactions ^{90}Zr (n, 2n) and ^{90}Zr (n, n'p), respectively, which have high energy thresholds (12.53 and 8.79 MeV, respectively). Consequently, if 14 MeV neutrons are moderated to an energy below the threshold of these reactions, it might be expected that the interfering influence of zirconium would be somewhat reduced. In the published studies, these peculiarities of the activation analysis of zirconium for the hafnium content have not been discussed.

In this work we discuss the possibilities of quantitative determination of hafnium in zirconium and its alloys, based on the use of a low-voltage generator of 14 MeV neutrons, which are additionally moderated in a paraffin block, as the source of activation. In addition, we studied the possibilities associated with the use of neutrons for the irradiation of an isotopic ^{238}Pu–Be source.

A pulsed generator of 14 MeV neutrons of the NGI-5 type with a yield of $\sim 3\cdot10^8$ neutrons/sec and an isotopic ^{238}Pu – Be source of neutrons with a yield of 10^8 neutrons/sec were used for the activation of the samples.

A paraffin block with dimensions 300 × 160 mm with several vertical channels, in which samples were placed for irradiation at different distances from the source, was used to moderate the fast neutrons. The induced activity was measured on a scintillation γ spectrometer was a NaI(Tl) crystal with dimensions 40 × 50 mm with a well.

Figure 1 presents the apparatus γ spectra of a sample of zirconium containing $\sim 0.3\%$ by weight hafnium; the sample was irradiated with neutrons from a NGI-5 generator for 1 min with various geometries. The spectrum 1 corresponds to an arrangement of the sample directly at the target of the generator without the use of a moderator, while spectrum 2 corresponds to an arrangement of the sample in a paraffin block at a distance of ~40 mm from the target. In the apparatus spectra, in addition to a photopeak with energy 0.217 MeV from ^{179m}Hf, photopeaks with energies 0.59 and 0.91 MeV from the isotope ^{89m}Zr and ^{89m}Y were observed. The results of the measurements showed that when the irradiated sample is removed from the target of the generator and a paraffin shield is used, the interfering background of the zirconium matrix in the region of 0.2 MeV of the apparatus spectrum is reduced by approximately 7-fold. In addition, intensity of the photopeak 0.217 MeV from ^{179m}Hf is increased, which is evidently explained by an increase in the fraction of slow neutrons, which induce the reaction ^{178}Hf(n, γ) ^{179m}Hf with a large cross section of activation (75 barns). The area of this photopeak proves to be a maximum when the sample is placed in a paraffin block at a distance of 40 mm from the target of the generators; moreover, it is five times as great as the intensity of the peak of the same sample placed at the target of the generator during irradiation.

Thus, the use of a paraffin block as a moderator in work on a generator of 14 MeV neutrons lowers the limit of measurement of hafnium in zirconium by more than 10-fold. The value of the lower limit of measurement of hafnium calculated according to the 2σ criterion (where σ is the standard deviation of the background in the region of 0.2 MeV), is $\sim 2\cdot10^{-2}\%$ by weight for a sample of zirconium weighing 10 g with a neutron yield of the generator $\sim 3\cdot10^8$ neutrons/sec. It should be noted that this value is only approximately three times poorer than the value obtained in [3] with a substantially larger yield of 14 MeV neutrons (10^{10} neutrons/sec).

The use of an isotopic α–Be source of neutrons even more effectively reduces the interfering influence of the zirconium matrix, since the bulk of these neutrons have an energy below the thresholds of the reactions on zirconium. The presence of slow neutrons in the energy spectrum of such a source increases the value of the useful reaction ^{178}Hf (n, γ) with the formation of the isotope ^{179m}Hf, according to which hafnium is determined. These data are confirmed by the nature of the apparatus γ spectrum of the zirconium sample with a hafnium content ~0.3% by weight (Fig. 2), irradiated with the neutrons of a ^{238}Pu – Be source. Only one photopeak is observed in the spectrum, with energy 0.217 MeV, from the isomer ^{179m}Hf.

The photopeaks with energies 0.59 and 0.91 MeV, which always appear when zirconium is irradiated on a generator of 14 MeV neutrons, are entirely absent in this case. The intensity of the photopeak 0.217 MeV is increased by 80%, if a 20 millimeter paraffin shield is placed between the isotope source and the sample during irradiation. The rate of count in the region of the γ peak 0.2 MeV in this case is $1.2\cdot10^5$

counts/min per gram of hafnium with a background of 100 counts/min from the zirconium sample weighing 10 g, which corresponds to a value of the lower limit of measurement of hafnium equal to $1.5 \cdot 10^{-3}$% by weight, with a yield of the isotope source 10^8 neutrons/sec.

Table 1 presents the results of an activation determination of hafnium in zirconium and alloys based on it, obtained by irradiation with an isotope source. The material to be analyzed was placed in a polyethylene ampoule, irradiated for 1 min, and 5 sec after the end of irradiation, the induced activity of ^{179m}Hf was measured for 40 sec according to the photopeak 0.217 MeV.

The hafnium content in the samples was determined by comparison with control samples, prepared on the basis of zirconium dioxide with the addition of hafnium dioxide.

From Table 1 it is evident that the results of activation determination of hafnium are in good agreement with the results of the spectral method. The coefficient of variation of the activation method for hafnium concentrations $\sim 5 \cdot 10^{-2}$% by weight in samples weighing ~3 g is ±8% rel. The time of one analysis is 4-5 min. The method described, using an isotopic ^{238}Pu – Be source of neutrons with a yield of 10^8 neutrons/sec, can be used successfully for the highly sensitive and rapid analysis of zirconium and its alloys for hafnium content.

LITERATURE CITED

1. W. Macintosh and R. Jervis, Analyt. Chem., 30, No.7, 1180 (1958).
2. G.V. Leushkina et al., in: Neutron Activation Analysis [in Russian], Fan, Tashkent (1971), pp.33-36.
3. V.T. Tustanovskii and U. Orifkhodzhaev, Zavod. Lab., 36, No.12, 1482 (1970).

NONOBSERVANCE OF SPONTANEOUS FISSION IN KURCHATOVIUM AT BERKELEY

V.B. Druin, Yu.V. Lobanov,
D.M. Nadcarni,* Yu.P. Kharitonov,
Yu.S. Korotkin, S.P. Tret'yakova,
and V.I. Krashonkin

UDC 546.799

Element 104, kurchatovium, was first observed experimentally in 1964 through the spontaneous fission of its isotopes [1]. Among the products of ^{242}Pu irradiation by ^{22}Ne ions in the internal beam of the 310-centimeter cyclotron there was observed three spontaneously fissioning activities with half-lives of 14 msec, ~0.3 sec, and several seconds. The first turned out to be the fissioning isomer ^{242f}Am. Of the others, the most thoroughly studied behavior was the activity with $T_{1/2} \approx 0.3$ sec which was identified as ^{260}Ku through measurement of the excitation function and cross irradiations.

In 1969–1970, the experimental studies of kurchatovium continued in the external beam of the accelerator. The half-life of ^{260}Ku was determined more precisely ($T_{1/2} \approx 0.1$ sec) [2] and a second isotope, ^{259}Ku ($T_{1/2} \approx 4$ sec), was also identified [3]. The identification of these isotopes was based on excitation functions and integral angular distributions of the recoil atoms.

Realizing the importance of chemical identification of the atomic number of the new element, I. Zvara et al. [4] developed a rapid method for chemical analysis of nuclear products. The first experiments on the identification of element 104 were carried out in 1966 in the internal beam of the cyclotron using frontal chromatography [5]. The experiments showed that the spontaneously fissioning activity produced in the irradiation of ^{242}Pu by ^{22}Ne ions passed rapidly through a four-meter column and an aerosol filter under conditions favoring the passage of hafnium tetrachloride molecules (typical representative of group IV elements) separated from actinide elements, i.e., it was an ekahafnium.

In 1970–1971, new chemical experiments were set up in which the kurchatovium was separated in the form of the chloride by gas-adsorption thermochromatography [6]. Irradiation conditions and the chromatographic procedures were chosen to be optimal for ^{259}Ku ($T_{1/2} \approx 4$ sec). In particular, the time of gas travel from the target to the portion of the column where group IV elements were deposited was 0.8 sec so that the ^{260}Ku ($T_{1/2} \approx 0.1$ sec) decayed in the beginning of the column and did not distort the shape of the chromatogram. The behavior of ^{44m}Sc and $^{170, 171}$Hf was investigated in the experiments at the same time. It was shown that the distribution of fission-fragment tracks from spontaneous fission of ^{259}Ku along the column reproduced the distribution of hafnium accurately. This demonstrated that the four-second spontaneously fissioning isotope belonged to group IV of the periodic table, i.e., it was element 104, and it was concluded that this element had also been detected in the chemical experiments of 1966.

Ghiorso and his associates [7] expressed doubts about the Dubna results for ^{260}Ku and ^{259}Ku. As an argument, they first presented different estimates of the lifetimes of these isotopes with respect to spontaneous fission mainly based on extrapolations of certain empirical relations. They attempted to observe spontaneous fission in a number of experiments but the technique they used was not sufficiently sensitive [8]. However, the apparatus and experimental results were not published in detail [8, 9].

A later report from Berkeley [10] asserted that spontaneous fission is not observed and should not be observed for ^{259}Ku produced in the interaction of ^{248}Cm with ^{16}O ions; on the basis of their experimental

*Bhaba Atomic Research Center, Bombay, India.

Translated from Atomnaya Energiya, Vol.35, No.4, pp.279–280, October, 1973. Original article submitted April 11, 1973.

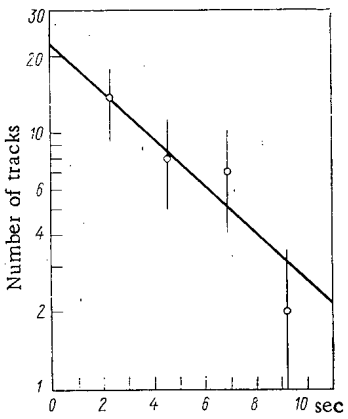

Fig. 1. Decay curve for ^{259}Ku. The solid line corresponds to $T_{1/2} = 3.2 \pm 0.8$ sec.

results, the spontaneous fission branching ratio did not exceed 20%, but it should not be more than 0.1% from their extrapolated estimates.

Because of this, the present work involving irradiation of ^{246}Cm by ^{18}O ions was undertaken in order to show that spontaneous fission of ^{259}Ku can be observed, and its branching ratio determined, for this target—particle combination with a technique of sufficiently high sensitivity.

EXPERIMENTAL METHOD

A ^{246}Cm (>99%) target with an admixture of ^{242}Cm (0.5%) was prepared by electrolytic deposition on a thin titanium backing (5 μm). The short-lived ^{242}Cm was introduced as a tracer which enables one to detect through its α activity slight contamination by target material of the most important parts of the experimental equipment (recoil-atom collector, detectors). Monitoring for α activity of curium showed that the possible background from spontaneous fission of ^{246}Cm was negligibly small.

The apparatus used in the experiments, having a tape recoil-atom collector transporter and phosphate glass fission-fragment detectors, was described previously in detail [2]. Additional shielding was provided for the fission-fragment detectors in order to prevent possible penetration by curium atoms ejected from the target because of elastic scattering of ^{18}O ions.

Irradiation of ^{246}Cm was accomplished in an external beam of ^{18}O ions accelerated in the 310 cm cyclotron at JINR. The energy of the accelerated ions at the target was 100 MeV, which corresponds to the maximum cross section for a reaction involving evaporation of five neutrons [9].

The average ion flux through a 1-cm^2 target was $2 \cdot 10^{12}$ particles/sec. The total ion flux was measured with a scanning device located between the beam collimator and target and calibrated with a Faraday cup.

For a fixed velocity of the collector tape (28 cm/sec), 31 tracks of fragments from spontaneous fission of product-nuclei in the reaction were observed in the detectors. The lifetime of the isotope was estimated from the distribution of tracks along the length of the detectors. Figure 1 shows the decay curve for the isotope produced in these experiments. It is clear that the half-life is 3.2 ± 0.8 sec on the basis of the measurements, which agrees rather well with the data for ^{259}Ku obtained from spontaneous fission [3] and α decay [11].

The partial cross section for ^{259}Ku production as measured from spontaneous fission and for an ^{18}O ion energy of 100 MeV, is $4 \cdot 10^{-34}$ cm^2. An estimate of possible background from the decay of ^{252}102 (SF ≈ 30%); which may be produced in the reaction ^{242}Cm (^{18}O, α4n)^{252}102, leads to a value of no more than 5-10% based on data for the cross sections of the nuclear reactions (^{22}Ne, α4n) [12] and (^{16}O, α4n) [9].

RESULTS AND DISCUSSION

Calculations made by Sikkeland of the cross sections for the nuclear reactions ^{246}Cm (^{18}O, 4-5n)$^{259, 260}$Ku and ^{248}Cm(^{16}O, 4-5n)$^{259, 260}$Ku have been reported [9]. The calculated values of the cross sections for the reactions with evaporation of five neutrons turned out to be 1.5-2 times less than the cross section for the ($^{16, 18}$O, 4n) reaction. It was pointed out, however, that in experiments on the synthesis of ^{259}Ku in the nuclear reaction ^{248}Cm(^{16}O, 5n)^{259}Ku, the measured cross section was approximately four times higher than the calculated value. This is in agreement with experimental results from studies of similar nuclear reactions such as (^{18}O, 4-5) in ^{238}U [13] and ^{242}Pu [14]. It was established that in the transition to heavier targets, the values of the corresponding cross sections are reduced by a factor of 10 and the cross section for the (^{18}O, 5n) reaction is 3-5 times greater than the cross section for the (^{18}O, 4n) reaction in both cases [13, 14]. It is possible that the ratio of the cross sections for reactions involving the evaporation of five and four neutrons observed with uranium and plutonium also holds for curium. One can then suppose that the maximum cross section for the nuclear reaction ^{246}Cm(^{18}O, 5n)^{259}Ku is $\sim 6 \cdot 10^{-33}$ cm^2 for an ^{18}O energy around 100 MeV.

From the ratio between the measured cross section for ^{259}Ku production derived from spontaneous fission and the estimated total cross section, a spontaneous fission fraction SF/$\alpha \approx 7\%$ is obtained. This value is in agreement with the limit SF/$\alpha \leq 20\%$ given in [10]. It should be noted that the critical remark

[10] with regard to the chemical separation of kurchatovium [6] were based only on an indirect analysis of the quantity SF/α for ^{259}Ku which led to the conclusion that this ratio should be less than 0.1%. The Berkeley authors then concluded that the cross section for the nuclear reaction ^{242}Pu(^{22}Ne, 5n) as measured by the spontaneous fission of ^{259}Ku should not exceed $5 \cdot 10^{-36}$ cm^2 and therefore kurchatovium must not have been observed in the chemical experiments [6].

The experimental data points up the unsoundness of such criticism. The yield of ^{259}Ku in the nuclear reaction ^{242}Pu(^{22}Ne, 5n)^{259}Ku in the chemical experiments [6] is in good agreement with our data if it is assumed that the total cross section for the reaction ^{242}Pu(^{22}Ne, 5n)^{259}Ku is $2 \cdot 10^{-33}$ cm^2, as also follows from the Sikkeland calculations [9]. The unwarranted faith of the authors of [10] in their semi-empirical extrapolations and their repeatedly expressed scepticism [9, 15] about the possibility of discovering the new element from spontaneous fission of its isotopes are cause for surprise.

Thus physical experiments on the spontaneous fission of kurchatovium isotopes supplemented by chemical methods for the identification of transactinide elements yield an unambiguous result relative to the synthesis of a new element.

In conclusion, the authors thank Academician G.N. Flerov for continuing interest in the work and for enthusiastic support; they also thank V.A. Davidenko and V.N. Polynov, whose valuable help determined the possibility of carrying out this work to a considerable extent. The authors are grateful to Yu.V. Poluboyarinov for help with the experiments and to the U-300 cyclotron group for providing efficient operation of the accelerator.

LITERATURE CITED

1. G.N. Flerov et al., At. Energ., 17, No.4, 310 (1964).
2. Yu.Ts. Oganesyan et al., At. Energ., 29, No.4, 243 (1970).
3. G.N. Flerov et al., Proceedings of International Conference on Heavy-Ion Physics, Dubna (1971), p.125.
4. I. Zvara et al., JINR Preprint D6-3281, Dubna (1967).
5. I. Zvara et al., At. Energ., 21, No.2, 83 (1966).
6. I. Zvara et al., Inorg. Nucl. Chem. Letters, 7, 1109 (1971).
7. A. Ghiorso and T. Sikkeland, Phys. Today, 20, 25 (1967).
8. A. Ghiorso et al., Report UCRL-18667, Berkeley (1968).
9. A. Ghiorso, Proc. 13 Conf. on Chemical Res., Houston (1969), p.107.
10. A. Ghiorso et al., Inorg. Nucl. Chem. Letters, 7, 1117 (1971).
11. A. Ghiorso et al., Phys. Rev. Letters, 22, 1317 (1969).
12. E.D. Donets, V.A. Shchegolev, and V.A. Ermakov, At. Energ., 16, No.3, 195 (1964).
13. E.D. Donets, V.A. Shchegolev, and V.A. Ermakov, Yad. Fiz., 2, 1015 (1965).
14. V.L. Mikheev, Yad. Fiz., 5, 1186 (1967).
15. M. Nurmia, Report LBL-666, Berkelye (1971), p.42.

XXIV SESSION OF PKIAE SEV

V. A. Kiselev

In line with the work plan drawn up by the COMECON Permanent Commission on the peaceful uses of atomic energy, the 24th session of the Commission was held on June 19-23, 1973, in Brno (Czechoslovakia).

Delegations from Bulgaria, Hungary, the German Democratic Republic, the Republic of Cuba, Poland, Rumania, the USSR, and Czechoslovakia took part in the work of the Commission. It was the first time that a delegation from Cuba had taken part in the Commission's deliberations.

Upon invitation by the Commission, a representative of the international nuclear instrumentation economic association known as Interatominiztrument also took part.

The session took up problems facing the Commission in the light of the resolutions adopted at the XXIV session of COMECON, sessions of the Executive Committee of the Council, and the Comprehensive Program of further deepening and improvements in collaboration and in the development of socialist economic integration of COMECON member-nations.

The Commission discussed measures and proposals on collaboration between COMECON member-nations involving development of a reactor facility (water-cooled and water-moderated reactor) of 1000 MW electric power output, procedures for safe disposal of radioactive wastes by burial, materials on shipping spent nuclear fuel, topics concerning radiation technology and equipment, nucleonic instrumentation, and other pertinent topics in nuclear science and engineering.

The Commission also discussed development of a draft program of scientific and technical collaboration between COMECON member-nations with a long-term perspective, on radiation safety in connection with the expanded use of atomic energy for peaceful purposes.

Appropriate recommendations and solutions are adopted on all of the topics discussed by the Commission.

Translated from Atomnaya Énergiya, Vol. 35, No. 4, p. 281, October, 1973.

COLLABORATION DAYBOOK

A conference on isotope production was held in Prague, April 9-13, 1973. Participating were authorized representatives of Bulgaria, Hungary, the German Democratic Republic, Poland, Rumania, the USSR, and Czechoslovakia.

The conference discussed a draft of an Agreement on multilateral international specialization and cooperation in the production of isotope wares, and agreed on a list of such products (numbering 500-odd items) to be a subject of specialized production in the period up to 1975. The list drawn up includes inorganic compounds, over a hundred tritium-labeled organic compounds, and about 300 ^{14}C-tagged compounds; also over 30 sets of medical isotope equipment and 20 types of sealed radiation sources, and so forth.

The conference judged it feasible to work out proposals aiming at further specialization in the production of isotope wares for the 1976-1980 period. In line with this assessment, member-nations of COMECON are scheduling engineering cost studies for the 1973-1974 period in this area. The conference discussed the progress of work on problems taken up under the PKIAE SEV work plan for 1973.

Appropriate decisions were arrived at on all of the topics under discussion.

* * *

The fifth session of the coordination scientific-technical council of COMECON member-nations on radiation equipment and technology (KNTS-RT) was held April 24-27, 1973, in Warnemunde (East Germany). Members of the council and experts from Bulgaria, Hungary, the GDR, Poland, Rumania, the USSR, and Czechoslovakia took part in the deliberations, as well as a COMECON Secretariat staffmember. Nine topics were placed on the agenda.

The council heard a report from the GDR delegation entitled "On industrial realization of radiation sterilization processes for medical wares," and pointed out that radiation sterilization is at present one of the most highly developed processes in this area, and that it has been engineered into a full-scale technological process in a number of capitalist countries. Radiation sterilization processes are in the pilot stage in the COMECON nations, and will be scaled up to industrial production conditions in the coming three to five years.

The council discussed measures for industrial utilization of radiation sterilization processes in interested COMECON member-nations. The burden of the measures discussed centered around working out engineering cost validations of radiation sterilization processes: comparisons of the radiation method of sterilization and other familiar technological approaches to the problem, selection of the optimum variant of a full-scale sterilization facility, and ascertaining volumes of production and demand.

The council approved a draft paper entitled "Procedures for determining cost aspects of radiation practice"; an agenda for a symposium on radiation processing of foodstuffs and agricultural products, to be held in Sofiya October 15-17, 1973; basic trends and structure of scientific forecasting of the development of radiation equipment and technology.

The council expressed its agreement with proposals on the structure and nature of the contents of Unified public health regulations pertaining to the design and operation of radiation facilities; heard information on the compilation of preparatory materials for the Unified dosimetric radiation technological process monitoring procedures; heard a report delivered by the KNTS-RT chairman on the balance of work done over the course of 2.5 years, and on ways of bringing measures worked out and approved by KNTS-RT

Translated from Atomnaya Énergiya, Vol.35, No.4, pp.281-282, October, 1973.

to fruition; confirmed a tentative agenda for the forthcoming sixth session.

* * *

A conference of specialists on radiation processing of foodstuffs and agricultural products was held in Moscow May 15-18, 1973. The conference was attended by food experts, public health personnel microbilogists, radiation experts, and other specialists from Bulgaria, Hungary, the GDR, Poland, Rumania, the USSR, and Czechoslovakia, who had been participating in the deliberations of the COMECON Permanent Commissions on the food industry and on the peaceful uses of atomic energy.

The delegates in attendance at the conference were brought up to date on work in progress in several countries on the development of technology for applications of radiation processing of foodstuffs with the object of lengthening storage time, cutting down losses, and intensifying technological processes. The greatest amount of interest was shown in research findings on combined methods of processing as the most promising approach on the horizon, as well as in biological and medical publich health oriented research on deactivation and decontamination of irradiated products.

The conference took note of the need:

- for performing and coordinating research work of a biological nature to be carried out by specialists in the food industry, and medical publich health research covering a broad range of topics connected with studies of deactivation and the nutritional value of irradiated foodstuffs;
- working out quality criteria for irradiated products;
- working out unified approaches in procedures and techniques to be employed in medical and public health assessments of irradiated foodstuffs, and drafts of unified legislative proposals on realization of such techniques and procedures in COMECON member-nations.

The conference also discussed proposals for a draft plan of joint research in the field of public health assessments of irradiated products, and some topics associated with various aspects of acceptance of the methods, and put finishing touches on the research program for the year 1973.

INFORMATION

SOVIET – FRENCH COLLABORATION IN THE FIELD OF PEACEFUL USES OF ATOMIC ENERGY

B.I. Khripunov

It is now more than a decade that France has occupied one of the leading places in international collaboration with the USSR State Committee on the peaceful uses of atomic energy. This collaboration has been taking place primarily on the basis of two agreements drawn up between the USSR GKAE [USSR State Committee on the Peaceful Uses of Atomic Energy] and the French Commissariat de l'Energie Atomique: one of these agreements covers joint research in high-energy physics using the 70 GeV accelerator (at Serpukhov) and the French Mirabel liquid-hydrogen bubble chamber, while the other, a general agreement dated May 20, 1967, covers a broad range of topics associated with the peaceful uses of atomic energy.

In the current year, the USSR GKAE and the French CEA envisage signing, within the framework of the above general agreement, a new statement on collaboration which covers a schedule of measures to be taken in the years 1973–1975. This statement will call for exchanges on fast reactors, plasma physics, and controlled thermonuclear fusion, desalination of sea water, and other topics.

In May and June of this year, the Soviet Union was visited by a delegation of leading activists of the French CEA headed by the body's general administrator André Giraud. The delegation was staffed by the head of the CEA's board of international liaisons M. Goldschmidt. The status of Franco-Soviet collaboration and the outlook for the development of further such collaboration in the coming years were the principal topics discussed during the visit.

The delegation visited the Institute of High Energy Physics at Serpukhov; where a large team of French specialists is currently engaged in research, and also visited scientific research institutes in Georgia and Armenia, as well as holding talks at the USSR GKAE center.

The two sides offered a high estimate of the results achieved through this visit. In a letter addressed to the USSR GKAE at the termination of the visit, M. Giraud expressed a "firm conviction that the development of collaboration between the USSR GKAE and the French CEA is necessary in an of itself, and also from the vantage point of improving mutual understanding between our two peoples."

Translated from Atomnaya Énergiya, Vol.35, No.4, p.283, October, 1973.

SESSION OF SOVIET – FRENCH COMMISSION ON SCIENTIFIC TOPICS

A.V. Zhakovskii

At a regularly scheduled session held May 22-24, 1973 at the IFVE center (High-Energy Physics Institute, Serpukhov), the Franco-Soviet commission discussed the progress of work with the Mirabel bubble chamber, and the status of joint experimental research on beams of separated particles using that chamber.

A report delivered by P. Preugny (Saclay) listed various problems that have come up in the operation and use of the Mirabel bubble chamber, and where notable success has been achieved in working toward solutions. These problems include: reliability of the expansion system, adjustment of thermodynamical parameters, minimization of dust on the walls of the chamber. Nonetheless, in order to achieve a quality of plates that would render automatic processing of bubble-chamber plates possible, work has to be continued on improving the performance of some of the systems of the chamber (the illumination system, the data box, and so on).

Reports on the performance of the separated particles channel in this chamber were made by V.I. Kotov. Four work sessions have been completed since adjustment of the optics of the No.7 channel and of the high-frequency separator was carried out. The separator was in operation a total of 1900 h (including adjustment time) during that period, and the chamber downtime due to malfunctions of the separator was kept to about 2%. It was also shown that it is in principle possible to obtain separated beams of K^--mesons, antiprotons, and deuterons with energies to 40 GeV.

E. Pauly (Saclay) and P.F. Ermolov provided the commission with information of the status of chamber experiments and on progress in processing data secured with the use of the chamber (studies of p – p interactions and a review verification experiment). On the basis of material obtained after a portion of the plates had been processed, it was proposed to present appropriate reports to the international conference on the physics of elementary particles scheduled for September 1973 at Aix-en-Provence (France).

The commission discussed a proposed experiment to be carried out on a beam of 32 GeV antiprotons, and recommended a further study of this proposal, while at the same time continuing a review verification experiment with antiprotons.

Reports by B. Delaire (Saclay) and V.I. Moskalev to the commission noted the work load that can be handled in processing in laboratories participating in the Mirabel bubble chamber program is estimated in the neighborhood of 500 to 600 thousand viewings of photographs a year as of 1975, and about 500,000 measurements.

The session of work with beams of K^+- and K^--mesons, with statistics of 30,000 photographs in either case, is now scheduled to follow next.

In conclusion, the commission took up several topics of an organizational nature.

Translated from Atomnaya Énergiya, Vol.35, No.4, p.283, October, 1973.

CONFERENCES

II ALL-UNION CONFERENCE ON MICRODOSIMETRY

V.I. Ivanov

The second All-Union conference on microdosimetry was held June 12-15, 1973 at the Moscow Order of the Labor Red Banner Engineering and Physics Institute [MIFI].

Microdosimetry is a comparatively young developing branch of applied nuclear physics. Microdosimetry is being enlisted in efforts to investigate processes involving transfer and distribution of absorbed energies within the confines of radiosensitive microstructures upon irradiation of living and nonliving objects by ionizing radiations. The term "sensitive microstructures" applies here to those formations in which observable radiation effects are brought about as a result of irradiation (e.g., the living cell or such subcellular structures as chromosomes).

In view of the tiny dimensions of sensitive microstructures, fluctuations in transferred energy are substantial. Methods and ways and means of simulating the energy transfer process accompanying interactions between ionizing radiations and sensitive microstructures are now being worked out, and the relationship between the microdosimetric variables to be measured and the radiation effects to be observed is being established.

The second All-Union conference on microdosimetry was staged in line with recommendations adopted at the first All-Union conference (also held at MIFI, February 5-6, 1970), which took note of the basic scientific trends extent in the field, and then laid the basis for coordinated research in this area. Balance sheets on the development of microdosimetric research over the ensuing three-year period were drawn up at the second All-Union conference on the topic, and a total of 32 scientific papers on the basic trends were heard and discussed; topics covered included: theoretical aspects of microdosimetry (including the structure of tracks), experimental equipment in microdosimetry, and interpretation of dose – effect curves on the basis of microdosimetric concepts. By the present time, a considerable amount of experimental and theoretical data has been accumulated on the distribution functions of the principal microdosimetric variables: the dimension of events and the specific energy, for equivalent tissue volumes with linear dimensions in the range from 0.1 to 10 μ. But these data have yet to be systematized, and even so do not encompass many conditions of irradiation which are of practical importance.

The most common method for measuring microdosimetric variables remains the ionization-pulse method based on the use of low-pressure proportional counters; wall-less counters have become increasingly popular in more recent years.

One of the main problems is how to determine the range of applicability of microdosimetry, and also how to establish the relationship between microdosimetric variables and radiation effects on the basis of analysis of the experimental data. The special features of the microscopic distribution of absorbed energy culminate in values of macroscopic dosimetric variables to be determined by the methods of conventional dosimetry not being in a one-to-one relationship with radiation effects, if the latter are due to damage done to the sensitive microstructures. The magnitude of the observable radiation effects should be correlated with microdosimetric variables and with the parameters of the distributions of those variables; the possibility of establishing some one-to-one relationship between them is what determines the applied value of microdosimetry.

Much space was given in the reports (and even more so in the discussions) to the practical significance of microdosimetry for radiobiology. Most of the reporters concluded that microdosimetry should be regarded as a tool which will enable radiobiologists to extract additional raw information on the absorbed

Translated from Atomnaya Énergiya, Vol.35, No.4, p.284, October, 1973.

energy of radiation, which will expand opportunities for predicting the magnitude of radiation effects on the basis of physical measurements. It has been pointed out that the possibilities inherent in microdosimetry should not be exaggerated insofar as the discovery of the mechanism underlying radiation damage is concerned. Only in those cases where the model reflecting the mode of damage is known will a juxtaposition of the magnitude of the radiation effect to the microdosimetric variables and to the parameters of the distributions of microdosimetric variables make it possible to find values of the constants used in the theory (e.g., the dimensions and number of targets).

The need for microdosimetric backup of radiobilogical experiments relying on equipment simulating radiosensitive microstructures of a concrete object to be irradiated immediately in the process of bombardment of that object by radiation was underlined at the conference, and the feasibility of extending microdosimetry techniques to the study of biological effects brought about by radiations emitted by radionuclides incorporated into the living organism; background concentrations are included here.

The conference constituted a demonstration of the rising level of research work on microdosimetry. Conferences of this type are contributing to the task of coordinating scientific research efforts. The third All-Union conference on microdosimetry is scheduled for two to three years hence.

MIFI SCIENCE CONFERENCE

V.V. Frolov and V.A. Grigor'ev

The regularly scheduled science conference of instructors, students, and colleagues of the Moscow Order of the Labor Red Banner Engineering and Physics Institute [MIFI] was held in January 1973. A total of 367 reports was heard at the sessions of the 24 panels.

The experimental nuclear physics panel heard an interesting report on research on cosmic γ photons, delivered by B.I. Luchkov et al. Work done by a team of MIFI colleagues conducting research with the artificial Earth satellite Kosmos-251 revealed a discrete source of high-energy γ photons located in the constellation Taurus, and tentatively identified with the peculiar galaxy SC 120. Four more sources of cosmic γ emission were detected, with the aid of a γ-ray telescope operating on board the Kosmos-264 satellite, in the neighborhood of the north pole of the local galaxy, but these also appear to be extragalactic. The report discussed some further pathways of development open to γ-ray astronomy.

A lively discussion was provoked by a report submitted by G.B. Bondarenko et al., on the first experiments designed in a search for the W-boson. The results obtained to date are indicative of the existence of new and unusual mechanisms at work in generating high-energy muons in nucleon–nucleon collisions.

A report on new nucleus-like systems presented by I.S. Shapiro was the most interesting one presented at the theoretical nuclear physics panel. The report went into bound states and resonant states of nucleons and antinucleons with lifetimes corresponding to level widths on the order of 10 to 100 MeV (quasinuclear mesons of mass $\approx$2 to 3 GeV). Theoretical investigation has demonstrated that there must exist an integral spectrum of quasinuclear mesons counting over ten levels. Experimental data appearing in the recent literature offers support to predictions based on theory.

The most interesting reports presented to the plasma physics panel dealt with building thermonuclear reactors. For example, a paper by O.A. Vinogradova et al., proposed a new design of electrostatic recuperator in the form of a system of beveled diaphragms with a linear potential distribution; this system is capable of producing a recuperation factor of the required value under conditions close to those found in thermonuclear reactions. Reports by A.A. Pisarev et al., discussed evolution of gas in response to particles becoming embedded in the vacuum containment shell of a thermonuclear reactor as the reactor interacts with plasma present. As a result of those experiments and computer calculations, the diffusion parameters and parameters of gas evolution were obtained under conditions of ion bombardment. It was shown, specifically, that virtually all of the hydrogen present is given off from metals forming the walls of a thermonuclear reactor at the reactor operating temperature.

The physics of separatory processes panel heard a report by N.A. Kolokol'tsov which outlined a theory of cascades with heavy enrichment at each stage, and provided formulas useful in calculating symmetrical and asymmetrical cascades.

The concluding plenary session of the conference heard an address by MIFI professor Academician M.D. Millionshchikov. The report offered an analysis of the role played by fundamental scientific research and by applied scientific research in the development of Soviet society, and in the construction of the material-technical base of communism, and also formulated problems facing science colleagues on the faculties of college-level institutions, both from the standpoint of their direct participation in scientific and technical progress, and in efforts to train cadres and skilled personnel to serve and manage the national economy of the country.

Translated from Atomnaya Énergiya, Vol.35, No.4, pp.284-286, October, 1973.

In addition, the plenary session also heard reports on some of the most interesting scientific advances achieved by MIFI colleagues. A report by V.G. Varlamov, Yu.P. Dobretsov, B.A. Dolgoshein, and V.G. Kirillov-Ugryumov cited experimental findings on the interaction between muons and atoms of the noble gases. It was shown that the reason for the absence of precession of the muon spin in inert gases immersed in a transverse magnetic field at the muon frequency, as detected in earlier work by those authors above, is the spin – orbital interaction between the muon and the electron shell of the muonic atom. When a muon is stopped in neon, a "mesonucleus" or "mesonuclide" $(\mu^{-20}Ne_{10})^{+9}$ is formed, and that is equivalent to the nuclide $^{20}F_9$ with the spin and magnetic moment of a negative muon. In collisions experienced with target atoms, the neon mesonucleus picks up the electron shell of the fluorine atom. The presence of the magnetic moment at the electron shell of the fluorine atom is responsible for the paramagnetic properties of the muonic atom manifested on the mesonucleus $(\mu^{-20}Ne_{10})$. Measurements were conducted with the gas target filled with a mixture of gases Ne (p = 42 atm) + Xe (p = 1 atm). It was shown that the experimental distribution of decay electrons produced as the total moment of the mesoneon atom precesses in weak magnetic fields (1.1 Oe and 2.1 Oe) contains precession frequencies corresponding to the expected theoretical values, which are approximately 100 times in excess of the precession frequency of a free muon.

The study of mesoneon type muonic atoms is opening up fundamentally new opportunities for research in muon physics and in applications of muon physics.

A paper by S.A. Gonchukov, M.A. Gubin, and E.D. Protsenko, which was awarded the Lenin Komsomol [Communist Youth League] prize, presented results of investigations into the properties of multimoded gas lasers It was specifically disclosed in the course of these investigations that a gas laser is capable of operating, under certain conditions, on two closely adjacent axial modes of oscillations. In that case the interaction or coupling between modes is so strong that otherwise insignificant losses or amplification of one of the interacting modes will bring about a drastic redistribution of the intensities of the modes. Utilization of this effect to advantage in lasers with a nonlinear absorbing cell has made it possible to enhance contrast in resonances by almost two orders of magnitude in power output, and to narrow the width of the resonances appreciably. That has resulted in frequency stability $\approx 10^{-14}$ with an averaging time of 100 sec (for a laser one meter in length).

A report submitted by M.A. Kuz'min and V.V. Khromov dealt with the development and practical acceptance in theoretical investigations of a set of ROKBAR programs designed to facilitate the search for the optimum variant of a fast reactor with due account taken on interactions between the thermal, neutronphysics, strength, and cost characteristics of such a reactor. The optimality criteria invoked in this approach are: specific computed losses in generating 1 kWh electric power, the doubling time of the system of breeder reactors, the specific fuel loading in the cycle, and so forth. The solution of the optimization problem is arrived at through an iterative procedure on the basis of the generalized theory of small perturbations and the method of linear programming.

Operating experience with this set of programs has shown that the ROKBAR program can be used to find ways of improving the engineering cost features of a nuclear power station based around fast reactors, with a substantial reduction in computer time.

A report by I.S. Shedrin dealth with the nation's first functioning U-30 electron accelerator, which operates in the three-centimeter wavelength range. Conversion to that range now expands possibilities for building miniature sources of radiation useful bringing about radiation effects in a variety of instruments and materials, for devising simulations of sources of β-radiation with flux density greater than 10^{10} $cm^{-2} \cdot sec^{-1}$, for simulation of certain other problems and verification of concepts related to design projects, and for designing large accelerator complexes, etc.

The U-30 accelerator is itself a variant of a stationary laboratory facility and is designed to raise the energies of the accelerated electrons to 2 MeV, with a mean current of 10 μA. The machine can be operated in conjunction with various focusing systems. The control and supply systems are transistorized, so that size is greatly reduced, while reliability is improved, and it is now possible to employ an automatic system for bringing the accelerator to operating conditions. The system is broken up in design terms into functional modules, is compact, transportable, and reliable in service. The external format of the accelerator conforms to current esthetic requirements. The U-30 model is the base model for a series of accelerators to be designed for the three-centimeter wavelength range. A possible new generation of 4.6 MeV and 8 MeV accelerators designed by size and concomitant increments in both the accelerator and the control system is in the wings.

SYMPOSIUM ON HEAVY-CURRENT FIELD-EMISSION PLASMA ELECTRONICS

G.O. Meskhi

For over thirty years, research on electric insulation provided by vacuum gaps, and on phenomena associated with breakdown in vacuum, has been carried on at many laboratories throughout the world. The nature of the insulating properties of vacuum and of discharges struck in vacuum is associated with a variety of phenomena occurring both on the surfaces of electrodes and in the vacuum gap per se. Extensive research on those phenomena over the course of recent decades has been rendered possible by the availability of equipment for shaping high-voltage pulses with widths of several nanoseconds, and by the development of methods for recording rapid processes. This research has culminated in the design of powerful sources of electrons and x-rays for this work.

We should take note of the two most salient trends in this area: 1) designing powerful CW and pulsed sources of electrons utilizing an arc discharge struck in a vacuum. The advances attained in this trend are characterized by the electron guns employed in various technological processes (such as welding, cutting metals in vacuum, etc.); 2) electron sources based on field emission and meeting the needs of the electronics industry, and specifically those widely utilized in electron microscopes, to which we can added powerful sources of electrons and x-rays that have been devised in recent years and which make use of the initial stage of vacuum breakdown (processes developing within the first 100 to 200 nsec after voltage is applied). Facilities useful in producing electron beams with currents as high as several megaamperes and energies to 15 MeV, with pulse widths to 100 nsec, are now available as an outcome of this work.

Symposia held once every two years in the USA since 1964 on coordination of research in the field of electrical insulation and discharges in vacuum were broadened to an international status starting with 1968.

A symposium on field-emission plasma heavy-current electronics organized by the Siberian Division of the USSR Academy of Sciences and the Ministry of Higher and Middle Special Education of the RSFSR (MV i SSO RSFSR) on the initiative of the Atmospheric Optics Institute of the Siberian Division of the USSR Academy of Sciences [IAO SO AN SSSR] and the Tomsk Institute of Automated Control Systems and Radio Electronics of the MV is SSO RSFSR, was held in Tomsk May 15-17, 1973. This symposium attracted over 130 scientists from various cities throughout the country. Fifty-odd original papers and tutorial review papers were presented. The work of the symposium took place in two panels: the first discussed electron emission properties of a stationary plasma and gas-discharge sources of electrons; the other discussed electron emission properties of nonstationary plasma and generation of powerful electron beams. The huge volume of information presented at this symposium rules out any but a brief coverage in this short article. We therefore restrict the discussion here to the basic problems under discussion at that gathering.

1. Elucidation of the mechanism of "explosive emission" and conditions governing the transition from field emission to "explosive emission." These topics were discussed in contributions by G.N. Fursei, G.A. Mesyats, S.P. Bugaev, and others.

The electric field responsible for emission of electrons from a metal is determined by the surface microgeometry, and can be increased by a factor of ten to a hundred, on microscopic corona points, over the field governed by the macrogeometry of the electrodes. The gain of such a field on microscopic corona points is a function of the ratio h/r, where h is the height and r the filleting radius of microasperities.

Translated from Atomnaya Énergiya, Vol. 35, No. 4, pp. 286-287, October, 1973.

When large currents are taken off an emitter in response to a strong electric field, and also as a result of Joule heating and the Nottingham effect, the corona micropoint explodes within a certain time, to form a cathode-sheath flare. From that instant on, the plasma of the cathode-sheath flare becomes the emitting zone. The rate of expansion of the plasma so formed is more or less the same $2 \cdot 10^6$ to $3 \cdot 10^6$ cm/sec, for several materials investigated (copper, tungsten, aluminum). A low rate of expansion of the flare has been detected in the case of lead ($\lesssim 10^6$ cm/sec). The time of onset of the "explosive emission" process, reckoned from the instant the voltage pulse is applied (time delay t_d), fluctuates over a wide range (approximately from 10 nsec to 10 μsec) and is associated with the density of the current being drawn off. The relationship $j^2 t_d \approx$ const is now established. This dependence has been confirmed in some theoretical and experimental research efforts. In this formula, the constant is dictated by the properties of the cathode material, and is $4.5 \cdot 10^9$ in the case of tungsten.

2. The development of cathodes in which the plasma prepared beforehand serves as the emitting zone.

D.I. Proskurovskii, G.P. Bazhenov, and colleagues have demonstrated through direct measurements that the plasma of the cathode-sheath flare stimulates effective emission of electrons from portions of the cathode enveloped by plasma. New cathodes based on emission of electrons from preorganized plasma were reported on at the symposium. The plasma can form in this case as a result of surface breakdown on a cathode, either in response to a preliminary pulse, or by preliminary filling of the anode – cathode gap.

3. The utilization of polymeric films in diagnostics of heavy-current relativistic beams of electrons.

Contributions by V.B. Sannikov discussion work using viniproz and astrolon type polymeric films sandwiched with thin conducting interlayers in order to eliminate space charge determine the geometric dimensions of the beams and the energy spectrum (according to the degree of fogging of the films when traversed by the electron beam). The film fogging mechanism remains obscure to date. The maximum allowable current density up to which the film remains intact is ≈ 5 kA/cm^2. The energy resolution in this method is several kiloelectron-volts at 100 keV electron energy.

4. Development of heavy-current electron accelerators through reliance on inducative shaping components.

Designs of electron accelerators using an inductance as the shaping component were discussed at the symposium, and well as experimental research findings obtained with such accelerators. Current switching on a diode is achieved by means of a circuit breaker which utilizes the explosion of thin wires and a high-pressure spark discharge switch. Pulses of electron current to 8 kA were produced with energies to 1 MeV, and pulse width $\lesssim$100 nsec. Work in this direction is being conducted by B.M. Koval'chuk and Yu.A. Kotov.

5. Development of powerful controlled commutators with triggering by an electron beam. A gas discharge switch with electron piercing features has been proposed for switching fast storage lines. The required current density (10^3 A/cm^2) and the electron energy needed to trigger the discharge switch (100 keV) have already been calculated. Heavy-current accelerators serve as the electron sources.

Great interest attaches to tutorial review papers submitted by E.M. Reikhrudel', G.A. Mesyats, and G.N. Fursei, which sketched out the complete picture of advances achieved to date, and which shed light on the problems that call for further investigation.

A resolution adopted at the closing session of the symposium stressed the need to convoke such forms on a regular basis (once every two years).

V/O IZOTOP AGENCY CONFERENCES AND SEMINARS

The "Applications of radioactive isotopes in the national economy" panel began its work in January 1973 at the Leningrad House of Scientific and Technical Publicity. It was organized by the Leningrad interrepublic division of V/O Izotop agency. Seminars of a program as part of the continual seminar "Applications of radioactive isotopes in industry and in scientific research" are being held systematically. Representatives of industrial enterprises and scientific research institutes are taking part in these seminars.

* * *

A technical conference with representatives of the Avtomatpishcheprom maintenance and adjustments board for the food industry and the Association of Breweries was held under the auspices of the Leningrad interrepublic division of V/O Izotop in February 1973. A decision was reached at the conference to study the performance of industrial enterprises within the Association with the object of gaining acceptance for radioisotope equipment and techniques, and conducting tests on radioisotope devices designed to ascertain the level of beer in tanks and vats during monthly inspections.

* * *

The "Power supplies packages for electronic physics research equipment" seminar organized by the Sverdlovsk division of V/O Izotop in conjunction with a branch of the Biophysics Institute of the USSR Ministry of Public Health was held in the demonstration hall of the Sverdlovsk interdistrict division of V/O Izotop in February 1973. Staff members of Sverdlovsk scientific research institutes took part in this seminar.

* * *

The "Radioisotope devices and specifications for maintenance, repair, and operation" panel was held in February 1973 under the auspices of the Sverdlovsk interdistrict division of V/O Izotop in collaboration with the District Council and the House of Industry of the Sverdlovsk Science and Industry Society (NTO). Participating were specialists of industrial enterprises, scientific research institues, and planning institutes in Sverdlovsk. Eleven papers were read at the seminar.

* * *

A seminar on the quality and operational features of radiation-protective equipment was held in March 1973 under the auspices of the Tashkent interrepublic division of V/O Izotop. Participating were representatives of 24 organizations (mostly consumers of protective equipment), as well as representatives of planning institues and scientific research institues. Seven reports were presented.

* * *

A seminar on "Experience and outlook for applications of radioisotope equipment in metallurgy, machinery manufacture, and radioisotope equipment in metallurgy, machinery manufacture, and in the chemical process industry" was organized by the Sverdlovsk interdistrict division of V/O Izotop agency in conjunction with the NTO District Council and the Sverdlovsk Municipal Central Scientific and Technical Institute in March 1973. Five papers were presented at this seminar.

* * *

Translated from Atomnaya Énergiya, Vol.35, No.4, pp.287-288, October, 1973.

A conference on applications of radioisotope techniques and instruments in the industry of the Podol'-sk area of the Kiev region was held in March 1973. The Kiev interrepublic division of V/O Izotop agency sponsored this conference, which attracted about 70 specialists from industrial enterprises, to hear seven papers.

* * *

A combined exhibit and seminar on "Applications of isotopes and radioisotope equipment in the machinery industry" was held in Gor'kii March 21-33, 1973. Reports were submitted by representatives of 26 industrial enterprises in the city. A radio report on the seminar and exhibit was organized from the exhibit hall with the object of broadening publicity on advanced experience acquired in the use of radioisotope equipment at the city's industrial enterprises. The inauguration of the exhibit was broadcast on local TV.

* * *

A conference on planning and organization aimed at gaining acceptance for radioisotope equipment in the national economy of the country was held in Tashkent during April 1973, organized by the V/O Izotop for the benefit of heads of departments of procurement dealing with such instruments in the territorial divisions of V/O Izotop. A new procedure for working on acceptance of radioisotope equipment by planning institutes, scientific research institutes, industrial enterprises, and the leading bodies of government ministries, was discussed at this conference.

* * *

A conference on "Applications and operation of KURA and SURM radioisotope level gages" was held under joint auspices of the V/O Izotop and the Kaliningrad TsNTI, and also the Leningrad maintenance and adjustments section of the Specialized board on maintenance, installation, and adjustments of radiation equipment in June 1973. This conference took place at the No.2 paper and pulp combine in Kaliningrad. The conference attracted representatives of twenty industrial enterprises in Kaliningrad. Five reports were presented. The conference participants were familiarized with the operation of the SURM radioisotope level gage, which has given satisfactory services on stream at the combine.

* * *

A seminar on "Radioactive isotopes and radioisotope equipment as a means of process automation in the food industry" was held in Odessa under the auspices of the Kiev interrepublic division of V/O Izotop in July 1973. This seminar was organized with the object of acquainting workers in services dealing with process measuring and monitoring instruments and automatic control instruments of the food processing industry in Odessa and surrounding region with the latest in radioisotope equipment. The seminar heard thirteen reports. Specimens of radioisotope devices in use in the food processing industry were displayed at an exhibit organized for the benefit of seminar participants. The seminar participants adopted recommendations to be published and disseminated to enterprises in the country's food industry.

VII INTERNATIONAL CONFERENCE ON NONDESTRUCTIVE TESTING (WARSAW, JUNE 1973)

A. N. Maiorov

The VII International Conference on nondestructive testing techniques in quality control of materials and products was held June 4-8, 1973 in Warsaw. The conference attracted 1200 delegates representing 31 countries, including socialist countries (Bulgaria, Hungary, East Germany, Poland, Rumania, the USSR, Czechoslovakia, Yugoslavia). The conference heard 245 reports presented (40 of these from the Soviet Union), and eight panel sessions were set up. Reports dealing with practical results on the utilization of nondestructive techniques and equipment were discussed in an informal free discussion setting at "round table" meetings.

The special distinguishing feature of this conference was the appearance of new sections designed to provide a forum for discussing work in standardization of techniques and equipment, the use of nondestructive testing in reactor technology, and in investigations of the physical properties of materials and of flaws appearing in materials, and also topics pertaining to automation of nondestructive testing, and training of qualified specialists in nondestructive testing.

Of the total number of reports presented, 89 dealt with ultrasonic inspection techniques, 48 with radiation techniques, 43 with magnetic and electromagnetic techniques, 11 with general topics in flaw detection, and 53 with miscellaneous methods of inspection (radio wave, thermal, capillary, optical, acoustical, etc.).

Reports presented at the conference bear witness to the further development and expansion of practical utilization of the principal techniques of radiation flaw detection: industrial radiography, radioscopy, and radiometry. New sources of ionizing radiations are being developed and those already in use have been undergoing improvements; new types of cermet x-ray tubes appearing on the scene feature high emission intensity at voltages to 500 kV and longer tube life (report by W. Hartl, West Germany); comparative investigations on low-energy sources of radiation from ^{170}Tm, ^{75}Se, ^{55}Eu, ^{241}Am, and ^{169}Yb in industrial radiography at short focal length have been complete (M. Dobrowolski et al., Poland); new types of accelerators, NDT betatrons, are now available (J. Janiczek et al., Poland; O. Bulaev et al., USSR), microtrons (J. Osterberg, Sweden; S. Kapitsa et al., USSR), and a 25,000 r/min·m linear accelerator (G. Wheeler, USA).

Detectors for use in radiation flaw detection are being improved, new characteristics of x-ray films have been suggested (R. Bollen et al., Belgium); a new approach has been worked out for discerning flaws withcontrast – noise characteristics of radiographic film taken into account (K. Panatescu, Rumania) so that conversion can be made to quantitative estimates of flaws in the interpretation of radiograms. Neutron radiography has been making advances with the possibility of the use of track-delinearing detectors under study (H. Berger, USA); a new microchannel image intensifier has been designed (V. Chalmeton, France); a procedure for optimizing the parameters of neutron detectors has been worked out (N.D. Tyufyakov et al., USSR). The possible use of a combination of fluoroscopic screen and photodiodes has been investigated (S. Schmidt and E. Kirgner, West Germany) as a means of visualizing latent radiation images; a radioscopic system based on a CsI(Tl) scintillation crystal, in which system the images can be "stored" not only with the aid of the commonly used magnetic tapes and disks, but also by means of special tubes which provide resolution of 120 television lines per millimeter when the screen diameter is 25 mm, a writing time of 0.01 sec, data storage time and data readout time of 10 to 12 min (R. Halmshaw, Britain).

Translated from Atomnaya Énergiya, Vol. 35, No. 4, pp. 288-289, October, 1973.

In recent years, a need has been felt for new procedures and new equipment in radiation flaw detection practice to meet the needs of industry. For example, automated self-propelled facilities capable of radiographing joints when equipment is moved through the interior of ducts or piping over distances from 2 to 10 km have been designed in some countries for radiographic quality control of welded joints in trunk pipelines (K. Sauerwein, West Germnay; I. Roualt, France). The BIX corporation (Britain) ran a viewing of a film illustrating applications of similar equipment in the construction of overland and sea-bottom gas pipelines and oil pipelines. New types of γ-ray flaw detection gear have made their appearance (V. Osuchowski et al., Poland), as well as x-ray introscopes (B.I. Leonov et al., USSR), betatron introscopes (V.I. Gorbunov et al., USSR).

Some of the papers submitted presented results of theoretical and experimental research on the selection and validation of parameters of radiometric flaw detection (Z. Godlewski, Poland; K. Sinclair et al., USA), on applications of such equipment in quality control of ceramic wares (Z. Godlewski, Poland) and in quality control of rolled steel products (V.I. Gorbunov et al., USSR). A trend toward automation of basic unit processes in radiation flaw detection practice has come to the fore in recent years: exponometry [metrology of exposure] (H. Basler, West Germany), digital computer interpretation of radiograms (V.G. Abramov et al., USSR; B. Doster et al., USA).

The "Nondestructive testing in reactor technology" panel heard 13 reports devoted to applications of automatic ultrasonic flaw detector sets (W. Deutsch, West Germany; A. Samoel, France; K. Abend et al., West Germany) and eddy-current flaw detection equipment (F. Forster and Meier, West Germany) designed to inspect the quality of fuel element tubes and steam generator tubes during the fabrication processes; development of automatic systems for monitoring the content and distribution of fissile isotopes in uranium and plutonium nuclear fuel – in fuel element form (N. Beyer et al., USA; M. Destribats et al., France); development and utilization of acoustical, ultrasonic, and radioisotope devices and equipment for quality control of pressure vessels and pipe connections of nuclear reactors while in service or during overhaul and repair (O. Reimhard, USA; W. Ratch, West German; A.N. Maiorov et al., USSR). Close attention is being given to integrated NDT systems and the interaction between NDT systems and fuel element fabrication technology, with a view to achieving appreciable improvements in the service life and engineering cost picture of fuel elements (H. Fedick et al., USA; P. Picard et al., France); to experience and results in comprehensive utilization of NDT to inspect 40 nuclear reactors of different design types over the 1963-1972 period in the USA, in the course of installation, repair, and operation (K. Lautzenweiser, USA); to applications of the AGA thermographic facility in inspection of filtration equipment used in the manufacture of nuclear fuel.

An organized specialized exhibit displaying up-to-date nondestructive testing equipment drew participation from 54 firms in 32 countries. Most broadly represented were x-ray equipment and radioisotope equipment (152 displays), ultrasonic devices (85) and electromagnetic devices (69). Worth special note among the newer devices are acoustic emission devices fabricated by Leonard (Franch) and Dunigan – Endevco (USA – Britain) for inspecting reactor pressure vessels while in service, a facility for x-ray television inspection manufactured by Philips – Muller and Seifert (West Germany), γ-ray flaw detection gear fabricated by AGC (France), K.S. Products (Britain), Picker – Anderks (USA – Denmark), etc., x-ray equipment manufactured by Balto (Belgium), Philips (West Germany), etc., ancillary equipment for industrial radiography manufactured by Lowol (West Germany), Geverken (Sweden), etc., automated sets for combined electromagnetic and ultrasonic inspection of austenitic and ferromagnetic tubes ranging up to 60 mm in diameter manufactured by ASIA (Sweden), 8 MeV linear accelerators Verian – Linatron-2000 (USA), generating 2000 p/min/m, and the 9 MeV Super-X linear accelerator (Britain) generating 1500 r/min/m. A new trend coming to the fore is an increase in the number of firms developing and manufacturing nondestructive testing equipment, alongside the obvious increase in the production volume and sales of NDT gear. But the leading positions in the field and in the market are still being held by major concerns which have been specializing in this area for quite some time, such as: Sauerwein of West Germany (γ-ray flaw detection gear), Forster of West Germany (electromagnetic instruments), Philips of West Germany and Balto of Belgium (x-ray equipment), and so on.

The technical level of the new equipment has been raised appreciable in recent years, with unitized modular makeup coming into its own, and the production volume of nondestructive testing equipment has expanded.

The conference and the exhibit were both organized under the auspices of the International Nondestructive Testing Committee.

III INTERNATIONAL SYMPOSIUM ON PLASMA CONFINEMENT IN TOROIDAL SYSTEMS

V.V. Alikaev, N.N. Brevnov,
and V.S. Mukhovatov

The III international symposium on plasma confinement in toroidal systems, organized by the Max Planck Plasma Physics Institute with support from the European Physical Society, was held March 26-30, 1973, at Garching (West Germany).*

The symposium participants paid respects to the memory of Academician L.A. Artsimovich.

The symposium was attended by 179 delegates from 12 countries, who heard 80 reports. Most of the reports were devoted to the generation, confinement, and heating of plasma in Tokamak type machines. The reports presented at the symposium were printed prior to the inauguration of the proceedings and distributed in printed form to the participants.

The reader will recall that, prior to 1969, Tokamak type systems were studied uniquely in the Soviet Union, and that it was only in the wake of the Dubna conference that research in that direction began to undergo intensive development in other countries. At the present time, a dozen or so Tokamak machines, close in size and dimensions to the T-4 machine, the largest such Soviet facility located at the I.V. Kurchatov IAE [Institute of Atomic Energy], have been built and put into service in other countries. On the eve of the conference, experiments were initiated on the TFR machine (at Fontenay-aux-Roses, France). This machine surpasses the T-4 machine by quite a bit in its design data (intensity of toroidal magnetic field 60 kOe, ratio of large radius of torus to small radius $R/a = 98/20$), and will figure as the largest such machine in the world for the coming year.

The experimental data obtained on the foreign machines are in basic agreement with the findings of Soviet research. A report by N. Furth (Princeton) noted that energy losses from the plasma on ST machines and ATC machines at discharge conditions typical of Tokamak type facilities (small radiative losses and current in plasma ≈60 kA) are described adequately well by the pseudoclassical formula put forth by L.A. Artsimovich. According to preliminary data, a departure from this formula in the direction of increased losses is observed at currents ≈120 kA. The plasma energy lifetime τ_E is ≈20 msec on the Japanese IFT-2 machine, and corresponds to the empirical formula $\tau_E \approx H_\theta a^2$ suggested by S.V. Mironov on the basis of experimental data obtained with the T-3 machine (built at the I.V. Kurchatov IAE). This formula is in its essentials similar to the pseudoclassical formula. It had been shown in earlier Soviet work that the pseudoclassical theory provides a rough description of the experimental results, and that it specifically falls short of accounting for the longer plasma confinement time in response to increased plasma density.

D. Duchs et al. (USA) presented a tutorial review paper summarizing results of numerical simulation of transfer processes in a Tokamak plasma. Five semi-empirical models producing poor correlation with experiment are known. According to all the models, the electronic thermal conductivity must exceed the neoclassical values by a factor ranging anywhere from several units to several tens. But these models either fail on the whole to take sufficient account of the effect of impurities or treat the effect of impurities in too inconsistent a manner. For example, a comparatively oversimplified treatment of the effect of impurities (in terms of Z_{eff} and radiative losses with linear emission) led American physicists working on the Ormak machine (Oak Ridge, USA) to the inference that the electronic thermal conductivity

*The first conference of this kind was held in 1966 at Princeton (USA), the second at Dubna (USSR) in 1969.

Translated from Atomnaya Énergiya, Vol.35, No.4, pp.289-291, October, 1973.

in their system was at best one-fifth the pseudoclassical value, and in fact close to the neoclassical value, while the diffusion rate was pseudoclassical. Several years ago, open disagreement between Soviet and American physicists was voiced on the relationship between the energy time τ_E and diffusion time τ_p of plasma confinement, i.e., essentially on which of the loss mechanisms, whether thermal conduction or diffusion, would exert the preponderant effect. It was inferred, on the basis of experimental findings obtained with the T-3 and TM-3 machines (I.V. Kurchatov IAE) that $\tau_p \gg \tau_E$, i.e., the anomalous electronic thermal conductivity predominating. It was affirmed in contributions by American physicists working with the ST machine and reporting out their results at the Madison 1971 conference and Grenoble 1972 conference, that $\tau_E \approx \tau_p$, and that there was no need to suggest the existence of anomalous electronic thermal conductivity as a relevant factor.

It is noteworthy that this view is shared by the physicists working on the Ormak machine. At the same time, results of the latest ST experiments, reported out at this symposium, show $\tau_E \approx \tau_p/5$.

Matters are somewhat different with the thermal conductivity of plasma ions. All of the available experimental data on ion temperatures are in close agreement with the familiar L.A. Artsimovich formula derived under the assumption that the sole mechanism of energy loss by ions is neoclassical thermal conduction, while the collision frequencies correspond to the plateau on the frequency dependence of the thermal diffusivity. On that basis, Soviet physicists several years ago inferred the classical nature of the behavior of ions in the Tokamak. That inference has not been at variance with results reported later by American investigators. While paying close attention to more recent indications that the ion temperatures continue to conform to the plateau formula, we see that the plasma parameters are indicated by estimates to correspond to the region of infrequent collisions. The same effect was encountered with the Ormak machine, where the shift observed was even further onto the region of infrequent collisions. The observed discrepancies between experimental data and neoclassical theory according to the Ormak findings can be eliminated by taking into consideration the fact that energy losses by ions occur through charge transfer. Consequently, the ionic thermal conductivity in the region of infrequent collisions apparently conforms to the neoclassical law. But that conclusion is based on the assumption that a coulomb mechanism of energy exchange between ions and electrons is operative. If the flow of energy from electrons to ions exceeds the coulomb variant, then the ionic thermal conductivity must be anomalous. A serious argument in support of the neoclassical ionic thermal conductivity, which is not associated with the above assumption, can be found in the experimental results on adiabatic compression of plasma on the ATC machine that were reported at the symposium.

One major problem is that of investigating whether a stable plasma can be obtained at low values of the stability ratio q. It is known that when q declines to three-quarters, there is a runaway instability in the plasma. A report devoted to research on the Ormak machine pointed out that a decline in q in the range $q(a) < 5$ (where a is the radius of the diaphragm) brings about a shorter plasma confinement time even in the absence of such a runaway instability. A report dealing with experiments on the T-6 machine (USSR) showed that discharges such that $q(a) \approx 1.2$, retaining their stability for 1-2 msec, can be successfully obtained in cases where the surface of the plasma pinch is situated fairly close to the surface of the conducting liner, i.e., $a/b > 0.8$ (where b is the radius of the transverse section through the conducting liner). On the basis of these data, as well as experiments conducted on the Alcator machine (USA), in which a relatively stable plasma was generated at $q \approx 1.7$, we can infer that the range of values $1 < q(a) < 2$ is not an absolutely forbidden region for the Tokamak type machine. A runaway instability also occurs at large $q(a)$ values if the plasma density exceeds a certain critical level (approximately $3 \cdot 10^{13}$ to $5 \cdot 10^{13}$ cm^3). A report by N. Furth went into some detail on the concept of radiative cooling of the periphery of a plasma pinch as one of the possible causes of contractive implosion of the current channel observed before the onset of the runaway instability. But the mechanism behind the runaway instability remains as obscure as ever. Photographs of emission from the plasma pinch on the ATC machine led N. Furth to the conclusion that the expansion of the pinch during the processes of runaway instability takes place as the result of the development of fine-scale perturbations, rather than large-scale perturbations, and the former exert virtually no effect at all on the shape of the surface of the plasma pinch.

Close attention was given to contamination of plasma by impurities originating in the walls of the chamber, at the conference, and also to energy losses from the plasma as a consequence of charge transfer processes involving ions on impurities and the neutral gas. Protecting the plasma from wall effects has been a focus of increasing attention in recent years. One of the possible approaches to a solution of this problem is reliance on the divertor; that variant was discussed in a report submitted by Japanese physicists. It became known at the symposium that a machine employing a local divertor is being built at

Culham (Britain). There is great interest in the work reported on concerning a "thimble" type Tokamak machine at the I.V. Kurchatov IAE. The transverse section through the plasma exhibits a prolate shape in that machine, in contrast to the shape found in a conventional Tokamak. The interest in such a system is accounted for by the fact that higher plasma parameters can be successfully attained in machines of that type, according to theoretical prediction.

Plasma confinement and plasma heating in stellarator type systems were amply discussed at the symposium. Satisfactory agreement between the rate of diffusion decay of plasma and predictions based on neoclassical theory was observed in work done on Heliotron D (Japan), Saturn (USSR), and Proto-Cleo (Britain) thermonuclear machines. Some substantial discrepancies with neoclassical theory both in absolute values of plasma lifetime and in the nature of the dependence of plasma lifetime on the parameters of the plasma and of the magnetic field have been observed in work on the JIPP (Japan) and Tor-1 (USSR) stellara tor machines.

Several reports presented were devoted to new designs of magnetic systems for generating a stellarator configuration magnetic field. A novel magnetic system – a single-helix Vint-20 torastron machine, is under study at KhFTI [Khar'kov Physics and Engng. Inst.] (USSR). This machine features a unique helical conductor accommodated within a vacuum chamber, and which generates both longitudinal and transverse components of the magnetic field. A design project involving the large W-VII stellarator, construction of which has already begun at the Garching Plasma Physics Institute (West Germany), was already reported on at the conference. This facility will feature a large radius of 200 cm, plasma radius of 22 cm, and magnetic field intensity to 40 kOe.

Of the reports dealing with systems with internal conductors, the one of greatest interest was a tutorial review paper on work being done with the levitating-ring spherator (Princeton, USA). The plasma lifetime increases with the temperature over the range of electron temperatures from 0.1 to 10 eV, and varies inversely with plasma density, as pseudoclassical theory would dictate. As the temperature is increased further, and the region of infrequent collisions is reached, the shape of the dependence alters and acquires a Bohm shape $\tau \approx \tau_{Bohm}$.

Several reports dealing with studies of Belt pinch configurations were presented. The parameters of the two large pulsed pinches constructed in West Germany, with over 1 MJ energy content in the power supplies, are of special interest. One of these, under construction at Garching, is to have its power package stepped up to 3 MJ, and longitudinal current flowing in the plasma will be raised to 0.9 MA. The second facility under construction at Julich (West Germany) will have a power package generating 1.1 MJ, so that current flowing through the plasma will be brought up to 0.5 MA. Physical research using these machines is scheduled to be in progress by the end of 1973.

A report discussing research findings in work with the Doublet-II machine (USA) showed that the doublet configuration exists only for a brief time interval (≈1 msec) and at currents of 500 kA. At lower currents (≈100 kA) and longer durations (≈20 msec), two pinches form in the plasma. It is proposed that the Doublet-II machine be redesigned into a thimble type Tokamak machine in 1974.

Plasma heating in closed-loop machines was the subject of a special session of the conference, at which high-frequency and microwave methods of plasma heating and heating by injection of fast atoms was discussed. The most interesting findings were forthcoming from work on the Uragan stellarator, where $nT \approx 10^{15}$ eV/cm was reported. It was shown that when a mixture of two gases is employed, heating is observed both in the neighborhood of the ion cyclotron frequency and in the neighborhood of the ion – ion resonance. Similar work has been done at Princeton on the ST machine, where 1 to 4 MW power is to be put into the plasma by the end of 1973, at the frequencies of the ion cyclotron resonance and its second harmonic. Preparations for plasma heating experiments in the range of frequencies of the lower hybrid resonance are underway at the Alcator facility (USA). At the present time, plasma heating by the magnetic pumping method is under investigation in Britain. Two reports submitted by French scientists deal with the theory behind this mode of heating. The Vega stellarator and the Petula Tokamak machine are being built at Grenoble (France), for research on radiofrequency methods of plasma heating.

Neutral injection into closed-loop machines was discussed in five papers. Injection of a beam of atoms, with 40 kW beam power, has been carried out at the Cleo machine (Britain). Similar experiments will be underway at the Ormak (USA), TFR (France), and ATC (USA) machines. Close attention is being given to the theoretical aspects of injection of fast atoms. Three papers discussed the effect of a neutral gas and inhomogeneity of the magnetic field on confinement of fast trapped ions, rotations of plasma in response to injection, etc.

Most of the theoretical contributions dealt with two major topics: plasma stability and transport processes in plasma. Some of the papers discussed the theory of linear stability in Tokamak type machines with prolate cross sections of the magnetic surfaces. A report by O. Rotherford (USA) presented a nonlinear theory of Thyring instability. Rosenbluth (USA) made an attempt to account for runaway instability in terms of a nonlinear development of a m = 1 corkscrew instability. The theoretically predicted voltage surges and displacements of plasma pinch turned out to be much smaller than those observed experimentally. But this remains the only theoretical model which correctly predicts the sign of the voltage surge and the direction of displacement of the pinch.

In conclusion, we may note that the symposium demonstrated the steadily increasing concentration of efforts on the part of most countries in investigation plasma behavior in Tokamak type systems. Most of the large machines of this type already in service or being built in the various countries provide grounds for hope that the outlook of this trend of research on the road toward successful construction of a thermonuclear reactor will become clearer in the immediate future.

NATIONAL MHD SYMPOSIUM IN USA

A. V. Nedospasov

The XIII national symposium on engineering aspects of magnetohydrodynamics was held at Stanford University (USA) March 26-28, 1973. These symposia are usually scheduled on an annual basis and draw renowned specialists not only from various points in the United States, but also from other countries.

There are three salient trends in the design of MHD generators: generators working on combustion products of fossil fuels (open cycle); generators working on inert gases with readily ionizable additives (closed cycle); and liquid-metal MHD generators. The symposium provided confirmation of the fact that research on the second trend, the purpose of which is to use MHD generators in the nuclear power industry in tandem with high-temperature gas-cooled reactors, is being sharply curtailed. It is indicative that, of the nine papers submitted on plasma generators with nonequilibrium conduction, only one such paper was forthcoming from the United States. That paper described an interesting experiment on conversion of 12.6% of the enthalpy of a neon plasma stream with cesium additive to electric power; this power conversion materialized in a shock tube. The stagnation temperature in this experiment, 3700°K, is too high for a nuclear reactor.

Of the other reports on this topic, we must take note of experimental and theoretical research on nonequilibrium MHD generators (Direct Conversion Laboratory at Frascati, Italy) and a detailed paper on the properties of turbulent plasma in such MHD generators (Max Planck Institute, Garching, West Germany). That paper offered a clear confirmation of the straightforward formula for the effective conductivity $\sigma_{eff} \approx \langle\sigma\rangle \beta_{crit}/\omega_m \langle\tau\rangle$ proposed and validated in some of the research efforts conducted at the I.V. Kurchatov Institute of Atomic Energy in the 1963-1967 period.

The curtailment of work on MHD generators with nonequilibrium conduction is dictated by the absence of programs geared to the design of high-temperature gas-cooled power reactors for the 1700-2000°C temperature range.

Materials on preliminary design work on a large power plant with a gas-phase nuclear reactor and an MHD generator were published at the symposium. The proposed range of temperatures of the working gas in this case is 3500-4500°K. According to what the author had in mind, such an electric power station could be put into an Earth satellite orbit and could transmit the power it generated back to Earth in the form of radio waves.

Certain difficulties still stand in the way of progress in the third trend, which involves nuclear power packages to operate on board spacecraft. Specialists on liquid-metal MHD generators have therefore initiated a more attentive study of the feasibility of earthbound applications of such MHD generators.

The symposium participants focused their closest attention on MHD generators using combustion products. Some of the new experimental MHD generators which make use of both combustion and detonation are described in papers submitted by American scientists. These are comparatively small systems operating on combustion products of liquid fuel in pure oxygen. The channel of the MHD generator in these systems is generally supersonic with electrode pairs connected diagonally in series. Electric power up to 0.5 MJ per kilogram of combustion products is generated by these systems.

Research in the USA on lengthening the operating time of MHD generators is undergoing further development. Continuous operation of a generator for several hours at power outputs on the order of several hundred kilowatts has been achieved with the Avco company's Mark-VI MHD machine. Prior to that, power generating time with that machine had been at best portions of a minute or several minutes.

Translated from Atomnaya Énergiya, Vol. 35, No. 4, p. 292, October, 1973.

Major research is underway in Japan, which is presently the third-ranking country (trailing behind only the USSR and the USA) in the volume of work being done on direct conversion of thermal energy to electric power by the MHD method. Finishing touches are currently being put on an experimental facility in Japan in which the MHD generator features a magnetic system with a superconducting coil.

The symposium coincided with the signing, in Washington, of an agreement on scientific and technical collaboration between scientists of the USSR and the USA in the field of power development. The terms of this agreement cover, in particular, extensive collaboration in the field of MHD generators, with which American scientists are presently linking plans for expanded research.

VISIT OF USSR GKAE DELEGATION TO SWITZERLAND TO LEARN ABOUT PLASMA PHYSICS RESEARCH PROGRAM

V.I. Pistunovich

In accordance with an agreement on collaboration in the field of peaceful uses of atomic energy, drawn up between GKAE SSSR [the USSR State Commission on peaceful uses of atomic energy] and the Science and Research Division of the Switzerland Department of the Interior, a delegation from the GKAE SSSR consisting of three persons visited Switzerland May 6-16, 1973.

The delegation members visited centers at which research in plasma physics is in progress, and made a study of engineering applications of plasma phenomena at those locations.

The principal center in these efforts is the Plasma Physics Research Institute attached to Federal Polytechnic School in Lausanne (director E.S. Weibel). The staff of the Institute totals 56, and the annual budget runs to three million Swiss francs.

Work on dynamic RF stabilization on straight and bent θ-pinch machines is being completed at the Institute. A plasma of density $3 \cdot 10^{16}$ cm^{-3}, with ion temperature 30 eV, has been generated on a 100 cm long straight θ-pinch with a 10 cm diameter. A procedure for measuring the radial density profile by means of a ruby laser interferometer has been worked out. A bent θ-pinch is constituted by a 1/3 torus with a 100 cm large radius and a 5 cm small radius, and with no longitudinal magnetic field. Electrodes through which RF current is passed at amplitude 6 kA are positioned at the ends of the machine. The current flows over a span of 4 μsec. The variable magnetic field is 20 kOe in intensity, with a period of 10 μsec. Plasma of density 10^{16} cm^{-3} with 50 eV electron temperature has been generated. The Kruskal – Shafranov limit is increased by about ten times in response to the RF current.

Experiments on stabilization of instabilities by feedback in a θ-pinch with a large beta, $\beta = 8\pi nT/H^2$ are being prepared. The machine in question extends about 100 cm in length, 5 cm in diameter, the energy of the bank of capacitators is 20 kJ at 36 kV voltage. These experiments are similar to those staged at Los Alamos (USA), and will be performed in contact with American specialists.

The effect of the rotating magnetic field on the behavior of plasma is being investigated on a facility 150 cm in length and 10 cm in diameter. The electrodes through which longitudinal current establishing an azimuthal magnetic field is passed are located at the ends of the tube. The energy generated by the bank of capacitors is 3 kJ, the current period 5 μsec. The longitudinal magnetic field is 2 kOe at a frequency 2.5 MHz from the 8 MW power generator, and the rotating magnetic field is established with the field of longitudinal current. A plasma of density 10^{15} cm^{-3} is generated.

A "plasma box" machine has been built for research on wave propagation through plasma of density 10^8 to 10^{10} cm^{-3} with electron temperatures 3-5 eV. This machine comprises a vacuum volume about 100 cm in diameter, within which permanent magnets are located, extended over the surface of the $50 \times 30 \times 30$ cm box; the magnets form a large number of what are termed antiprobkotrons.* The magnetic field is zero at the center, and 2 kOe in the magnetic mirrors. Research on laser diagnostics is well advanced at the institute. Research on CO_2 lasers is also in progress.

Another research center operating in the field of plasma physics is the Physics Institute attached to the Friburg University (director O. Huber). The team working on plasma physics consists of 12 staff-members. The principal research topic is investigation of the magnetosonic resonance. A fast θ-pinch

*Probkotron – Soviet term for open-ended mirror system – translator's note.

Translated from Atomnaya Energiya, Vol.35, No.4, pp.292-293, October, 1973.

with capacitor bank energy content 120 kJ is employed to generate the plasma. At the present time a facility with a 10 kOe quasistationary magnetic field is being built. It is proposed that 400 kA current be passed along the axis within 80 μsec. Electrical conduction in a decaying plasma is being investigated on the Sigma machine. This research is being pursued with the object of simulating phenomena at work in a cosmic weakly ionized plasma.

There is also a facility designed to study a HCN laser at wavelength 0.3 mm, and here 1 A current is being passed at 10^3 V through a mixture of H_2 and CN gases.

Research on plasma physics is also being conducted by some teams in higher educational institutions in Bern and Zurich. The Bern team deals mainly with laser generation of plasma, and is working out plans for laser applications in thermonuclear studies.

Abosrption of helicon type waves in plasma of density 10^{13} cm^{-3}, electron temperature 20 eV, magnetic field 30 G, is under investigation at Zurich.

Applied research is being conducted mainly by private concerns. The Pierre Holding company has divisions in the towns of Thun and Vabern, and is studying interaction between laser radiation and matter. Completely automated laser facilities have been designed to pierce tiny holes in the ruby gems employed in the manufacture of watches. There are CO_2 lasers, argon lasers, and mercury lasers at Vabern.

The Brown Boveri firm (center located at Baden) has designed an instrument to be used in measuring the velocity profile in the flow of liquids, gases, and plasma. This instrument is based on the Doppler effect in scattering of laser light from particles of additive sized to 1 μ. It is capable of measuring the flow-speed of liquids over the range from 10^{-3} to 10^5 cm/sec. Work is in progress on holography using a ruby laser, and on designing current breakers for service up to 500 kA, within about 20 msec response time. Superconducting NbTi wire solenoids designed for magnetic fields of up to 45 kOe are being fabricated at a division of the Brown Boveri firm in the Zurich area.

EXHIBITIONS

LOW-TEMPERATURE PLASMA IN THE SERVICE OF THE NATIONAL ECONOMY

E.S. Trekhov

The development of research on the physical and chemical properties of low-temperature plasma, and the invention of plasma generators with a broad spectrum of technical characteristics, have paved the way to achieving far-reaching acceptance of plasma processes in practical production work today. As a consequence of the broad range of parameters, low-temperature plasma is now not only a convenient means of intensifying already existing production processes of several types, and lowering process costs into the bargain, but also contributes to the development of some fundamentally new technological arrangements. In these novel approaches, the specific properties of plasma are entirely inseparable either from the characteristics of the process per se (in that the process would not even be realizable to begin with under other conditions) or from the properties of the end product.

Experience accumulated to date in the industrial exploitation of plasma processes, and the status of various promising developments that have yet to win acceptance in industry, as well as problems pertaining to the further development of processes, have prompted the need for a special All-Union interdepartmental series of measures geared to attracting all organizations concerned with practical applications of low-temperature plasma in the USSR and all the organizations conducting experimental and theoretical research in this field.

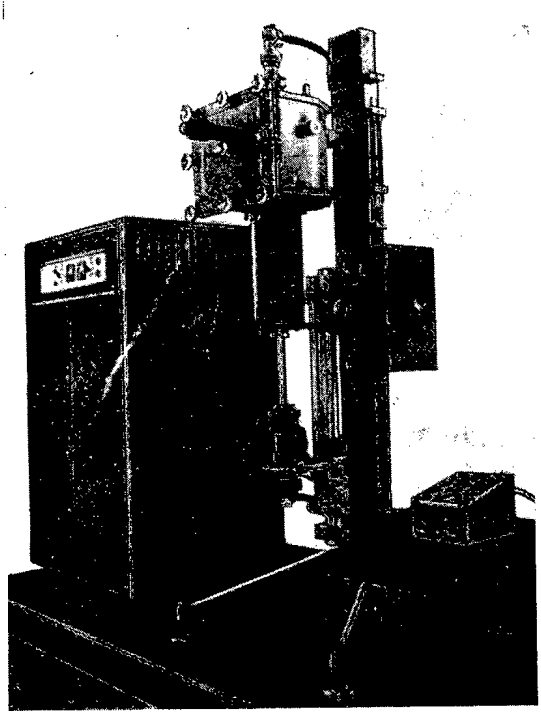

Fig. 1. The Monokristall PD-3 plasma arc facility.

This measure was carried out on the initiative of GKAE SSSR by utilizing the facilities of the VDNKh [Exposition of Achievements of the USSR National Economy] from September 1972 through February 1973. The "Atomic Energy" pavilion at the VDNKh was chosen as the site for a topical exhibit on "Varieties of facilities utilizing low-temperature plasma," around which were centered conferences and seminars relevant to topic, with meetings organized to meet specialists in the field.

The exposition afforded 400 m^2 of floor area to house some 52 exhibits and displays. Most of these were operating models or specimens manufactured in quantity production by Soviet industry, while some were pilot-scale prototypes. The exhibit comprised five sections arranged according to subtopic, four of them being devoted to industrial facilities in plasma-chemical, metallurgical, machinery, mining, and other branches of industry, and the fifth to plasma investigation techniques.

Most of the full-scale industrial facilities were developed on the basis of dc arc plasmatrons. We can consider the problem of service life as solved in the case of most low-output and medium-output (to 50 kW) arc plasmatrons: the service life is determined by the durability or life of the electrodes, and impressive advances have been registered in the design of electrodes. This has made it possible to

Translated from Atomnaya Énergiya, Vol. 35, No. 4, pp. 293-295, October, 1973.

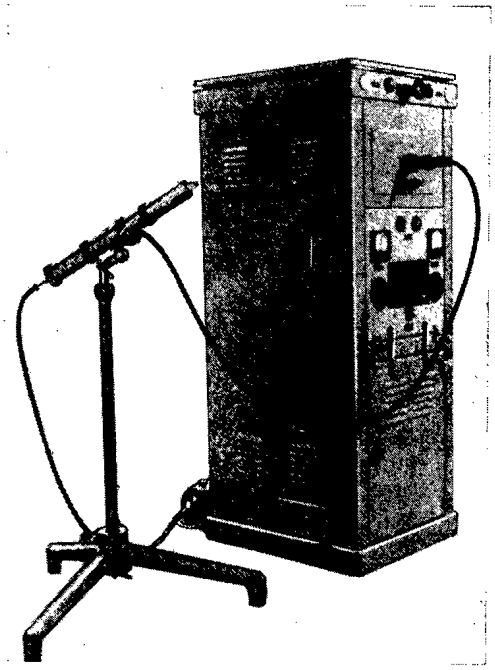

Fig. 2

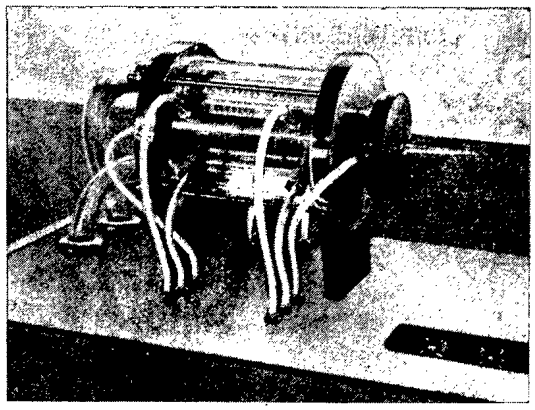

Fig. 3

Fig. 2. Laboratory model LFP-3 torch plasmatron.

Fig. 3. Arc plasma source for investigating emission spectra in vacuum ultraviolet region.

design such facilities for automatic control or semiautomatic control, thereby improving the engineering cost picture. Among the large-scale facilities scaled up to in-plant operating size, we must single out the SGU machine manufactured at the Avtogenmash plant in Odessa. This facility is provided with a 50 kW output Kiev arc plasmatron employing air as the plasma-forming gas. This machine handles automatic cutting to match an irregular shaped template in work on sheet metal or plate in sizes 2000 × 8000 mm and 60 mm thick (aluminum). The use of air-plasma cutting increases cutting speed 10-15% over that attainable with an inert gas plasma torch, according to plant data, and that results in impressive savings. The ITEF-20m machine, designed for plasma-arc cutting of metals, is a highly sophisticated facility that won great favor at the exhibit. While the exhibit was on, the machine was installed at five enterprises throughout the country (and orders placed for the machine are more impressive than that figure would indicate).

In addition to facilities making use of the thermal effect of the plasma jet to process metals by cutting and welding, a prominent place was occupied at the exhibit by instruments whose operation is based on the transport properties of plasma jets. By utilizing the high temperature and high velocity of plasma jets to good advantage, these machines are capable of applying coatings to either ceramic or metal surfaces, whatever the size of the work and whatever the configuration. These machines include the UMP-5 developed by VNIIavtogenmash institute and now in quantity production. Using various plasma-forming gases, nitrogen included as working gases, the facility has the capability of applying as much as 5 kg of tungsten metal within an hour, or as much as 3 kg zirconia (zirconium oxide) and other materials in that time, at 30 kW power output level. This is a versatile general-purpose machine, and can be used in heat treatment, welding, cutting, and also in chemical processes.

Arc plasma-chemical reactors were represented at the exhibit by the novel-design three-phase ZPG plasma generator, developed at Kazan' Polytechnic Institute. This generator is capable of heating its working gas to 15,000°C at power output to 100 kW, and at a gas (hydrogen) flowrate of 4 c/sec. Consequently, the ZPG generator is a highly promising facility whose power can be put to use either in the metallurgical industry or in the chemical process industry, and which is capable of operating for several hundred hours.

The A.A. Baikov Institute of Metallurgy of the USSR Academy of Sciences exhibited the Monokristall PD-3 plasma-arc machine, a facility which operates on inert gases. This machine is capable of growing single-crystal rods of refractory metals (molybdenum, tungsten) up to 40 mm in diameter and extending to

1 m in length in a continuous process and without benefit of a vacuum enclosure (Fig.1).

The exhibits mentioned do not come near exhausting all of the possibilites inherent in applications of the arc plasmatrons displayed, but they do offer a fairly complete picture of the pathways open for developing further uses of plasma jets in the national economy. It should be recalled that plasma generation in plasmatrons of this type, and the region within which the working gas is heated, are separated spatially from the site where the plasma is used.

Plasmatrons in which the plasma is generated and heated through the interaction between the plasma-forming gas and an RF electromagnetic field figured prominently at the exhibit. The special interesting feature of FR plasmatrons is the way they can combine the effective volume and the plasma heating region. Moreover, RF plasmatrons can function at low flowrates of the plasma-forming gas. The absence of parts that can wear out or become consumed (electrodes) renders the service life of RF plasmatrons virtually independent of anything but the operating characteristics of the RF oscillator energizing the facility. Thanks to the qualities enumerated, this type of plasma generator appears to hold great promise, particularly when we consider that the state of the plasma can be made markedly nonequilibrium, with a substantial discontinuity between the electron temperature and the gas temperature.

Of the two types of RF plasmatrons, distinguished by the mode of coupling between the plasma and the RF field, the exhibit displayed only torch RF plasmatrons. The LFP-3 laboratory torch plasmatron put on display by the Moscow Engineering and Physics Institute [MIFI] feeds power up to 1 kW into the plasma at plasma temperatures up to 6000°C(pressure atmospheric) depending on which plasma-forming gas is used (see Fig.2). The jet velocity runs as high as 100 m/sec, and the flow of heat energy through the nozzle critical section runs as high as 1 kW/cm^2. The special distinguishing feature of this plasmatron is the use of an RF torch discharge in which the sources of heat are kept out of contact with the walls of the plasmatron, so that pure plasma jets are brought about along with clean plasma volumes having prespecified degree of nonequilibrium. RF power can be supplied to the plasmatron via a flexible cable, so that the plasmatron can be kept mechanically separate from the RF generator.

A suspended-bed type plasma-chemical reactor presented by Tomsk Polytechnic Institute consists of a conventional suspended-bed (or fluidized-bed) processor connected to a torch type plasmatron. The plasma temperature (up to 5000°K) is used to advantage in speeding up chemical processes. Power intake can be as high as 7 kW, and the generator frequency ranges from 5 to 40 MHz.

Some interesting devices designed to take measurements of different plasma parameters for plasma diagnostics purposes, and for control of plasmatron performance, were displayed in the last section of the exhibit.

The High Temperature Institute of the USSR Academy of Sciences [IVT AN SSSR] displayed a device designed for continuous automatic plasma temperature measurements by the spectral method. This device is the first of its kind, and can be used in automatic control of the state of the plasma in any technological process.

A series of arc type plasma sources with arc stabilized by cooled walls, was exhibited by the High Temperatures Institue of the USSR Acedemy of Sciences. These sources facilitate study of electrical conductivity, thermal conductivity, viscosity, and spectral emissivity of various states of the plasma as the parameters vary with the temperature.

The advantages offered by these devices are their high operating stability, the high plasma temperatures (all the way to 30,000°C), which render them also convenient and practical in many instances as irreplaceable sources of continuous radiation over a broad spectral range. Also on view at the exhibit was a very compact and conveniently handled source of radiation designed for installation directly on the spectral instrumentation bench.

A similar facility was exhibited by the Moscow Engineering and Physics Institute – an arc type plasma source designed to facilitate research on radiation and absorption of gases in the vacuum ultraviolet region of the spectrum. The channel arc of this source, thanks to reliance on a gas blanket system to protect the arc electrodes, and also thanks to the presence of gas optical windows transparent in the 2500–1000 Å region of the spectrum, operates on any gas, including air, carbon dioxide, and oxygen at atmospheric pressure. An external view of this facility is seen in Fig.3. This source can be used as a standard source in calibrating spectral equipment in the vacuum ultraviolet region, since it offers, in addition to high stability, virtually unlimited length of service life.

The exhibit, in providing an effective base for training specialists hailing from different branches of the national economy, successfully carried out its other assigned tasks as publicist and stimulator of new achievements in the field of plasma technology.

breaking the language barrier

WITH COVER-TO-COVER ENGLISH TRANSLATIONS OF SOVIET JOURNALS

in mathematics and information science

Title	# of Issues	Subscription Price
Algebra and Logic *Algebra i logika*	6	$120.00
Automation and Remote Control *Avtomatika i telemekhanika*	24	$195.00
Cybernetics *Kibernetika*	6	$125.00
Differential Equations *Differentsial'nye uravneniya*	12	$150.00
Functional Analysis and Its Applications *Funktsional'nyi analiz i ego prilozheniya*	4	$110.00
Journal of Soviet Mathematics	6	$135.00
Mathematical Notes *Matematicheskie zametki*	12 (2 vols./yr. 6 issues ea.)	$185.00
Mathematical Transactions of the Academy of Sciences of the Lithuanian SSR *Litovskii Matematicheskii Sbornik*	4	$150.00
Problems of Information Transmission *Problemy peredachi informatsii*	4	$100.00
Siberian Mathematical Journal of the Academy of Sciences of the USSR Novosibirski *Sibirskii matematicheskii zhurnal*	6	$195.00
Theoretical and Mathematical Physics *Teoreticheskaya i matematicheskaya fizika*	12 (4 vols./yr. 3 issues ea.)	$145.00
Ukrainian Mathematical Journal *Ukrainskii matematicheskii zhurnal*	6	$155.00

Back volumes are available.
For further information, please contact the Publishers.

SEND FOR YOUR FREE EXAMINATION COPIES

PLENUM PUBLISHING CORPORATION
Plenum Press • Consultants Bureau
• IFI/Plenum Data Corporation
227 WEST 17th STREET
NEW YORK, N.Y. 10011

In United Kingdom
Plenur Publishing Co. Ltd., Davis House (4th Floor)
8 Scrubs Lane, Harlesden, NW10 6SE, England